BIOCHEMICAL AND MOLECULAR ASPECTS OF *NEUROSPORA CRASSA*

THESIS
SUBMITTED TO THE
UNIVERSITY OF PUNE
FOR THE DEGREE OF
DOCTOR OF PHILOSOPHY
IN
CHEMISTRY (BIOCHEMISTRY)

BY
URMILA BALBIRSINGH RAWAT

DIVISION OF BIOCHEMICAL SCIENCES
NATIONAL CHEMICAL LABORATORY
PUNE 411 008, INDIA

FEBRUARY 1998

To my parents and brothers....

ACKNOWLEDGEMENTS

At this moment when I look back, I recollect many a faces who have been with me through all the moments of ecstasy and pain, excitement and frustration. I take this opportunity to thank them all.

Without a guide, a journey is directionless. Here I express my deep sense of gratitude to Dr. (Mrs.) Mala Rao for guiding me through with her knowledge and experience. She was always there in times of difficulty. I thank her for being my constructive critic which helped immensely.

I express my gratitude towards Dr. M.C. Srinivasan, former Head of Biochemical Sciences Division, NCL for the knowledge of microbiology imparted, Dr. (Mrs.) V.V. Deshpande for valuable discussions and Dr. V. Jagannathan for the scientific discussions held during the assessments of my Ph.D program. Their talks of encouragement always kept up the motivation in me.

I am highly indebted to Prof. S. Mitra, T.I.F.R. Bombay for permitting the use of CD facility; Dr. K.N. Ganesh, NCL for the use of spectrofluorometer, and also Dr.'s Aditi Pant, Sourav Pal, Ashish Lele and Premnath for their timely help.

Well started is half the job done. I am thankful to Dr. A.M. Bodhe for the practical help during the initial stages of my work. Thanks are also due to the scientists of Biochemical Sciences Division, NCL for the help rendered on various occassions..

I am thankful to Dr. Paul Ratnaswamy, Director, NCL and Dr. P.K. Ranjekar, Head of Biochemical Sciences Division for granting permission to submit this work in the form of thesis.

The fellowship received from the Council of Scientific and Industrial Research and the partial financial support from the Department of Science and Technology is also duly acknowledged.

The immeasurable help extended by Ajitha and Ganga during the prepartion of this thesis will always be remembered. I thank them for the untiring efforts and also Meena, Tripathi, Sathi, Bhavana and Badri Viswanathan for the help when it was needed the most. Thanks are also due to Narsimha and Ganga for the helpful discussions. Rohini, Rangarajan, Vaishali, Suchitra, Anu, Veena, Amutha, Shamim and Madhura provided friendly assistance on various ocassions. I thank them all for the moments of joy and laughter which made the lab a better place to work.

Thanks are also due to Dr's Jyoti, Abhay and Sangita, and Kavita, Neeta, CV, Sudeep, Aparna and Jui. I am also grateful to Dr. Mohini and Devyani for the constant support, encouragement and sharing the lighter moments.

I appreciate the efficiency of our office staff, Ms. Usha Deshpande & Indira Mohandasan and thank them for the help rendered.

It was a delight to see equipments in working condition whenever required. I gratefully acknowledge the services of Mr. M. Kamthe and Mr. V.Karanjkar for the same.

I also express my sincere appreciation to our lab attendent Mr. Ramakant Lambathe who was of great help in day to day routine work.

Throughout the course of my Ph.D Sneha was always there by my side as a friend and companion. Her untiring efforts went a long way in the preparation of this thesis. I certainly fall short of words in expressing my feelings towards her.

I owe all that I am to my parents and, brothers Anirudha and Sudeep. Without their constant encouragement and support it would have been difficult to emerge through the turbulent waters of life and submit this work.

Above all I thank the Almighty

Urmila Rawat

TABLE OF CONTENTS

DECLARATION

This is to certify that the work incorporated in the thesis entitled **Biochemical and Molecular aspects of *Neurospora crassa*** submitted by Urmila B. S. Rawat was carried out under my supervision at Biochemical Sciences Division, National Chemical Laboratory, Pune. Material obtained from other sources has been duly acknowledged in the thesis.

Mala Rao

Dr. (Mrs) Mala Rao

(Research Guide)

ABBREVIATIONS

ANS	8-Anilinonapthalene-1-sulfonic acid
ATP	Adenosine 5'-triphosphate
AMP-PNP	5'-adenyl imidodiphosphate
CD	Circular dichroism
DTT	Dithiothreitol
DEP	Diethyl pyrocarbonate
EA adduct	1-(β-hydroxyethylthio)-2-β-hydroxyethyl isoindole
EDC	1-ethyl-3[3-(dimethylamino)-propyl]-carbodiimide
FCAL	Fluorescent chemoaffinity labeling
Gdn/HCl	Guanidine hydrochloride
GdmCl	Guanidinium chloride
HNBB	2-Hydroxy-5-nitrobenzyl bromide
NADPH	Reduced nicotinamide adenine dinucleotide phosphate
NADH	Reduced nicotinamide adenine dinucleotide
NAD^+	Oxidized nicotinamide adenine dinucleotide
NBS	*N*-Bromosuccinimide
NEM	*N*-Ethylmaleimide
OPTA	*o*-Phthalaldehyde
PHMB	*p*-Hydroxymercury benzoate
PMSF	Phenylmethylsulfonylfluoride
TNBS	2,4,6-Trinitrobenzene sulfonic acid
XD	Xylitol dehydrogenase
XI	Xylose isomerase
XR	Xylose reductase
XR-u	Unfolded state of XR
XR-m	Molten globule state of XR

SYNOPSIS

The efficient utilization of hemicellulose is necessary for the commercial exploitation of the lignocellulosic materials. D-xylose the predominant sugar of hemicellulose is not readily fermented by micro-organisms. We have earlier identified a strain of *Neurospora crassa* NCIM 870 with the unique ability to directly convert biomass to ethanol.This organism exhibits both depolymerase and fermentative activities and can ferment both D-glucose and D-xylose. The biotechnological implication of ethanol production by this organism prompted us to investigate the enzymes catalyzing the initial reactions in the conversion of xylose to ethanol. The main features of the work done are:

[A] D-XYLOSE CATABOLIZING ENZYMES IN *NEUROSPORA CRASSA*– The production of D-xylose catabolizing enzymes, xylose reductase (XR) and xylitol dehydrogenase (XD) by *Neurospora crassa* was studied The enzyme activities were induced by D-xylose under aerobic conditions. However, D-glucose was an effective repressor and low enzyme activties were obtained. The induction of NADPH-linked XR preceeded NADH-linked XR and the ratio of NADH to NADPH-linked XR activity displayed variation from 0.02 to 0.2 suggesting the presence of two different XR. Aerobic conditions were required by *N. crassa* for cell growth but not for ethanol production. Maximum ethanol of 0.3 g/g of D-xylose was produced when shifted to semiaerobic condition where high NADH-linked XR and NAD-linked XD activities were observed.

The production of xylose isomerase (XI) another D-xylose catabolizing enzyme was detected for the first time in the cell extracts of *N. crassa.* Of the various carbon sources tested, highest XI was obtained with D-xylose when *N. crassa* was grown for 72 h. The enzyme exhibited maximum activity at pH 8.0 and 70 °C and retained 100 % activity at 45 °C for 30 min at pH 8.0. XI was activated by 8 mM Mg^{2+} whereas 2 mM Co^{2+} afforded protection against inactivation by heat. The K_m for D-xylose was 10 mM and 22 mM for XI and XR respectively at 28 °C and pH 7.0. The present investigation revealed that the conversion of D-xylose to D-xylulose in *N. crassa* is mediated not only by the oxido-reductive pathway involving XR and XD, but also by an alternate pathway involving XI.

[B] PURIFICATION AND CHARACTERIZATION OF XYLOSE REDUCTASE AND XYLITOL DEHYDROGENASE– The purification and characterization of XR and XD the enzymes catalyzing the initial reactions in the conversion of xylose to ethanol by *N. crassa* has been described. XR was purified to homogeneity by ammonium sulfate fractionation, DEAE-Cellulose, CM-Sephadex and Sephacryl S-200 chromatography with 90 fold purification and specific activity of 73 $U.mg^{-1}$. The molecular mass of the native enzyme when determined by Sephacryl S-200 gel filtration was found to be 60 kDa whereas on SDS-PAGE a value of 29 kDa was obtained indicating the presence of two similar subunits. XR was most active at pH 6.3 and 40 °C. It exhibited maximum stability at pH 5.5 and 4 °C. The initial velocity and product inhibition studies revealed that the *N. crassa* XR follows an *iso-ordered bi bi* mechanism. The enzyme was highly specific to NADPH as the coenzyme and no activity was observed in the presence of NADH alone. However, in the presence of NADPH the non phosphorylated coenzyme enhanced the XR activity. Fluorescence studies revealed the presence of a single NADH and NADPH binding site per dimer of XR with K_{NADPH} and K_{NADH} values of 0.85 and 19 μM respectively.

XD was purified to homogeneity by fractional ammonium sulfate precipitation followed by column chromatography on DEAE-Cellulose, Sephacryl S-200 and β-NAD-agarose with 81.5 fold purification and specific activity of 15 $U.mg^{-1}$.The purified enzyme had a native molecular mass of 87 kDa (gel filtration) and was composed of two similar subunits of molecular mass 43.6 kDa (SDS-PAGE). XD exhibited maximum activity at pH 8.4 and 28 °C. It was most stable at pH 7.0 and at 4 °C. The enzyme was activated by Mg^{2+} and stabilized by Ca^{2+}, Mg^{2+} and Mn^{2+}. The enzyme was found to be highly specific to NAD^+ (K_m 0.7 mM) as the coenzyme and exhibited maximum activity in the presence of the sugar alcohols xylitol (K_m 28.5 mM) and sorbitol (K_m 100 mM).

[C] ACTIVE SITE CHARACTERIZATION OF XYLOSE REDUCTASE– The importance of various functional groups for the activity of XR was investigated by the use of chemical modifiers with restricted amino acid specificity, under the conditions which did not alter the enzyme conformation. XR was inactivated by the modifier *N*-bromosuccinimide (NBS) suggesting the presence of an essential Trp in XR. NADPH afforded 90% protection against inactivation. Kinetic analysis of the NBS modified XR and

acrylamide quenching studies confirmed the involvement of Trp at the coenzyme binding site of XR. Chemical modification studies in combination with ANS binding experiments revealed that the Trp residues of XR are essential for maintaining the hydrophobicity of the NADPH binding site and thus permitting its efficient binding to the enzyme.

The inhibition of XR by the modifiers *p*-hydroxymercury benzoate (PHMB), *o*-phthalaldehyde (OPTA) and 2,4,6-trinitrobenzenesulfonic acid (TNBS) indicated the presence of essential Cys and Lys residues at the active site of XR. Double inhibition studies showed that Cys residues involved in the reaction with PHMB (SH_I) and OPTA (SH_{II}) are distinctly different and essential for XR activity. Experimental evidence has been presented that serves to implicate that SH_I located in a hydrophobic microenvironment at the high affinity NADPH binding site of XR plays a role in the binding of the coenzyme to XR; whereas, SH_{II} serves to maintain the conformation of the active site essential for catalysis by interacting with the NH_2 group of an essential Lys residue situated at a distance of 3 Å.

The k_{cat}/K_m profile of XR reaction at varying pH yielded pK_a values of 5.5 and 7.0 Comparison of the pH-k_{cat}/K_m profile of XR measured in water and 20% ethanol indicated that the pK_a values of 5.5 and 7.0 may be ascribed to an ionizable His and carboxyl group respectively. Further, the role of these residues in the mechanism of action of XR was delineated using chemical modification studies. The differential reactivity of native and diethylpyrocarbonate (DEPC) modified XR towards xylose isomers indicated the presence of an essential His in XR and its involvment in binding and directing the specificity of aldose substrates within the active site of the enzyme. The involvement of carboxyl group in the catalytic action of XR was investigated by using the modifier 1-ethyl-3[3-(dimethylamino)-propyl]-carbodiimide (EDC).

[D] CONFORMATION AND MICROENVIRONMENT OF THE ACTIVE SITE OF XYLOSE REDUCTASE– In the present investigation the conformation and microenvironment of the active site of XR from *N. crassa* has been probed. XR was completely inactivated by low concentrations of Gdn/HCl which was used as a active site perturbant. Fluorescence studies revealed that the inactivation of XR by Gdn/HCl precedes gross conformational change and the possibility of secondary conformational change was eliminated by acrylamide quenching studies. The change in the active site conformation was

monitored by fluorescent chemoaffinity labeling (FCAL) using OPTA as a chemical initiator. OPTA reacts with XR at the active site resulting in the formation of a fluorescent XR-isoindole derivative. The enzyme inactivated by low concentrations of Gdn/HCl retained its ability to form the isoindole derivative indicating that inactivation was not due to conformational changes at or near the active site of XR. Gdn/HCl also had no effect on the binding of NADPH to XR. Energy transfer experiments further revealed the structural integrity at the active site of the Gdn/HCl-inactivated XR. Changes in the fluorescence emission maximum of 1-(β-hydroxyethylthio)-2-β hydroxyethylisoindole (EA adduct) in solvents of varying polarity was studied. The data obtained was utilized to interpret the fluorescence behaviour of XR-isoindole derivative and assess the polarity at the active site. Experimental evidence presented in this work serves to implicate that the active site of XR is less fragile and is located in a microenvironment of low polarity.

[E] CHAPERONE-ASSISTED FOLDING OF XYLOSE REDUCTASE– Present investigations were undertaken to understand the folding of XR using the multimeric protein α-crystallin as a molecular chaperone. Denaturation studies using the structure-perturbing agent guanidinium chloride (GdmCl) indicated that XR folds through a partially folded state that resembles the molten-globule. Fluorescence and delay experiments revealed that α-crystallin interacts with the molten-globule state of XR (XR-m) and prevents its aggregation. Cold-lability of α-crystallin-XR-m interaction was revealed by temperature-shift experiments implicating the involvement of hydrophobic interactions in the formation of the complex. Reconstitution of active XR was observed on cooling the α-crystallin-XR-m complex to 4 °C or on addition of ATP at 37 °C. ATP hydrolysis is not a pre-requisite for XR release since the nonhydrolyzable analogue 5'-adenylyl imidodiphosphate (AMP-PNP) was capable of reconstitution of active XR. Experimental evidence has been provided for temperature and ATP mediated structural changes in the α-crystallin-XR-m complex that shed some light on the mechanism of reconstitution of active XR by this chaperone. The relevance of the finding to the role of α-crystallin *in vivo* is discussed.

LIST OF PUBLICATIONS

1. **Rawat, U. B.** & Rao, M. B. (1998) Interactions of chaperone α-crystallin with the molten-globule state of xylose reductase: Implications for reconstitution of the active enzyme. *J. Biol. Chem.* **273,** 9415-9423.
2. **Rawat, U. B.** & Rao, M. B. (1997) Site and significance of cysteine residues in xylose reductase from *Neurospora crassa* as deduced by fluorescence studies. *Biochem. Biophys. Res. Commun.* **239**, 789-793.
3. **Rawat, U. B.** & Rao, M. B. (1997) Conformation and microenvironment of the active site of xylose reductase inferred by fluorescent chemoaffinity labeling. *Eur. J. Biochem.* **246**, 344-349.
4. Phadtare, S., **Rawat, U. B.** & Rao, M. B. (1997) Purification and characterization of xylitol dehydrogenase from *Neurospora crassa. FEMS Microbiol. Lett.* **146**, 79-83.
5. **Rawat, U. B.**, Phadtare, S. U., Deshpande, V. V. & Rao, M. B. (1996) A novel xylose isomerase from *Neurospora crassa. Biotechnol. Lett.* **18**, 1267-1270.
6. **Rawat, U. B.** & Rao, M. B. (1996) Purification, kinetic characterization & involvement of tryptophan residue at the NADPH binding site of xylose reductase from *Neurospora crassa. Biochem. Biophys. Acta* **1293**, 222-230.
7. **Rawat, U. B.**, Bodhe, A. M, Deshpande, V. V. & Rao, M. B. (1993) D-xylose catabolizing enzymes in *Neurospora crassa* and their relationship to D-xylose fermentation. *Biotechnol. Lett.* **15**, 1173-1178.
8. **Rawat, U. B.** & Rao, M. B. (1998) Evidence for the presence of non-catalytic NADH-binding site in NADPH-linked xylose reductase and its implications for the enzyme activation (manuscript under preparation).
9. **Rawat, U. B.** and Rao, M. B. (1998) Role of Histidine and carboxyl group in the catalytic mechanism of xylose reductase from *Neurospora crassa*: Implications of a hydrophobic microenvironment (manuscript under preparation).

ABSTRACTS/PRESENTATIONS

1. **Rawat, U. B.,** Phadtare, S., Deshpande, V. & Rao, M. B. D-xylose catabolizing enzymes in *Neurospora crassa*: with special reference to xylose isomerase. Abstract accepted for Annual Conference of Association of Microbiologists of India, Dec' 1996.
2. Phadtare, S., **Rawat, U. B.** & Rao, M. B. Studies on xylitol dehydrogenase from *Neurospora crassa.* Abstract accepted for National Symposium on Current Trends in Biochemistry and Biotechnology of Fungi, India in Oct'1996.
3. **Rawat, U. B.** & Rao, M. B. Role of carboxyl group in the catalysis of xylose reductase from *Neurospora crassa.* Abstract accepted for Annual Meeting of Society of Biological Chemists, India in Nov'1996.
4. **Rawat, U. B.** & Rao, M. B. Involvement of tryptophan residue at the NADPH binding site of xylose reductase from *Neurospora crassa.* Poster presented at the XIV International Union of Biochemistry and Molecular Biology Congress at Bangalore, India in Sept' 1994.

CHAPTER 1

General Introduction

General Introduction

Necessity has been the mother of all inventions. This was proved true when the world faced its major oil crisis during the mid seventies. It was then that an interest was generated towards the utilization of lignocellulosic biomass for the production of fuel and chemical feedstock. Hemicellulose represents one third of the polysaccharide content of plant biomass. D-Xylose the predominant hemicellulosic sugar can be easily recovered from hemicellulose by acid hydrolysis than can D-glucose from cellulose (Jeffries, 1983). However, while the technology employing yeast and bacteria to produce chemicals from hexoses is well known, the ability of these organisms to ferment pentoses has been considered problematical. The efficient utilization of D-xylose is necessary both from economical and environmental point of view. Hence technologies are now emerging for the commercial exploitation of the hemi- cellulosic residues.

D-Xylose utilizing organisms

Bacteria– In the absence of oxygen, bacteria such as *Bacillus macerans*, *B. polymyxa*, *Aeromonas hydrophila*, *Aerobacter* sp., *Leuconostoc* sp., *Lactobacillus* sp. and *Klebsiella pneumoniae* (Rosenberg, 1980; Gong *et al*, 1983) readily convert xylose to a variety of products which include ethanol, butanediol, lactic acid, acetic acid and acetone. The product formed depends on the diverse metabolic pathways which operate under anaerobic fermentation and on the species, strains and the cultural conditions used. *Clostridium thermocellum* in coculture with *C. thermosaccharolytium* or *C. thermohydrosulfuricum* has been employed for the conversion of the polymer xylan to ethanol. *C. thermocellum* exhibits xylanase activity but is unable to utilize the D-xylose formed resulting in its accumulation; however, the presence of second organism such as *C. thermosaccharolyticum* or *C. thermohydrosulfuricum* ferments D-xylose to ethanol, lactic acid and acetic acid (Curtis, 1974; David & Wiesmeyer, 1970).

Yeasts– Generally yeasts are known to ferment hexoses mainly D-glucose to ethanol. Few yeasts strains such as *Pachysolen tannophilus, Candida shehatae, Pichia stipitis* and *Kluyveromyces marxianus* have been reported to ferment xylose to ethanol under semi-aerobic conditions (Jeffries, 1981; Watson *et al*, 1984; Schnider 1989). Majority of

yeasts belonging to *Candida, Brettanomyces, Saccharomyces, Schizosaccharomyces, Pachysolen* and *Kluyveromyces* lack the abilty to ferment D-xylose instead they utilize D-xylulose an isomer of D-xylose both oxidatively and fermentatively (Gong *et al,* 1983; Skoog & Hahn-Hagerdal, 1988).

Fungi– Several fungal species belonging to the genera *Fusarium, Rhizopus* (Perlman, 1950), *Monilia* (Gong *et al*, 1981a) and *Neurospora crassa* (Deshpande *et al*, 1986) have been reported with the ability to ferment D-xylose as well as D-glucose. Some potentially useful fungal strains belonging to *Monilia* sp. (Gong *et al*, 1981b), *N. crassa* (Rao *et al*, 1983; Deshpande *et al*, 1986) and *F. oxysporum* (Christakopoulos *et al*, 1989; Kumar *et al*, 1991a,b) also have the potential for the direct conversion of cellulose/hemicellulose to ethanol.

D-Xylose metabolism

Conversion of D-xylose to D-xylulose-5-phosphate

Once xylose is taken up by the cells it is first converted to D-xylulose and then subsequently phosphorylated by the action of the enzyme xylulokinase to yield D-xylulose-5-phosphate (Fig. 1). Bacteria, yeasts and fungi differ in their mode of conversion of D-xylose to D-xylulose. Bacteria generally achieve this conversion by employing the enzyme xylose isomerase (XI; EC 5.3.1.5) (Horecker, 1962; Chen, 1980); whereas, yeasts and fungi use a two step oxido-reduction reaction wherein D-xylose is first reduced to D-xylitol by NAD(P)H linked xylose reductase (XR; EC 1.1.1.21) which is further oxidized to D-xylulose by an NAD^+-linked xylitol dehydrogenase (XD; EC 1.1.1.9) (Chiang & Knight, 1960).

Metabolism of D-xylulose-5-phosphate

D-Xylulose-5-phosphate formed by the action of the enzyme xylulokinase is further metabolized *via* two major routes –

a) by the pentose phosphate pathway (PPP) which yields hexose phosphates or other intermediate compounds capable of entering the glycolytic pathway (Dickens, 1938).
b) by cleavage of pentoses with the formation of a three carbon unit and another two carbon unit compound using the enzyme phoshoketolase (Racker, 1948).

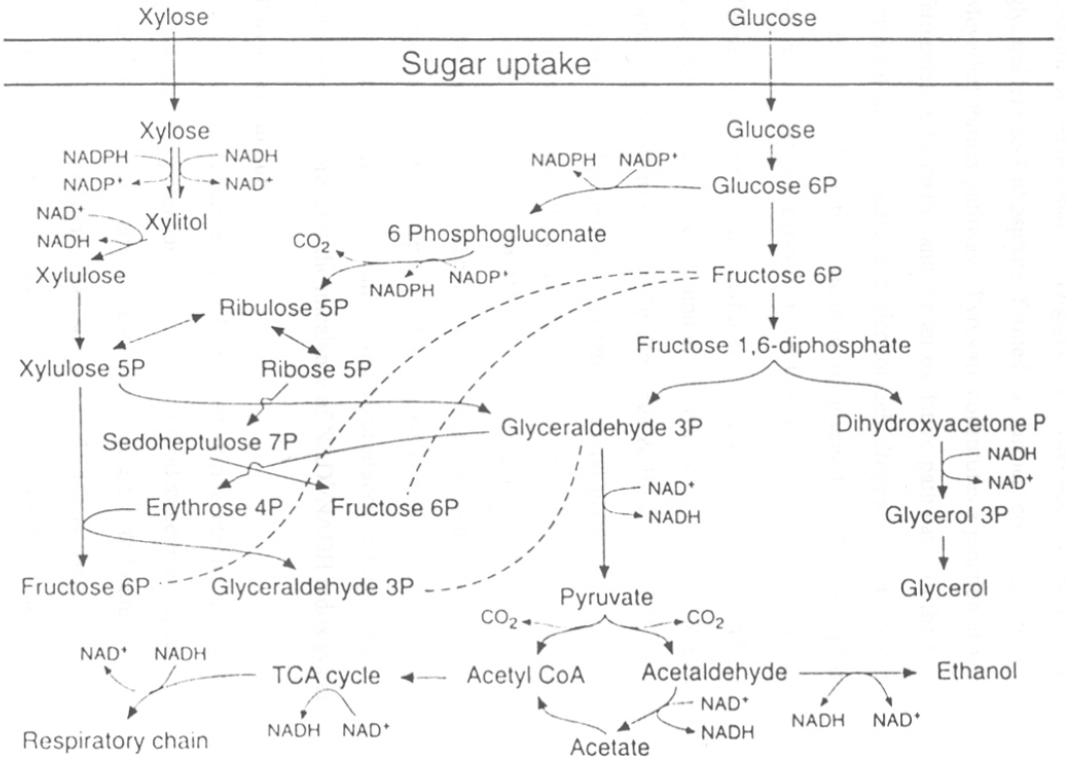

Fig. 1 Proposed pathway for the fermentation of xylose and glucose in the xylose fermenting yeasts

Pentose phosphate pathway- Xylulose-5-phosphate is metabolized *via* the pentose phosphate pathway wherein the enzymes transaldolase and transketolase convert D-xylulose-5-phosphate to D-glyceraldehyde-3-phosphate (Chakravorty *et al*, 1962). The glyceraldehyde-3-phosphate formed is further converted to pyruvate *via* the Embden-Meyerhof-Parnas pathway. Pyruvate constitutes a junction at which the cells may follow a fermentative pathway and /or an oxidative pathway. In the former pathway the enzymes pyruvate decarboxylase and alcohol dehydrogenase convert pyruvate to ethanol and the NADH formed in the oxidation of glyceraldehyde-3-phosphate is reoxidized. In the presence of oxygen, pyruvate is oxidized through the TCA cycle and the respiratory chain.

Phosphoketolase- In addition to the pentose phosphate pathway the enzyme phosphoketolase has been found in the yeasts. *R. graminis*, *R. glutinis*, *C. tropicalis* and *C. humicola* (Sgorbati *et al*, 1976; Ratledge & Botham, 1977). This enzyme catalyses the cleavage of D-xylulose-5-phosphate to acetyl phosphate and glyceraldehyde-3-phosphate which can further be converted to ethanol. The catalytic activity of phosphoketolase is inhibited by NADH, NADPH, ATP and acetyl CoA and is reduced in the presence of transketolase which competes with it for the same substrate. Girio *et al* (1989) have suggested that the phosphoketolase bypass is also essential because the reduction of acetyl phosphate to ethanol oxidizes NADH produced during the conversion of xylitol to D-xylulose which prevents the imbalance of NAD^+/NADH redox system.

Polyol production

Xylitol is formed as a byproduct during ethanol production from D-xylose. This polyalcohol has potential use as a natural food sweetener especially as a sugar substitute for diabetics and its use reduces dental caries (Culbert & Wang, 1986). The relative sweetness of xylitol (1.9) is higher than sucrose (1.4) and is almost equal to that of fructose (2.0). Hence xylitol is used as a sweetner in various food products like jams, jellies and chewing gums. Owing to its biotechnological applications various investigations have been carried out to maximize xylitol production. Gong *et al* (1981) have reported a mutant strain of *Candida* sp. which can efficiently convert D-xylose to xylitol with yields approaching 90 % of the theoretical . The yeasts *Candida* sp. B-22 and *C. guilliermondii* NRC 5578 have been found to be the best xylitol producers with yields upto 249 and 300 $g.L^{-1}$ respectively

(Meyrial *et al*, 1991). Recently, a recombinant *S. cerevisiae* strain transformed with the gene encoding XR of *P. stipitis* and requiring a cosubstrate for cofactor regeneration due to lack of XD activity gave a 95 % conversion of xylose to xylitol (Hallborn *et al* 1991). The oxygen supply has to be carefully regulated to maximize xylose reduction with minimal loss of xylitol to further metabolism. Barbosa *et al* (1988) reported that an increasing oxygen limitation enhanced xylitol production and decreased ethanol productivity. Industrially xylitol is produced from xylose by Ni^{2+}-catalyzed hydrogenation using gaseous hydrogen under high pressure at elevated temperature. However, the extensive purification steps involved render xylitol production by this route expensive (Hyvönen & Koivistoinen, 1983; Meyrial *et al*, 1991). In contrast, the microbiological conversion of xylose is a highly selective process.

Factors affecting D-xylose fermentation

pH and temperature

The optimum choice of initial pH depends on the type of media being fermented and the microbial strain carrying out the process. The initial pH values generally employed by various workers for fungal fermentation are within the range 5.0-6.0 (Rao *et al*, 1983; Kumar *et al*, 1991a). However, *Paecilomyces* sp. NF1 has a wide range of pH optima which varies from 2.2 to 7.0 (Wu *et al*, 1986). In case of yeasts the pH optima varies from 2.5-5.5 (du Preez *et al*, 1984; Dellweg, 1990). The pH range for the growth of thermophilic and mesophilic bacteria is in the range 4.5-8.0 with optima between 6.0-7.0. (Rosenberg, 1980)

The effect of temperature depends on the microbial strain employed for the fermentation. The optimum temperature for most pentose fermenting fungal species is between 28-37 °C (Wu *et al*, 1986; Deshpande *et al*, 1986). The yeasts have an optimum temperature range of 30-32 °C (Silinger *et al*, 1982; du Preez 1984). However, *P. stipitis* and *P. tannophilus* can grow at 37 °C and 37-42 °C respectively (Barnett *et al*, 1983; Kurtzman, 1984). The optimum temperature for the growth of thermophilic and mesophilic pentose fermenting bacteria ranges from 60-70 °C and 20-32 °C respectively (Wiegel, 1980; Banerjee, 1985).

Nutritional factors

Besides pH and temperature several nutritional factors exert a profound effect on D-xylose fermentations. The source of nitrogen supplied to the culture plays a crucial role in determining how the cell regulates its metabolic machinery. NH_4^+ salts have been found to stimulate the growth and enhance ethanol production by *S. cerevisiae*. Glucose-6-phosphate dehydrogenase is inhibited by NADPH; however, as the incorporation of NH_4^+ into α-keto glutarate requires NADPH, the addition of NH_4^+ salts decreases the intracellular level of NADPH, derepresses glucose-6-phosphate dehydrogenase, thereby increasing the activity of pentose phosphate pathway. It has been reported that the form of nitrogen supplied also affects the pentose phosphate pathway. When *C. utilis* was grown on nitrate the levels of glucose-6-phosphate dehydrogenase and transketolase were 2.5 times higher than when the cells were grown on a complex medium containing amino acids which may be due to a greater demand for NADPH in the nitrate grown cells. Studies performed by Banerjee (1985) indicated that $(NH_4)_2SO_4$ was the best nitrogen source for *K. pneumoniae*. This has been attributed to the fact that this compond also supplies sulfate ions which are essential for the synthesis of amino acids methionine and cysteine and the coenzyme lipoic acid, and CoA.

In *C. tropicalis* (Skoog & Hahn-Hagerdal, 1988), *P. tannophilus* (Dellweg *et al*, 1984) and *P. stipitis* (du Preez, 1986) the cell growth and ethanol production was enhanced in the presence of biotin and thiamine supplied *via* yeast extract. Trace elements such as Fe^{3+}, Zn^{2+}, Cu^{2+}, Mn^{2+} and growth factors like thiamine increased the growth of *P. anceps* (Perlman, 1949). Addition of low concentrations of lipids such as ergosterol have also been reported to increase ethanol production in *P. tannophilus* which has been attributed to increase in the ethanol tolerance of the organism (Dekker, 1986).

It has been reported by various workers that the presence of D-glucose retards D-xylose fermentation by *C. shehatae*, *P. stipitis* and *Pachysolen tannophilus* (Lee, 1992; Jeffries & Sreenath, 1988). This is in agreement with the finding that D-glucose partially represses the production of XR and XD. In *C. shehatae* the facilitated diffusion system involved in the transport of xylose is competitively inhibited by glucose while the proton symport is non-competitively inhibited (Bicho *et al*, 1988; Lucas & van Uden, 1986).

However, in case of *P. tannophilus* the addition of small amounts of D-glucose enhanced ethanol production (Jeffries *et al*, 1985) suggesting that the amount of pyruvate metabolized by the ethanol pathway was increased by glucose metabolism (Schneider, 1989).

Oxygen limitation

Oxygen supply is an important environmental factor affecting the rate and yield of ethanol production by yeasts and fungi. Oxygen is required for growth (Bruinenberg *et al*, 1984), mitochondrial function and to generate energy for xylose transport (Hofer & Nassar, 1987). Xylose fermentation is greatly enhanced by limited oxygen supply probably due to the role of oxygen as terminal electron acceptor which is required to relieve the partial redox imbalance generated by the action of the enzymes XR and XD catalyzing the initial two steps in xylose metabolism (Bruinenberg, 1984). A decrease in the specific oxygen uptake rate results in the inability of the electron transfer system to reoxidize the NADH produced by respiration and /or fermentation, as a consequence the intracellular levels of NADH increases which inhibits the NAD-linked XD activity further decreasing the ethanol yield (Rizzi *et al*, 1989a,b).

Metabolic inhibitors

As oxygen levels play a crucial role in the D-xylose fermentation several workers have studied the effect of metabolic inhibitors on the fermentation process. Azide can prevent contamination, block respiration and repress by-product formation. The use of this repiratory inhibitor increased the ethanol yield in *C. tropicalis* and *P. tannophilus* while a decrease in the production of xylitol was observed (Hahn-Hagerdal *et al*, 1985; Manderson & Newland, 1987). Presence of other inhibitors such as trichlorophenol and dinitrophenol also resulted in similar observations. In case of *F. oxysporum* the addition of azide, dinitrophenol and polyethylene glycol to the medium resulted in a shift in the product formation from acetate to ethanol (Singh *et al*, 1991). The respiratory inhibitor antimycinA improved the ethanol yield of *P. tannophilus* (Kotter & Ciriacy, 1993).

Inhibitors present in lignocellulosic hydrolysate

Acid hydrolysates of lignocellulosic materials used for ethanol production contain a number of metabolic inhibitors which include acetic acid formed from acetyl groups on

xylan, furfural produced from D-xylose, and tannins,terpenes and phenols. Inhibitory metal ions such as Cr^{3+}, Cu^{2+}, Fe^{3+} and Ni^{2+} may also be present probably as a result of corrosive metal parts of the apparatus used for the hydrolysates (Watson *et al*, 1984). The presence of these inhibitory factors markedly affect microbial growth and ethanol production. Resistance to inhibitors can be enhanced by acclimatization (involving exposure to increasing concentration of the hydrolysate) or by using isolates that have been recycled in the hydrolysate (Yu *et al* 1987; Parekh *et al*, 1988).

Ethanol tolerance

The fermentation rates in many bioprocesses depend on the cellular resistance of microbes to the end product. Various workers have investigated the influence of ethanol on the growth and metabolism of microorganisms (Ingram & Buttke, 1984; Ingram, 1986; van Uden, 1989). The studies revealed that the inhibition of xylose fermentation by ethanol may be due to a) changes in the cell membrane b) accumulation of acetaldehyde and acetate.

For many ethanologenic organisms the potency of alcohol as an inhibitor has been correlated with lipid solubility (Ingram & Buttke, 1984), implying that the hydrophobic site of the membrane is a prime target of ethanol inhibition. Among the various functions of the membrane, alcohol inhibits the uptake of various nutrients such as glucose, ammonium ions and amino acids; changes the physicochemical properties of the membrane and also causes leakage of various essential cofactors (Ingram, 1986; D'Amore & Stewart, 1987).

The oxidation of ethanol is accompanied by the formation of acetaldehyde and NADH which may lead to redox imbalance. At concentrations above 0.5 mM acetaldehyde reacts with the cellular amino groups and thus inhibits the cellular functions (Lieberthal *et al*, 1979). The enzyme acetaldehyde dehydrogenase catalyzes the conversion of acetaldehyde to acetate (Fig. 1) with the production of the coenzyme NADH thus amplifying the redox imbalance (Jones, 1989). The acetate formed is either excreted accumulated or oxidized *via* the TCA cycle. The accumulation of acetic acid results in the acidification of the cell which alters the proton gradient across the cell membrane. This results in an uncoupling of the energy production and transport systems which are dependent on proton gradient (Pampulha & Loureiro-Dias, 1989; Herrero *et al*, 1985).

Strain improvement for ethanol production

Genetic engineering

The bioconversion of D-xylose to ethanol by various yeasts and bacteria is subjected to various limiting factors such as conversion rate, low ethanol tolerance and product yield. Studies have been carried out by several workers for the selection of strains and their genetic improvement by using recombinant DNA technology. Recently the construction of yeasts with the ability to convert D-xylose to ethanol has been reported by various workers. So far the development of efficient recombinants was hampered because of the absence of a useful transformation system for the xylose fermenting yeasts. Few yeasts like *S. cerevisiae*, lack the ability to utilize D-xylose but are able to produce ethanol from D-xylulose a ketoisomer of D-xylose. (Skoog & Hahn-Hagerdal, 1988). Thus these species have the ability to produce ethanol if transformed with a gene coding for the enzyme that can convert xylose to xylulose and is expressed in yeast. However, most yeasts do not efficiently utilize D-xylose due to the cofactor (NADPH/NADH) regulation (Batt *et al*, 1986). Hence, attempts have been made to circumvent the oxido-reductive pathway that involves the enzymes XR and XD by transformation with a XI gene. This results in the direct cofactor free conversion of D-xylose to D-xylulose. The *E. coli* XI gene has been expressed in. *S. cerevisiae* and *Schizosaccharomyces pombe*. However, with the cloned strains low yields of ethanol 3% w/v were obtained which was attributed to the low expression of the XI gene (Chan *et al*, 1989). Further attempts were made for construction of an isomerase gene under the control of a highly active yeast promoter so as to improve its expression (Chan *et al*, 1989). Amore *et al* (1989) expressed XI genes from *Bacillus* and *Actinoplanes* in *S. cerevisiae* but was not catalytically active. In order to enhance ethanol production from xylose another approach employed cloning and expression of the xylose uptake gene from *E. coli* (Kurose *et al*, 1987) and the xylulokinase gene from *P. tannophilus* (Stevis *et al*, 1987) and *S. cerevisiae* (Ho & Chang, 1989). Recent reports on the cloning and expression of the genes coding for D-xylose catabolizing enzymes XR and XD have been summarized in Table 1.

Table. 1 Molecular cloning of xylose reductase and xylitol dehydrogenase

Parent	Host	Description	Reference
P. stipitis	*S. cerevisiae*	*P. stipitis* cDNA library was screened using antisera against *P. stipitis* XR and XD, respectively. The resulting cDNA clones served as probes for screening a *P. stipitis* genomic library. The XYL2 gene was isolated and actively expressed in *S. cerevisiae* tranformants. *S. cerevisiae* cells transformed with the plasmid, pRD1, containing XYL1 and XYL2 genes encoding XR and XD respectively were able to grow on xylose as the sole carbon source.	Kotter, 1990
P. stipitis	*S. cerevisiae*	The *P. stipitis* XYL1 gene was cloned and expressed in *S. cerevisiae*. The expression of XYL1 in *S. cerevisiae* increased nearly ten-fold when cloned under the strong promoter of yeast alcohol dehydrogenase gene (ADC1).	Chen, 1993
P. stipitis	*P. stipitis*	The *P. stipitis* XYL1 was inserted into an autonomous plasmid that *P. stipitis* maintains in multicopy. The plasmid pXOR with XYL1 insert or a control plasmid pJM6 without XYL1 was introduced into *P. stipitis*. When grown on xylose under aerobic conditions, the strain with pXOR had 1.8-fold higher XR activity than the control strain. However, the XR activity of the two strains grown on xylose were similar under oxygen limitation. When grown on glucose under aerobic and oxygen-limited conditions, the XR activity of the experimental strain was 10-fold higher than that of control. Ethanol production decreased with the introduction of pXOR compared to the control which may be attributed to nonspecific effects of the plasmid.	Dahn, 1996
P. stipitis	*S. cerevisiae*	*S. cerevisiae* was transformed with *P. stipitis* XYL1 and XYL2 genes. The genes were placed under the control of alcohol dehydrogenase 1(ADH1) and phospho glycerate kinase (PGK1) promoters in the yeast vector YEp24. On varying the vector constructions the ratio of XR by XD activity of the transformed *S. cerevisiae* varied from 17.5 to 0.06. A strain with an XR:XD ratio of 17.5 formed more xylitol; whereas, the strain with an XR:XD ratio of 0.06 formed more ethanol.	Walfridsson, 1997

Mutation studies

Various approaches using mutants have been developed to improve the performance of microbes for pentose utilization. Using UV mutagenesis, mutants have been selected for their ability to utilize xylose for ethanol production (Gong *et al*, 1981a; Mc Cracken, 1983). In these mutants the specific activity of XD and xylulokinase was high which enabled them to shift from xylitol to ethanol production. It has been reported that *P. tannophilus* produces and respires ethanol simultaneously. Lee *et al* (1986) obtained mutants unable to utilize ethanol as the carbon source which has been attributed to their deficiency in malate dehydrogenase, the enzyme involved in the metabolism of two carbon compound either by TCA or glyoxalate cycle. Presence of high content of D-glucose in lignocellulosic hydrolyzates has been shown to repress the utilization of D-xylose by microorganisms. Wedlock and Thorton (1989) reported that hexokinase is associated with the catabolite repression in *P. tannophilus* and *S. cerevisiae*. By selecting for resistance to 2-deoxyglucose Wedlock *et al* (1989) obtained hexokinase deficient mutants with the ability to ferment D-glucose and D-xylose simultaneously. Presence of nitrate in the growth media is known to induce elevated levels of pentose phosphate enzymes, glucose-6-phosphate dehydrogenase, xylose reductase and xylitol dehydrogenase (Bruinenberg *et al*, 1983). Therefore mutant strains with the ability to grow efficiently on nitrate should have higher levels of these enzymes. Xylitol is metabolized slowly by microorganisms; hence, mutant strains capable of more rapid growth on this substrate should be efficient xylose fermenters (Clark & Cronan, 1980). Jeffries (1984) selected *P. tannophilus* mutants by enriching and plating on nitrate-xylitol medium. These mutants exhibited both rapid growth on xylitol agar and higher specific ethanol productivity rates compared to the parent strains.

Protoplast fusion

The merging of genomes from disparate strains has been attempted using the technique of protoplast fusion to obtain strains with improved fermentative ability. The hybrids obtained by protoplast fusion between *S. cerevisiae* and *P. tannophilus* were able to produce and tolerate 10% ethanol (v/v) from molasses; however, the ethanol yields were lower (Wang & Wang, 1989). Gupthar (1992) attempted hybridization of *C. shehatae* and

P. stipitis with ethanol tolerant *S. cerevisiae* so as to obtain hybrids that would grow on xylose at high ethanol levels.

Present investigation

The present study deals with the various aspects of D-xylose catabolizing enzymes from *N. crassa.* The findings have been presented in the following five chapters

1] D-xylose catabolizing enzymes in *Neurospora crassa*

2] Purification and characterization of xylose reductase and xylitol dehydrogenase

3] Active site characterization of xylose reductase

4] Conformation and microenvironment at the active site of xylose reductase

5] Chaperone assisted folding of xylose reductase

CHAPTER 2

D-Xylose Catabolizing Enzymes in *Neurospora crassa*

Summary

The production of the D-xylose catabolizing enzymes XR and XD by *Neurospora crassa* was studied. The enzyme activities were induced by D-xylose under aerobic conditions. However, D-glucose was an effective repressor and low enzyme activities were obtained. The induction of NADPH-linked XR preceeded NADH-linked XR and the ratio of NADH to NADPH-linked XR activity displayed variation from 0.02 to 0.2 suggesting the presence of two separate enzymes. Aerobic conditions were required by *N. crassa* for cell growth but not for ethanol production. Maximum ethanol of 0.3 g/g of D-xylose was produced when shifted to semiaerobic condition where high NADH-linked XR and NAD-linked XD activities were observed.

The production of XI another D-xylose catabolizing enzyme was detected for the first time in the cell extracts of *N. crassa*. Of the various carbon sources tested, highest XI was obtained with D-xylose when *N. crassa* was grown for 72 h. The enzyme exhibited maximum activity at pH 8.0 and 70 °C and retained 100 % activity at 45 °C for 30 min at pH 8.0. XI was activated by 8 mM Mg^{2+} whereas 2 mM Co^{2+} afforded protection against inactivation by heat. The K_m for D-xylose was 10 mM and 22 mM for XI and XR respectively at 28 °C and pH 7.0. The present investigation revealed that the conversion of D-xylose to D-xylulose in *N. crassa* is mediated not only by the oxido-reductive pathway involving XR and XD, but also by an alternate pathway involving XI.

Introduction

Numerous fungi have been reported with the ability to degrade both cellulose and hemicellulose but only a few, especially *Fusarium* (Christakopoulos *et al*, 1990; Kumar *et al*, 1991a,b) and *Monilia* (Gong *et al*, 1981b) species exhibit both depolymerase and fermentative activity. Identification of fungal systems which would ferment cellulose and hemicellulose directly to ethanol is significant commerically but have never been seriously considered for developing process technology. This is understandable in view of the rapid fermentation of sugars by yeast. Generally, yeast are unable to metabolize cellulose and hemicellulose. From our laboratory we have shown the production of extracellular cellulase and xylanase activities and direct conversion of biomass to ethanol by *N. crassa* (Rao *et al*, 1983; Deshpande *et al*, 1986). The biotechnological implications of ethanol production by *N. crassa* prompted us to investigate the enzymes involved in xylose fermentation. Earlier it has been reported that bacteria yeast and fungi differ in their mode of conversion of D-xylose to D-xylulose, the first step in the conversion of xylose to ethanol. Bacteria generally achieve this conversion by employing the enzyme XI whereas, yeasts and fungi use a two step oxido-reduction reaction wherein D-xylose is first reduced to D-xylitol by NAD(P)H-linked XR which is further oxidized to D-xylulose by an NAD^+-linked XD. The presence of XI has been reported in the bacteria *Streptomyces violaceoruber* (Callens *et al*, 1986), *Escherichia coli* (Schellenberg *et al*, 1984) and *Lactobacillus pentosus* (Lokman *et al*, 1991). The oxido-reductases have been detected in the cell extracts of the yeasts *Candida albicans* (Viega *et al*, 1960), *Candida utilis* (Batt *et al*, 1986), *Pichia stipitis* (Verduyn *et al*, 1985), *Cephalosporium chrysogenum* (Birken & Pisano, 1976), *Pachysolen tannophilus* (Smile & Bolen, 1982) and *Fusarium oxysporum* (Suikho *et al*, 1983). The enzymes have been reported to be induced by D-xylose under aerobic conditions (Bolen & Detroy, 1985; Neirinck *et al*, 1984)

The present study reports the presence of D-xylose catabolizing enzymes namely xylose reductase, xylitol dehydrogenase and xylose isomerase in *N. crassa*. The correlationship between the enzyme activities and ethanol production by *N. crassa* has also been discussed.

Materials and Methods

Materials

N. crassa NCIM 870 was obtained from National Collection of Industrial Microorganisms; Pune, India. The organism was routinely maintained on MGYP slants containing malt extract (0.3%), glucose (1%), yeast extract (0.3%) and peptone (0.5%).

Methods

Fermentation conditions

The organism was grown aerobically by inoculating a heavy spore suspension in a 500 ml flask containing 50 ml of medium ($Na_3C_6H_5O_7$, 0.26 %; KH_2PO_4, 0.5 %; NH_4NO_3, 0.2 %; $MgSO_4$, 0.01 %; $CaCl_2$, 0.008 % w/v and trace elements) (Rhodes *et al,* 1971) and 2 % D-xylose as the carbon source. The flasks were shaken at 220 rpm (24 h) and were transferred to aerobic, semi-aerobic and anaerobic conditions at 28 °C. Under the aerobic conditions the organism was grown in 1 L flask containing 200 ml medium and 2% D-xylose at 220 rpm. The experiments under semi-aerobic condition were carried out by transferring the contents of the growth flask to a 100 ml stoppered flask with a capillary opening at the top containing 2% D-xylose. For anaerobic conditions the contents of the growth flask were transferred aseptically to 100 ml flask with 2% D-xylose. The flasks were gassed with nitrogen before and after the transfer of the cell mass. Ethanol was determined by gas chromatography as described earlier (Rao *et al*, 1983).

Preparation of cell extract

The *N. crassa* cell mass was suspended in 0.05 M sodium phosphate buffer pH 7.2, containing 2 mM each of β-mercaptoethanol, phenylmethylsulphonylfluoride and $MgCl_2$. The cells were sonicated for 10 min and the cell debris was removed by centrifugation (15,000 g at 4 °C for 20 min). The supernatant was used for studies on XR and XD. The cell extract for studies on XI was obtained as described above except that the cell mass was suspended in 0.05 M sodium phosphate buffer pH 7.2, with 0.5 M $CoCl_2$ and 1 mM $MgCl_2$.

Enzyme assays and protein determination

Xylose reductase– The assay mixture (1 ml) contained 0.1 M sodium phosphate buffer pH 6.3, 0.05 mM NADPH or NADH and an appropriate amount of cell extract. The reaction was started by the addition of D-xylose to a final concentration of 0.2 M and A_{340} decrease was measured.

Xylitol dehydrogenase– The assay mixture (1 ml) contained 0.05 M Tris/HCl buffer pH 8.2, 0.01 M $MgCl_2$, 0.2 mM NAD^+ and an appropriate amount of cell extract. The reaction was started by the addition of xylitol to a final concentration of 0.2 M and the A_{340} increase was measured.

XR and XD activities were assayed spectrophotometrically at 30 °C. The reaction rates were linearly proportional to the amount of extract added and were corrected for endogenous NAD(P)H consumption or production. Enzyme units are defined as *n*moles of nicotinamide nucleotide reduced or oxidized min^{-1}.

Xylose isomerase– The reaction mixture contained 0.05 M Tris/HCl buffer pH 8.0, 5 mM xylose, 5 mM $MgSO_4$, 0.5 mM $CoCl_2$ and suitably diluted enzyme. The mixture was incubated at 60 °C for 20 min. The reaction was stopped with the addition of 2 ml of 0.5 M perchloric acid and the xylulose formed was measured by the cysteine carbazole method (Dische & Borenfreund, 1951).

Glucose isomerase– The enzyme activity was measured under the conditions described for XI except that 0.02 M glucose was used as the substrate. After incubation at 60 °C for 20 min, the reaction was stopped by adding 2.0 ml of 0.5 M perchloric acid. The produced fructose was assayed by the cysteine carbazole method.

One unit of xylose/glucose isomerase is defined as the amount of enzyme producing 1 μmole of D-xylulose or D-fructose per min respectively under the assay conditions.

Specific activities have been expressed as units mg^{-1} of protein. The protein concentrations of the oxido-reductases and isomerases were determined by the method of Lowry *et al*, (1951) and Bradford (1976) respectively, using bovine serum albumin as the standard.

Results and Discussion

Production of XR and XD

XR and XD activities in *N. crassa* were induced by D-xylose whereas D-glucose was an effective repressor. The similar extent of repression (90%) of XR and XD by glucose suggests that these enzymes may be under co-ordinate control. In case of *P. stipitis* a similar type of glucose repression was observed whereas in *Pachysolen tannophilus* XD was repressed to a greater extent than XR (Bicho *et al*, 1988). The inducibility of these enzymes by xylose has also been reported in *F. oxysporum* (Singh & Schugerl, 1992) and *S. cerevisiae* (Batt *et al*, 1986).

Table 1. Induction of XR and XD activities in *N. crassa*

Carbon source	Enzyme Activities (U. mg^{-1})		
	XR		XD
	NADPH-linked	NADH-linked	NAD-linked
Xylose (2 %)	585	120	620
Xylose (1 %) + Glucose (1 %)	99	18	99
Glucose (2 %)	54	10	62

N.crassa was grown under aerobic condition for 24 h and then shifted to semiaerobic condition (48h). The enzyme activities were determined as described under materials and methods.

During the growth under aerobic conditions the specific activity of NADPH-linked XR and NAD-linked XD increased more rapidly and at an earlier stage compared to the NADH-linked enzyme (Fig. 1). The specific activity of NAD-linked XD (520 $U.mg^{-1}$) was considerably higher compared to the NADP-linked activity (12 $U.mg^{-1}$). The traces of NADP-linked XD activity may be attributed to the affinity of XD for the coenzyme (reverse reaction) (Bruinenberg *et al*, 1984). When aerobically grown cultures of *N. crassa* were shifted to semiaerobic stage, NADPH-linked XR remained constant whereas there was an

increase in NADH-linked XR and NAD-linked XD activities (Fig. 2). The enzyme levels under anaerobic conditions were similar to those observed under semiaerobic condition.

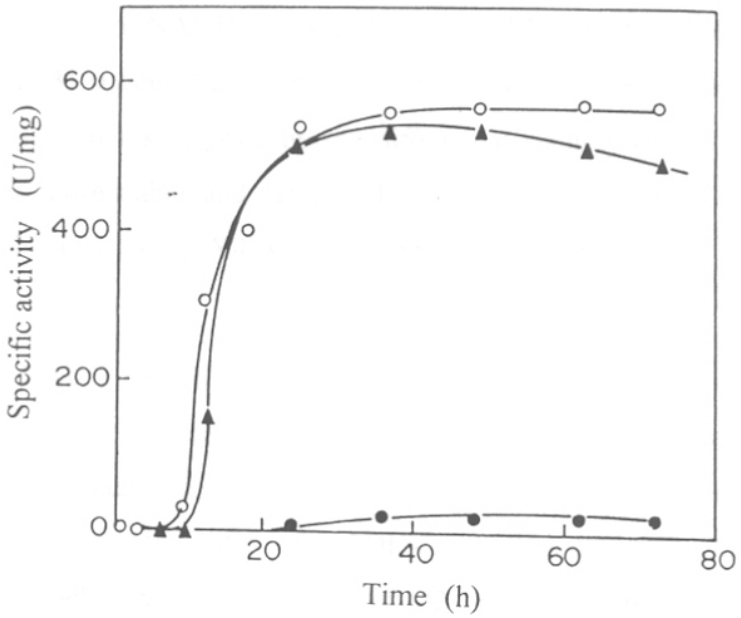

Fig. 1 **Levels of D-xylose catabolizing enzymes under aerobic conditions.** NADH- (•), NADPH- (o) linked XR and NAD-linked XD (▲) activities .

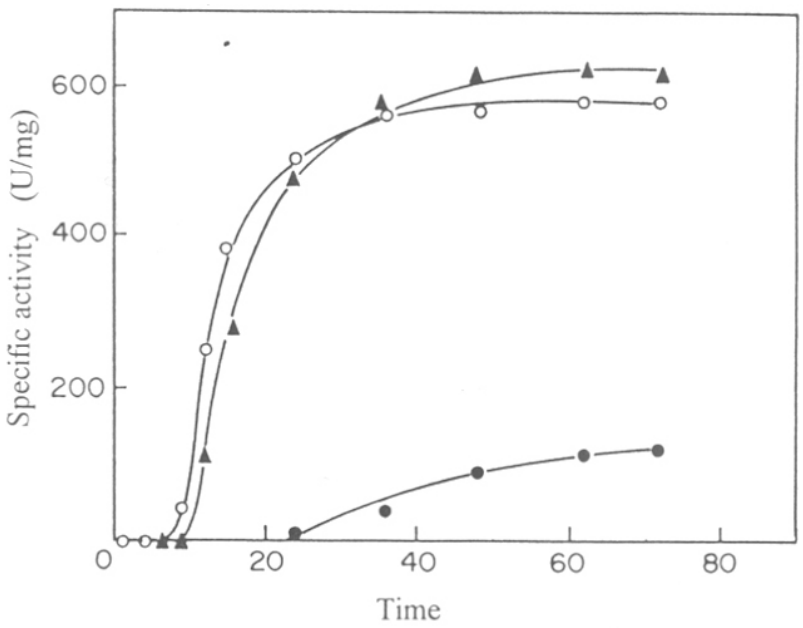

Fig. 2 **Levels of D-xylose catabolizing enzymes under semiaerobic conditions** NADH- (•) , NADPH- (o) linked XR and NAD-linked XD (▲) activities.

Presence of NADPH- and NADH-linked XR in *N. crassa*

As shown in Fig. 1 & 2 the induction of NADPH-linked XR preceeded NADH-linked XR. The ratio of NADH- by NADPH-linked XR activities displayed variation from 0.02 to 0.2 (Fig. 3) suggesting the presence of two different enzymes in *N. crassa*. This observation was further supported by the differential stability of the enzymes. NADPH-linked XR was more stable and retained 100 and 70% activity at 4 °C (24h) and 40 °C (2 min) whereas NADH-linked XR lost 80 and 100% of its activity at 4 °C and 40 °C respectively.

Correlation of NADH-/NADPH-linked XR to ethanol production

Aerobic batch cultures of *N. crassa* did not produce ethanol from D-xylose. However, under semiaerobic conditions an increase in ethanol production was observed which was dependent on the ratio of NADH-/NADPH-linked XR. Maximum ethanol of 6 $g.L^{-1}$ was obtained at a maximum ratio of 0.2 (Fig. 3). These results revealed that the NADH-linked XR probably plays a crucial role in the conversion of D-xylose to ethanol by *N. crassa* which may be attributed to its ability to prevent the imbalance of NAD^+/NADH redox system generated by the action of the enzymes XR and XD.

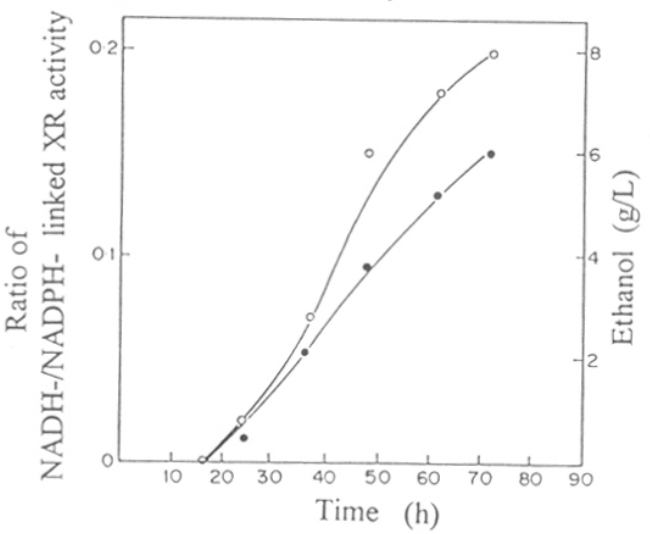

Fig. 3 **Correlation between NADH-/NADPH-linked XR activity and ethanol production by *N. crassa* under semiaerobic conditions.**
NADH-/NADPH-linked XR activity (o) and ethanol (•).

Production of XI

The presence of XI, another D-xylose catabolizing enzyme from *N. crassa* was studied. As shown in Fig. 4, the intracellular XI activity increased during the exponential phase of the organism and reached a maximum (0.014 $U.mg^{-1}$) at 72 h. The effect of different carbon sources on the production of XI revealed that maximum enzyme activity was obtained in the presence of 1% D-xylose (Table 2). XI activity was not detected in the extracellular culture filtrates of *N. crassa*.

Table 2. Effect of carbon sources on XI production

Carbon Source (1%)	Activity (%)	Carbon Source (1%)	Activity (%)
Xylose	100	Lactose	11
Xylan	36	Wheatbran*	7
Glucose	20	Glycerol	5

* concentration of wheatbran (5%)

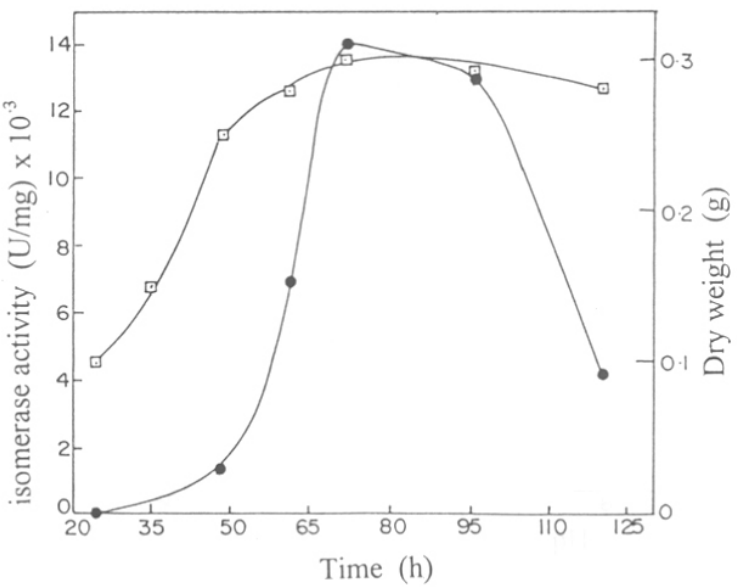

Fig. 4 **Induction of XI by *N. crassa* under aerobic conditions**
Growth curve (□) XI activity (•)

Characterization of XI

Influence of pH and temperature on the activity and stability of XI

The pH optimum of XI was determined by assaying the enzyme activity in presence of 0.1 M citrate buffer (pH 5-6), phosphate buffer (pH 7-8) and carbonate buffer (pH 9-10). It was observed that XI exhibited maximum activity at pH 8.0 (Fig. 5). To check the pH stability of XI, the enzyme was incubated with the above buffers at 37 °C for 30 min. The enzyme was found to be most stable at pH 8.0 and showed 50 and 70% loss in activity at pH 9 and 10 respectively. At pH 5-7, XI retained 45-55% of its activity (Fig. 5).

The optimum temperature of XI was determined by assaying the enzyme activity in the range 37-90 °C and was found to be 70 °C. The thermostability was examined by incubating the enzyme at various temperatures. It was observed that the enzyme retained 100% activity when incubated at 45 °C and showed 85% activity in the temperature range of 50-80 °C. However, the enzyme was rapidly inactivated beyond 80 °C (Fig. 6).

The enzymatic response of the *N. crassa* XI to temperature and pH was almost the same as that reported for bacterial enzymes (Kitada *et al*, 1989; Kwon *et al*, 1987). However, it showed optimum pH and temperature higher than that observed in case of the thermophilic fungus *Malbranchea pulchella* var: *sulfurea* TMD-8 (Bannerjee *et al*, 1994).

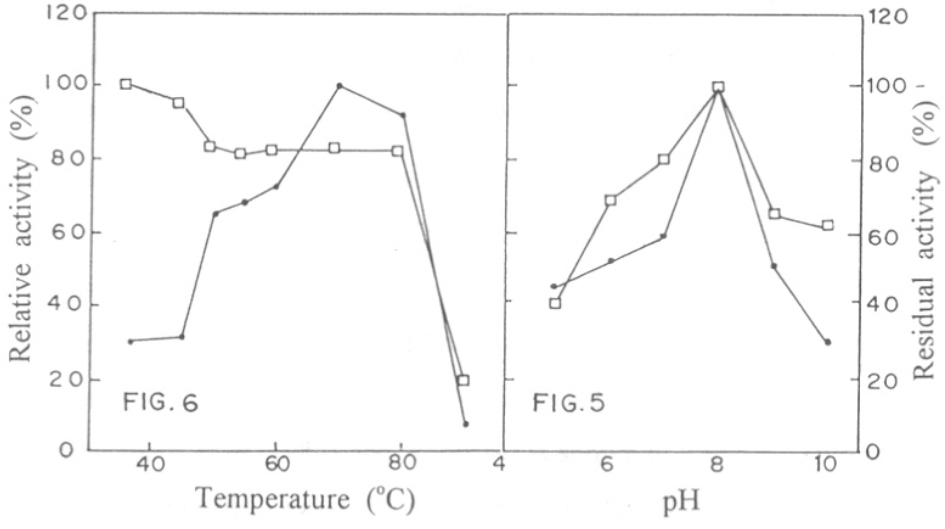

Fig. 5

Optimum pH and pH stability
Activity (□) and stability (•) of XI

Fig. 6

Optimum temperature and thermal stability
Activity (•) and stability (□) of XI

Influence of metal ions

The metal free XI obtained after dialysis against EDTA showed negligible activity when assayed in 0.05 M MOPS (3-[N-morpholino]propanesulfonic acid) buffer. Maximum activation of XI (70%) was observed with Mg^{2+} (8 mM); whereas, Co^{2+} (2 mM) afforded protection (80%) against heat inactivation. Similar roles of Mg^{2+} and Co^{2+} in bacterial isomerases have been attributed to their ability to stabilize the quaternary structure of the enzyme (Kasumi *et al*, 1982; Callens *et al,* 1988; 1986).

Substrate specificity

XI from *N. crassa* was unable to utilize D-ribose and L-arabinose at a concentration of 5 mM each; however, in the presence of D-xylose (5 mM) maximum activity (0.014 $U.mg^{-1}$) was observed. The enzyme also showed activity towards D-glucose (0.0135 $U.mg^{-1}$) as observed in many bacterial isomerases (Kitada *et al*, 1989). Thus maximum isomerization was observed with the substrates having hydroxyl groups at carbon 3 & 4 in the equatorial position as in glucose and xylose.

Affinity of XI and XR for D-xylose

The Michaelis constant (K_m) for the substrate D-xylose was determined by incorporating varying concentrations of the substrate (2-50 mM) for XI and (10-100 mM) XR in the reaction mixture. The data obtained was analyzed by Lineweaver-Burk plots and K_m values of 10 and 22 mM were obtained for XI and XR respectively.

Correlation between activity of D-xylose catabolizing enzymes and ethanol production

The maximum activity of NADPH-linked XR and NAD-linked XD was observed in 24 h grown culture of *N. crassa* (Fig. 1 & 2). However, ethanol was obtained at 72 h which was attributed to the increasing levels of NADH-linked XR activity (Fig. 3). The correlation between the ratio of NADH/NADPH-linked XR and ethanol yield by yeast species (Bruinenberg *et al*, 1984) and *N. crassa* is shown in Table 3. Higher ethanol yield (5.0 $g.L^{-1}$) was obtained in yeasts when the ratio of NADH-/NADPH-linked XR activity was greater than 0.4. However, in the case of *N. crassa* maximum ethanol was obtained at a ratio of 0.2. NADH-linked XR has been shown to play a crucial role in the production of ethanol probably by preventing the imbalance of the NAD^+/NADH redox system thus

allowing the efficient conversion of xylose to ethanol (Bruinenberg *et al*, 1984). Inspite of lower levels of NADH-linked XR activity in *N. crassa* a quantitative yield of alcohol comparable to that of other yeasts was produced. Hence, studies were undertaken to investigate the presence of an alternate xylose utilizing pathway in *N. crassa.*

Table 3. Correlation between the ratio of NADH-/NADPH-linked XR and alcohol production in yeasts and *N. crassa*

Organism	CBS No.	NADH/NADPH-linked XR	Ethanol g. L^{-1}
Candida tenuis	615	0.02	< 0.3
Candida tenuis	4113/4285	0.50	> 5.0
Candida shehatae	5813	0.40	> 5.0
Pichia segobiensis	6857	0.60	> 5.0
Neurospora crassa		0.20	> 5.0

In various bacteria such as *Streptomyces violaceoruber* (Callens *et al*, 1986), *Aerobacter aerogenes* (Mortlock & Wood, 1964), *Escherichia coli* (Schellenberg *et al*, 1984) and *Lactobacillus pentosus* (Lokman *et al*, 1991) the enzyme XI catalyses the isomerization of D-xylose to D-xylulose, the first step in the major pathway of conversion of D-xylose to ethanol. Although the oxido-reductive pathway involving XR and XD seems to be an obligatory pathway for xylose metabolism in yeasts and fungi, the presence of an inducible XI has also been reported in the yeast *C. utilis* (Tomoyeda *et al*, 1964) and the thermophilic fungus *Malbranchea pulchella* var: *sulfurea* TMD-8 (Bannerjee *et al*, 1994). The present study indicated for the first time presence of XI in the cell extracts of the fungus *N. crassa.* It was observed that the level of XI activity was maximum at 72 h (Fig. 4) when maximum ethanol production was observed (Fig. 3) indicating that XI plays a key role in the efficient conversion of xylose to ethanol by *N. crassa.* The higher affinity of XI for D-xylose (K_m 10 mM) than that of XR (K_m 22 mM) further supported this observation. Altogether the present investigations revealed that the conversion of D-xylose to D-

xylulose in *N. crassa* is mediated not only by the oxido-reductive pathway involving XR and XD, but also by an alternate pathway involving XI as illustrated below.

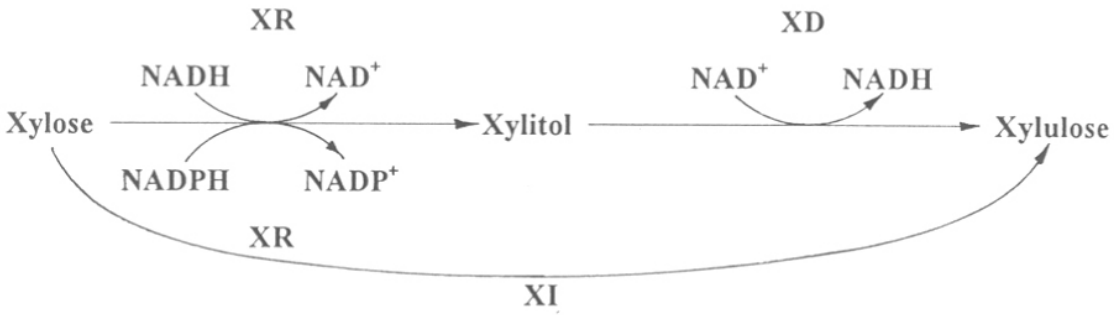

Fig.7 Pathway for the conversion of D-xylose to D-xylulose in *N. crassa*

CHAPTER 3

Purification and Characterization of Xylose Reductase & Xylitol Dehydrogenase

Summary

The purification and characterization of the enzymes XR and XD involved in the conversion of xylose to ethanol by *N. crassa* has been described. XR was purified to homogeneity by ammonium sulfate fractionation, DEAE-Cellulose, CM-Sephadex and Sephacryl S-200 chromatography with 90 fold purification and specific activity of 73 $U.mg^{-1}$. The molecular mass of the native enzyme when determined by Sephacryl S-200 gel filtration was found to be 60 kDa whereas on SDS-PAGE a value of 29 kDa was obtained indicating the presence of two similar subunits. XR with an isoelectric point of 8.3 was most active at pH 6.3 and 40 °C. It exhibited maximum stability at pH 5.5 and 4 °C. The initial velocity and product inhibition studies revealed that *N. crassa* XR follows an *iso-ordered bi bi* mechanism. The enzyme was highly specific to NADPH as the coenzyme and no activity was observed in the presence of NADH alone. However, in the presence of NADPH the non phosphorylated coenzyme enhanced the XR activity. Fluorescence studies revealed the presence of a single NADH and NADPH binding site per dimer of XR with K_{NADPH} and K_{NADH} values of 0.85 and 19 μM respectively.

XD was purified to homogeneity by fractional ammonium sulfate precipitation followed by column chromatography on DEAE-Cellulose, Sephacryl S-200 and β-NAD agarose with 81.5 fold purification and specific activity of 15 $U.mg^{-1}$. The purified enzyme had a native molecular mass of 87 kDa (gel filtration) and was composed of two similar subunits of molecular mass 43.6 kDa (SDS-PAGE). XD exhibited maximum activity at pH 8.4 and 28 °C. It was most stable at pH 7.0 and 4 °C. The enzyme was activated by Mg^{2+} and stabilized by Ca^{2+}, Mg^{2+} and Mn^{2+}. It was found to be highly specific to NAD^+ (K_m 0.7 mM) as the coenzyme and exhibited maximum activity in the presence of the sugar alcohols xylitol (K_m 28.5 mM) and sorbitol (K_m 100 mM).

Introduction

XR catalyzes the conversion of D-xylose to D-xylitol and is a key enzyme involved in the fermentation of xylose to ethanol. The enzyme also has potential application in the synthesis of xylitol an acariogenic non-caloric sweetener used in many food products (Emodi *et al*, 1978; Kulbe *et al,* 1972). XR's from several yeasts have been purified, some of their properties are listed in (Table 1). The enzymes are monomers or dimers with an optimum pH in the range 6-7. They have been reported to be specific to NADPH or NADH as the coenzyme (Ditzelmuller, 1985); however, its dual coenzyme specificity has also been reported by Verduyn *et al* (1985). It has been suggested that the NADH-linked XR plays a crucial role in anaerobic fermentation of xylose to ethanol by preventing the imbalance of NAD^+/NADH redox system generated by the action of the enzymes XR and XD (Bruinenberg *et al*, 1984).

XD catalyzes the oxidation of xylitol to D-xylulose which is phosphorylated to form D-xylulose-5-phosphate, a key intermediate in the reaction pathway involved in the conversion of xylose to ethanol. The action of XD results in the production of the reducing equivalents NADH. The non-phosphorylated coenzyme has to be oxidized either by respiration or by NADH-linked XR; otherwise, its accumulation results in the inhibition of XD further decreasing the ethanol yield (Slininger *et al,* 1985). Inspite of the importance of XD in xylose metabolism there are few reports on its purification and characterization which may be attributed to its labile nature. Some of the characteristics of XD from various sources have been listed in Table 2. The enzymes are specific to NAD^+ as the coenzyme and have an optimum pH in the range 8-10 while their molecular masses range from 82 to 300 kDa.

The present study describes the purification and characterization of XR and XD, the oxido-reductases catalyzing the initial crucial reactions in the major pathway for the conversion of xylose to ethanol by the fungus *N. crassa*.

Table. 1 Physicochemical properties of xylose reductases

Organism	K_m (xylose) (mM) varied coenzyme		K_m (μM)		Molecular mass (kDa)		Optimum pH	Reference
	NADH	NADPH	NADH	NADPH	Gel filtration	SDS-PAGE		
P. tannophilus	N.A.	162	N.A.	59	35-40	35-40	7.0	Ditzelmuller, 1984
P. stipitis	42	42	21	9	65 +4	34 +2	6.0	Verduyn, 1985
P. stipitis	97	67	40	3.2	63	32	6.0	Rizzi, 1988
Cryptococcus lactativorus	8.6	9.1	170	6	62	33	6.9	Kise, 1988
N.crassa *	N.A.	22	N.A.	9	60	29	6.3	Rawat & Rao, 1996
C. tenuis	87	72	25.4	4.8	48	43	6.0	Neuhauser, 1997

N.A. Not applicable

* Present study

Table. 2 Physicochemical properties of xylitol dehydrogenases

Organism	K_m (xylitol) mM	Molecular mass (kDa)		Optimum		Reference
		Gel filtration	SDS-PAGE	pH	Temp °C	
Cephalosporium chrysogenus	N.D.	300	29	9-10	N.D.	Birken & Pisano 1976
P. tannophilus	10	120	40	9.1-10	55	Morimoto *et al*, 1986
P. stipitis	26	63	32	9	35	Rizzi *et al*, 1989
C. shehatae	18.5	82	40	8.6	N.D.	Yang *et al*, 1990
N. crassa *	28.5	87	43.6	8.4	28	Phadtare *et al*, 1996

N.D. Not determined

* Present study

Materials and Methods

Materials

NADPH (reduced nicotinamide adenine dinucleotide phosphate), NADH (reduced nicotinamide adenine dinucleotide), NAD^+ (oxidized nicotinamide adenine dinucleotide), xylitol, D-xylose, DTT (dithiothreitol), β-ME (mercaptoethanol), PMSF (phenylmethyl sulphonylfluoride), DEAE-Cellulose, CM-Sephadex, β-NAD agarose, protein molecular weight markers for SDS & gel filtration were purchased from Sigma Chemical Co.,USA; Sephacryl S-200 from Pharmacia, Sweden; and Centricon-50 concentrators from Amicon. All chemicals used were of analytical grade.

Methods

Enzyme assays and Protein determination

XR activity was determined as described earlier by Verduyn *et al* (1985) with some modifications. The assay mixture (1 ml) contained 0.05 M sodium phosphate buffer pH 6.3, 0.15 mM NADPH and an appropriate amount of enzyme. The reaction was started by the addition of D-xylose (final concentration 0.25 M) and monitored spectrophotometrically by the decrease in NADPH absorption at 340 nm.

XD activity was determined spectrophotometrically as described by Chakravorty *et al*, (1962). The assay mixture (1 ml) contained 0.1 M Tris-HCl buffer, pH 8.4, 0.01 M $MgCl_2$, 0.01 M NAD^+ and an appropriate amount of enzyme sample. The reaction was started by the addition of xylitol to a final concentration of 0.1 M and the increase in absorbance at 340 nm was measured.

Enzyme units are defined as μmoles of nicotinamide nucleotide reduced or oxidized per min. Protein concentration has been determined by the method of Bradford (1976) using bovine serum albumin as a standard.

Purification of XR

All steps were performed at 4 °C unless stated otherwise. Concentration and desalting of the protein was carried out using Centricon-50 concentrators. The *N. crassa* cell mass (10 g wet wt.) was thawed and suspended in chilled 0.05 M sodium phosphate

buffer pH 7.5, containing 2 mM each of PMSF and EDTA. Cell extracts were prepared by disrupting the cells by sonication followed by centrifugation for 20 min at 4 °C and 15 000 g to remove the cell debris. The supernatant was then subjected to ammonium sulfate fractionation (65-75% saturation). The precipitate obtained was dissolved in 0.02 M sodium phosphate buffer, pH 7.5, and after dialysis against the same buffer was applied to DEAE-Cellulose column (25 x 3.5 cm) equilibrated with 0.02 M sodium phosphate buffer, pH 7.5. XR did not bind to the column and was eluted with the equilibration buffer at a flow rate of 15 $ml.h^{-1}$. The pooled XR fractions were concentrated and dialysed against 0.02 M sodium phosphate buffer, pH 6.0. This was further subjected to chromatography on CM-Sephadex column (20 x 2 cm) equilibrated with 0.02 M sodium phosphate buffer, pH 6.0. The adsorbed proteins were eluted with a linear gradient of NaCl (0-0.5 M) in equilibration buffer, pH 6.0. Fractions containing XR activity were pooled, desalted and concentrated. The enzyme was further purified by gel filtration using Sephacryl S-200 column (90 x 2.0 cm) which was equilibrated with 0.05 M sodium phosphate buffer pH 7.5 and then eluted with the same buffer at a flow rate of 12 $ml.h^{-1}$. Fractions containing enzyme activity were pooled concentrated and stored at 4 °C. The purity of the enzyme was determined by 10% SDS-PAGE according to the method of Laemmli (1970) followed by silver staining (Helmut *et al*, 1987).

Purification of XD

The cell extract for the purification of XD was obtained as described for XR except that the cell mass was suspended in 0.05 M sodium phosphate buffer pH 7.2, containing 2 mM each of DTT and $MgCl_2$ (Buffer A). The supernatant obtained was subjected to fractional ammonium sulfate precipitation (55-65%) and the precipitate obtained was dissolved and dialyzed against 0.02 M Buffer A. The dialysate was subjected to DEAE-Cellulose column chromatography at pH 7.2. The enzyme adsorbed on the column was then eluted with 0.02-0.3 M buffer gradient. The fractions showing XD activity were pooled, concentrated and dialyzed using Centricon-50 microconcentrators. The enzyme was further purified by gel filtration on Sephacryl S-200 column equilibrated with 0.05 M Buffer A. XD fractions from this column were further subjected to affinity purification on β-NAD agarose column equilibrated with 0.01 M Buffer A and 3.4 mM NAD^+. The bound enzyme was

eluted with 7 mM NAD^+. The fractions were tested for XD activity and protein. The purity was checked by SDS-PAGE (Laemmli, 1970) followed by Coomassie Blue staining.

Characterization of XR and XD

Determination of molecular mass

The molecular mass of the enzymes were determined by gel-filtration on Sephacryl S-200 according to the method of Andrews (1965). Alcohol dehydrogenase (150 kDa), bovine serum albumin (66 kDa), ovalbumin (45 kDa) and carbonic anhydrase (29 kDa) were used as the standard molecular markers. The subunit molecular mass was determined by 10% SDS-PAGE according to the method of Laemmli (1970). Bovine serum albumin (66 kDa), ovalbumin (45 kDa), glyceraldehyde-3-phosphate dehydrogenase (36 kDa) and carbonic anhydrase (29 kDa) were used as standard marker proteins.

Influence of pH on activity and stability

The optimum pH of the enzymes were determined by estimating the enzyme activity at different pH values ranging from pH 4-9. 0.1 M of citrate buffer (pH 4-6), sodium phosphate buffer (pH 6-8) and carbonate buffer (pH 9) were used. The effect of pH on stability was studied by incubating the enzyme with above buffers at 4 °C for 4 h.

Influence of temperature on activity and stability

The optimum temperature of XR and XD was determined by assaying at different temperatures ranging from 10-50 °C. The thermal stability was examined by determining the residual enzyme activities on incubation at varying temperatures (4-50 °C) for 4h.

Determination of isoelectric point

The isoelectric point (pI) of XR was determined by the U tube method (Pawar *et al*, 1988) using the ampholines in the pH range 3-10.

Kinetic studies

The various kinetic parameters of XR were determined in the forward NADPH-dependent D-xylose reduction reaction at pH 6.3. The substrate D-xylose was varied over a concentration range while the coenzyme NADPH was employed at a constant saturating concentration. The primary and secondary plots of bisubstrate reaction kinetics as described by Segel (1976) were used to determine the various kinetic constants. Discrimination

between different plausible kinetic mechanisms was performed by product inhibition studies (Segel, 1976). By using different concentrations of xylitol or $NADP^+$ as inhibitors, a series of kinetic measurements were performed at saturating concentrations of D-xylose or NADPH with the other substrate NADPH or D-xylose being varied. To determine the K_m and V_{max} of XD for the substrates xylitol, sorbitol and NAD^+ the enzyme was assayed in the presence of varying concentrations of the respective substrates. The data obtained was analyzed by Lineweaver-Burk plots.

Determination of coenzyme binding to XR

Fluorescence studies were performed to investigate the binding of the coenzymes NADPH and NADH to XR. The enzyme (0.14 μM) in 0.05 M sodium phosphate buffer pH 6.3, was titrated with varying concentrations of NADPH and the formation of XR-NADPH complex was followed by progressive quenching of protein fluorescence at 326 nm with the excitation wavelength fixed at 295 nm. The data obtained was evaluated according to the equation

$$L_o/\alpha = K_d/1\text{-}\alpha + E_o$$

where α is the fractional saturation and is equal to ratio of ΔF by ΔF_{max} , ΔF is the amount of fluorescence reduction at a specified coenzyme concentration and ΔF_{max} is the limiting amount of fluorescence at fully saturating concentration, L_o is the total concentration of the ligand, E_o is the total active site concentration and K_d is the dissociation constant. A plot of $1/(1\text{-}\alpha)$ versus L_o/α yields a straight line with x-axis intercept equal to concentration of the binding sites and reciprocal equal to binding constant (Stinson & Holbrook, 1973)

To investigate the binding of NADH to XR the enzyme (1 μM) in sodium phosphate buffer pH 6.3, was titrated with varying concentrations of the non-phosphorylated coenzyme. Assuming various values of n the concentrations of bound and free NADH were derived according to the equation

$$S_b = n\,[E_t]\,(\Delta F/\Delta F_\infty) \quad \text{and} \quad S_f = [S]\text{-}[S_b]$$

where $[E_t]$ and n denote the concentration and number of binding sites of the enzyme respectively, S_b and S_f are the concentrations of bound and free NADH respectively. ΔF is the amount of fluorescence change at the substrate concentration [S] and ΔF_∞ is the fluorescence change when all enzyme molecules are complexed with substrate. The ratios of

bound [NADH] /free [NADH] were plotted against bound [NADH] and the K_{NADH} (slope^{-1}) values were determined. The horizontal axis intercept yielded the values for $n[Et]$. The values of n and K_{NADH} were chosen which gave the best fit to the $n[E_t]+K_d$ value obtained by the intersection of the tangent of the initial part of F vs $[S]$ curve and its asymptote (Lefevre *et al*, 1980).

Results and Discussions

Studies on xylose reductase

Purification of XR

XR from *N. crassa* was purified to homogenity as analyzed by SDS-PAGE (Fig. 1) with 90 fold purification and specific activity of 73 $U.mg^{-1}$ (Table 3).

Table 3. Purification of XR from *N. crassa*

Purification step	Total Protein (mg)	Activity ($U. mL^{-1}$)	Specific activity ($U.mg^{-1}$)	Fold purification
Crude extract	3315	2652	0.8	1.0
Freezing and thawing	1390	2593	1.9	2.3
$(NH_4)_2SO_4$ fractionation	210	2254	10.7	13.3
DEAE-Cellulose	60.2	1272	21.0	27.0
CM-Sephadex	1.8	100.8	42.7	70.0
Sephacryl S-200	0.47	34.47	72.5	90.0

Physicochemical properties of XR

The M_r of XR when determined on Sephacryl S-200 gel filtration was found to be 60 kDa whereas on SDS-PAGE a value of 29 kDa was obtained indicating the presence of two similar subunits. XR with a pI of 8.3 exhibited maximum activity at pH 6.3 and 40 ^0C. It was most stable at pH 5.5 and 4 ^0C. The enzyme exhibited a broad specificity with aldoses and maximum activity was observed in presence of D-xylose (Table 4).

Table 4. Substrate specificity of XR from *N. crassa*

Substrate (0.25 M)	Relative activity (%)	Substrate (0.25 M)	Relative activity (%)
D-Xylose	100	D-Galactose	26
D-Glucose	14	D-Ribose	22

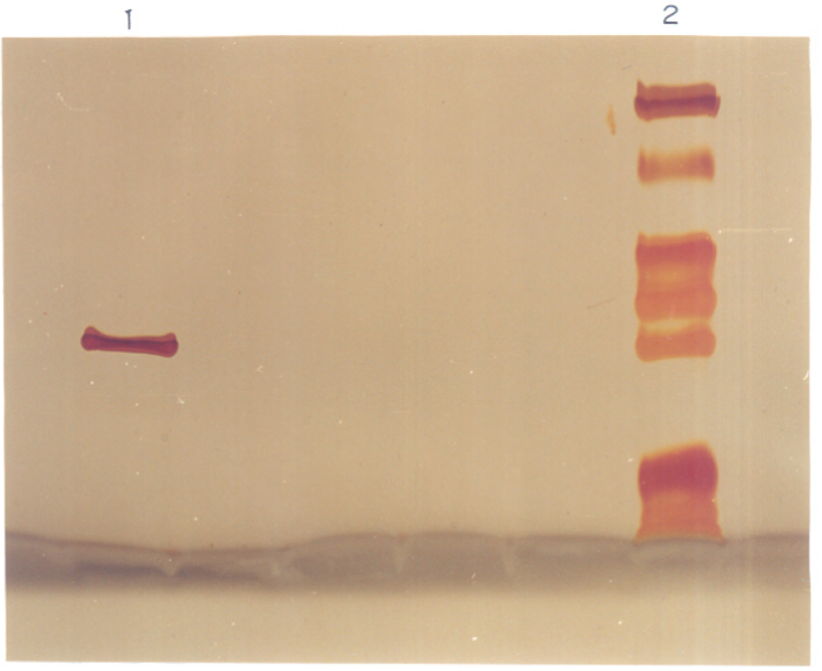

Fig. 1 **SDS-PAGE of purified XR**

Lane 1 XD (2.0 μg) and Lane 2 with the following protein standards: bovine albumin (66 kDa), ovalbumin (45 kDa), glyceradehyde-3-phosphate dehydrogenase (36 kDa), carbonic anhydrase (29 kDa), trypsinogen (24 kDa), trypsin inhibitor (20.1 kDa) and α-lactalbumin(14.2 kDa).

Initial velocity studies

Initial velocity measurements were performed to evaluate the reaction mechanism of XR in *N. crassa*. Fig. 2A shows a double reciprocal plot of initial velocity when the substrate D-xylose was varied over a range of concentration while the coenzyme NADPH was employed at a constant saturating concentration. The secondary plots (Fig. 2B) were used to determine the various kinetic constants which are tabulated in Table. 6 Unlike observed in case of XR from *P. stipitis* (Rizzi *et al*, 1986), a parallel initial velocity pattern was obtained which is consistent with a Ping Pong mechanism. Critical analysis of the initial velocity data is essential since kinetic mechanisms other than Ping Pong also yield double reciprocal plots of initial velocity which are a series of parallel lines (Segel, 1976).

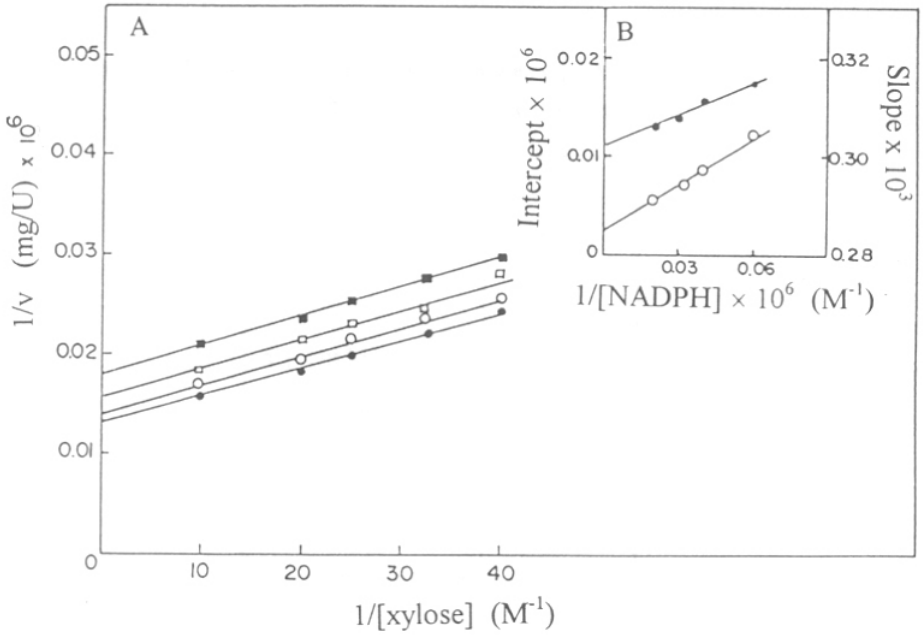

Fig. 2 **Primary and Secondary plots of the bisubtrate reaction kinetics for XR reaction.**

A. XR reaction with xylose varied at NADPH concentrations 50 μM (•), 31 μM (o), 25 μM (□) and 16 μM (■).

B. Secondary plots of primary intercepts (•) and slopes (o) of Fig. 2A versus reciprocal NADPH concentration.

In case of a sequential mechanism where B is the variable substrate and A is the changing fixed substrate

$$1/v = K_B/V_{max}(1+K_{iA}/[A])1/[B] + 1/V_{max}(1+K_A/[A]) \quad (1)$$

whereas, for a Ping pong mechanism

$$1/v = K_B/V_{max}(1/[B]) + 1/V_{max}(1+K_A/[A]) \quad (2)$$

where V_{max} is the maximum velocity, K_{iA} is the dissociation constant of E-NADPH complex, K_A and K_B represent Michaelis constants for NADPH and xylose and A and B are concentrations of NADPH and xylose. When $K_{iA} << K_A$ then (eq. 1) approximates (eq. 2) and the lines appear parallel. Thus the intersection of the lines at a point depends on the ratio of $K_{iA} : K_A$. In case of XR values of 1.05 and 9 μM were obtained for K_{iA} and K_A. Hence the possibility that the reaction mechanism of XR may be sequential was considered.

Table 6. Kinetic parameters of *N.crassa* XR as determined by bisubstrate reaction kinetics.

V_{max} (U.mg^{-1})	77
k_{cat} (min^{-1})	4638
K_A (μM)	9
K_B (mM)	22
K_{iA} (μM)	1.05
k_1 (μM^{-1}min^{-1})	515
k_2 (min^{-1})	541

Product inhibition studies

Inhibition studies were performed to investigate the order of substrate binding to XR. The data obtained was analyzed according to (Segel,1976). Inhibition of the enzyme by $NADP^+$ with saturating levels of NADPH for variable concentration of xylose was studied. $NADP^+$ was found to be uncompetitive with xylose and a value of 90 μM was obtained for K_{iq} the iso-inhibition constant. The inhibition pattern revealed that *N. crassa* XR may follow an i*so-ordered bi bi* mechanism or *iso-theorell-chance* mechanism.

Further to distinguish between these two mechanisms, inhibition studies were carried out using xylitol as an inhibitor with varying concentrations of xylose at saturating levels of NADPH (Fig. 3A). A non competitive inhibition pattern was observed which is in accordance to an *iso-ordered bi bi mechanism*. The inhibition constant K_{ip} obtained from the plots of intercepts of (Fig. 3A) against xylitol concentration (Fig. 3B) was 0.385 M. Altogether the initial velocity and product inhibition studies revealed that XR from *N. crassa* follows an *iso-ordered bi bi mechanism* as depicted below, where E, A, B, P, Q, and E' represent XR, NADPH, xylose, xylitol, $NADP^+$ and the isomerized enzyme respectively.

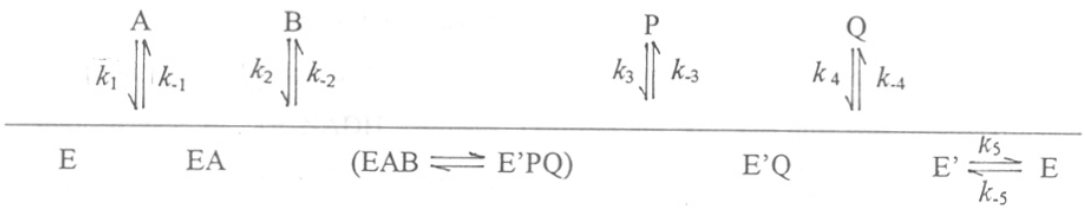

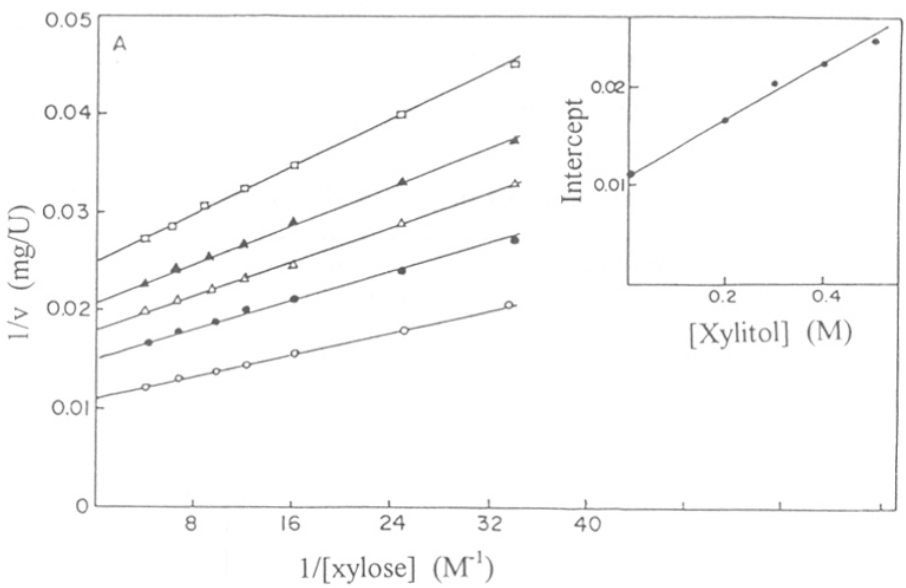

Fig. 3 **Inhibition of XR by xylitol**

A. Concentration of xylitol 0 M (o) , 0.2 M(•) , 0.3 M (Δ) , 0.4 M (▲) and 0.5 M (□) at saturating level of NADPH (0.25 mM) and varying concentrations of xylose.

B. Secondary plot (o) of primary intercepts of Fig.3A versus xylitol concentration.

Coenzyme specificity of XR

The purified XR from *N. crassa* was found to be specific to NADPH as the coenzyme and no activity was observed in the presence of the nonphosphorylated coenzyme NADH. This observation was further confirmed by fluorescence studies. Addition of the coenzymes NADPH or NADH to XR (0.25 μM) at a concentration of 0.15 mM each, quenched the tryptophanyl fluorescence (λ_{ex} 295 nm; λ_{em} 326 nm) indicating the formation of the respective E-coenzyme complexes. Further, addition of xylose (0.2 M) to XR-NADPH complex (λ_{ex} 295 nm; λ_{em} 326 nm) resulted in an increase in the fluorescence intensity indicating that xylose was in part reduced by the bound NADPH with a concomitant generation of $NADP^+$ form of the complex. In contrast, no change in the fluorescence of XR-NADH complex (λ_{ex} 295 nm; λ_{em} 326 nm) was observed indicating that XR lacked the ability to reduce xylose in the presence of the nonphosphorylated coenzyme. The effect of the coenzyme NADH on the XR reaction in the presence of the saturating concentration of NADPH (90 μM) was investigated. As shown in Table 7, an increase in XR activity was observed with an increase in NADH concentration with maximum activity at the coenzyme concentration of 180 μM.

Table 7. Increase in XR activity at varying concentrations of NADH

Ratio of NADPH to NADH	Increase in XR activity (%)
1:0	Nil
1:0.5	22
1:1	38
1:1.5	58
1:2.0	75

In order to investigate whether NADH was oxidized by XR in the presence of NADPH, activity measurements were performed in the presence of equimolar concentrations (0.15 mM each) of NADH and NADPH. It was observed that on completion of the reaction a residual absorbance of 0.92 was obtained indicating that the activity observed may be due to complete/partial oxidation of NADH or NADPH. To shed more light on this observation the above reaction mixture was passed through Centricon-3 microconcentrators to separate the XR (retentate) from the reaction products (filtrate). Further, the pH of the filtrate was adjusted to 8.4 and the change in its absorbance was measured on addition of *N. crassa* NAD-linked XD (1.5 μM) and the substrate xylitol (final concentration 0.1 M). It was observed that the presence of dehydrogenase failed to influence the coenzyme absorbance at 340 nm indicating that the enhanced activity of NADPH-linked XR may not be due to NADH taking part in the reaction. The oxidation of NADH by XR would have resulted in the formation of NAD^+ which would have been reduced by XD resulting in an increase in absorbance at 340 nm. Altogether the results revealed that NADH does not take part in the reaction but its binding to XR possibly induces a conformational change that results in realigning of the catalytic groups at the active site further increasing the enzyme activity.

Coenzyme binding studies

Binding of NADPH to XR– XR was titrated with varying concentrations of NADPH and the formation of E-NADPH complex was followed by progressive quenching of protein fluorescence (λ_{ex} 295 nm; λ_{em} 326 nm). Saturation was reached at coenzyme concentration of 3.5-8 μM (Fig. 4A). The quenching data was analyzed by the Stinson & Holbrook (1973) and values of 0.85 and 0.12 μM were obtained for the dissociation constant (K_d) of XR-NADPH complex and concentration of NADPH binding sites (E_o) (Fig. 4B). These studies revealed the presence of a single NADPH binding site/ dimer of XR.

Binding of NADH to XR– Addition of incremental amounts of NADH led to a progressive decrease in XR fluorescence (λ_{ex} 295 nm; λ_{em} 326 nm) (Fig. 5A). The fluorescence data was analyzed by the Scatchard plot (Fig. 5B) which revealed the presence of a single binding site per molecule of XR with a dissociation constant of 19 μM.

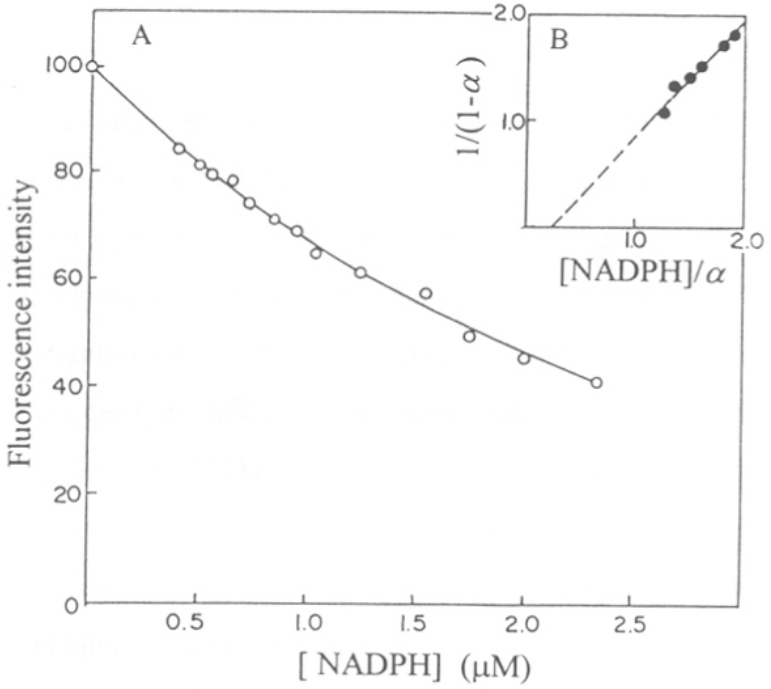

Fig. 4 **Titration of XR with NADPH**

A. Tryptophanyl fluorescence of XR at varying concentrations of NADPH

B. Plot of 1/1-α versus NADPH/α

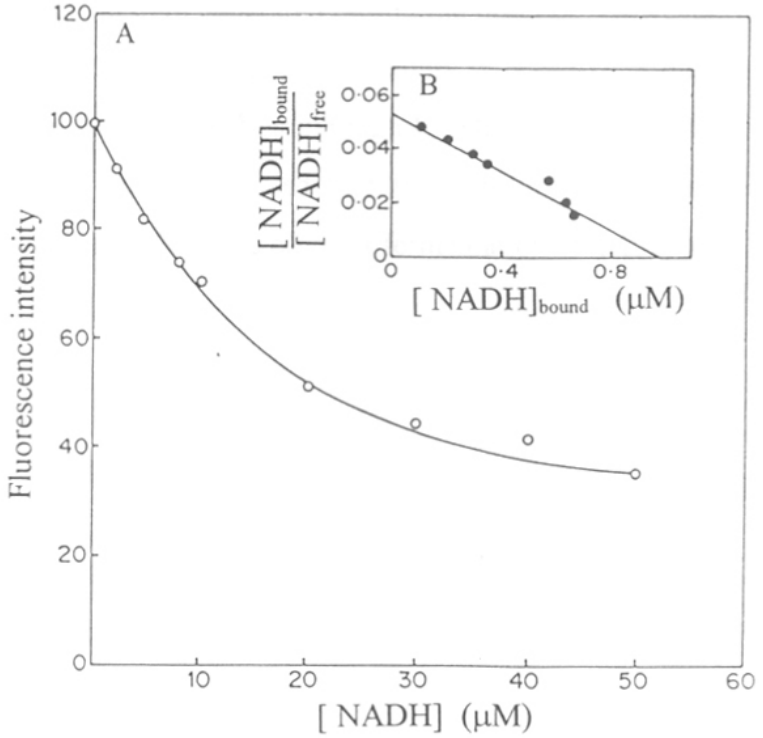

Fig. 5 **Binding of NADH to XR**

A. Quenching of tryptophanyl fluorescence of XR (λ_{ex} 295 nm; λ_{em} 326 nm) at varying concentrations of NADH.

B. Plot of bound [NADH]/free [NADH] *versus* bound [NADH]

Earlier it has been reported that XR may be specific to NADPH and /or NADH as the coenzyme. Ditzelmuller (1985) reported the presence of two XR's in *P. tannophilus* one with coenzyme specificity to NADPH and the other specific to NADH. The XR from *P. stipitis* has been shown to exhibit a dual coenzyme specificity (Verduyn *et al*, 1985). The present investigations revealed that the purified XR from *N. crassa* was highly specific to NADPH as the coenzyme and failed to exhibit activity in the presence of NADH alone. However, in the presence of NADPH the non-phosphorylated coenzyme enhanced the XR activity. This observation along with the fluorescence data supported the notion that the inability of XR to catalyze NADH dependent reduction of xylose cannot be attributed to the absence of NADH binding site on XR.

It was of particular interest to assign a physiological role to the increase in XR activity by NADH. Bruinenberg *et al* (1984) reported that under oxygen limited conditions NADH-linked XR plays a crucial role in xylose fermentation by preventing the imbalance of NAD^+/NADH redox system generated during the process. However, it was observed that in spite of low levels of NADH-linked XR activity in *N.crassa*, a quantitative yield of alcohol comparable to that of yeasts possessing high NADH-linked XR activity was produced (*refer chapter 2*). These studies revealed that the NADH-mediated increase of XR reaction possibly plays a crucial role in the efficient fermentation of xylose by *N. crassa*.

Studies on xylitol dehydrogenase

Purification of XD

XD was purified to homogenity as analyzed by SDS-PAGE (Fig. 6) with 81.5 fold purification and specific activity of 15.5 $U.mg^{-1}$ (Table 8).

Table 8. Purification of XD from *N. crassa*

Purification step	Total protein (mg)	Total units	Specific activity ($U. mg^{-1}$)	Fold purification
Cell-free extract	115	22	0.19	1.0
$(NH_4)_2SO_4$ fractionation	16	18	1.125	5.9
DEAE-Cellulose	6.0	14	2.33	12.2
Sephacryl S-200	3.2	11	3.4	17.8
β-NAD agarose	0.138	2.14	15.5	81.5

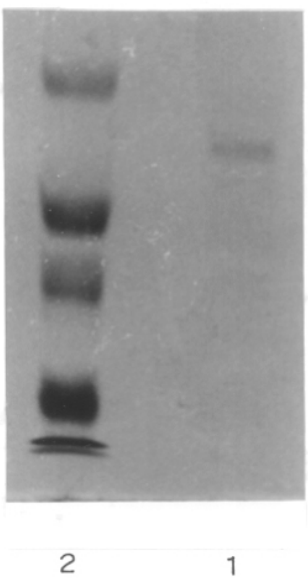

Fig. 6 **SDS-PAGE of purified XD**

Lane 1 XD (2.0 µg) and Lane 2 with the following protein standards: bovine albumin (66 kDa), ovalbumin (45 kDa), glyceradehyde-3-phosphate dehydrogenase (36 kDa), carbonic anhydrase (29 kDa).

Physicochemical properties of XD

Molecular mass

The molecular mass of XD was estimated to be 87 kDa by gel filtration. It showed a single band of molecular mass 43.6 kDa on SDS-PAGE (Fig. 6) in the absence as well as in the presence of β-mercaptoethanol indicating the absence of interchain disulfide bonds. Hence, *N. crassa* XD is a dimer with two similar subunits of molecular mass 43.6 kDa.

Influence of pH and temperature on activity and stability

N. crassa XD showed maximum activity at pH 8.4. It was most stable at neutral pH, 4 °C for 4h and was completely inactivated at pH 4.0 (Fig. 7). The activity and stability profile of *N. crassa* XD at different temperatures is shown in Fig. 8. It was observed that the enzyme was most active at 28 °C and maximally stable at 4 °C above which the stability gradually decreased. XR retained more than 60% activity when incubated at room temperature for 4h whereas 50 % of its activity was lost within 15 days at 4 ° C. Freezing and thawing of the enzyme solution resulted in complete inactivation of the enzyme.

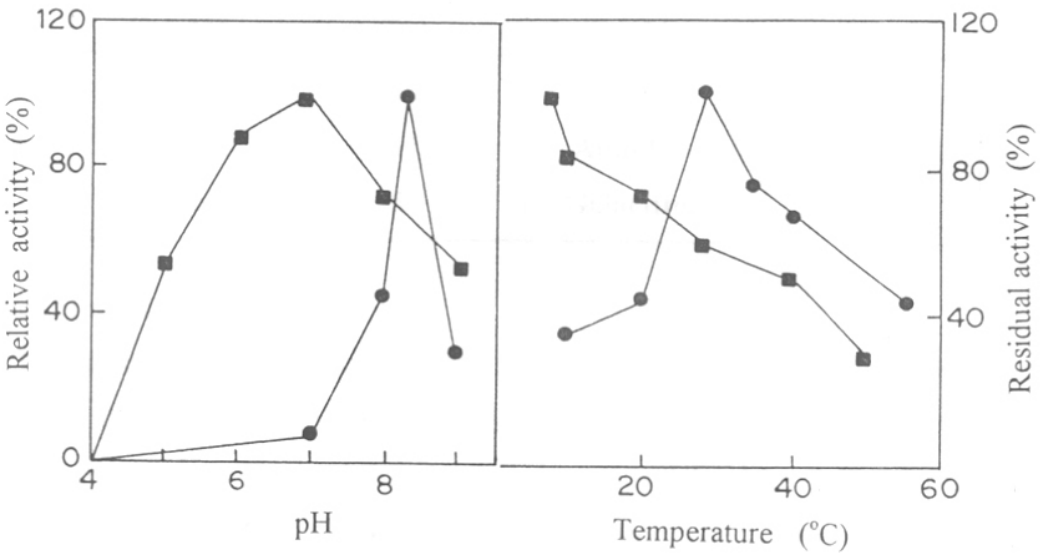

Fig. 7

Optimum pH and pH stability
Activity (•) and stability (■)

Fig. 8

Optimum temp and thermal stability
Activity (•) and stability (▪)

Coenzyme and substrate specificity

The *N. crassa* XD was found to be highly specific to NAD^+ as the coenzyme. It exhibited maximum activity in the presence of the sugar alcohols xylitol and sorbitol but no activity was observed in the presence of galactitol, mannitol and allitol (Table 8). These observations revealed that XD was most active on substrates having the configuration I and II (Fig. 9) wherein the secondary alcohol group and its hydroxyl must be in the L-configuration with respect to the primary alcohol group. In addition, the hydroxyl at C4 must also possess an L configuration; whereas, the hydroxyl on C3 may be either in the D or the L form. Similar type of coenzyme and substrate specificities have been reported for enzymes from *Rhodotorula* (Soumalainen *et al,* 1989), *P. stipitis* (Rizzi *et al*, 1989) and *P. tannophilus* (Morimoto *et al*, 1986); however, the enzyme from *C. utilis* (Scher & Horecker, 1966) was active in presence of polyols possessing configurations I-III

Table 8. Substrate specificity of XD

Substrate (0.1 M)	Relative activity (%)	Substrate (0.1 M)	Relative activity (%)
Xylitol	100	**Mannitol**	0
Sorbitol	95	**Allitol**	0
Ribitol	58	**Galactitol**	0

Influence of metal ions

The effect of various metal ions (10 mM) on the XD stability was determined by preincubating the enzyme with various metal ions for 1 h at 28 °C and then determining the residual activity. It was observed that the enzyme was stabilized by Ca^{2+} and Mg^{2+}, while the metal ions such as Co^{2+}, Cu^{2+} and Fe^{3+} had an inhibitory effect. The metal-ion free XD obtained on dialysis against EDTA (5 mM) had negligible activity which was restored by the addition of Mg^{2+} ions (2mM).

Kinetic studies

Michaelis constant for the coenzyme NAD^+ (K_m 0.7 mM) and the substrates xylitol (K_m 28.5 mM) and sorbitol (K_m 100 mM) were obtained from Lineweaver-Burk plots and

are tabulated in Table 9. It was observed that the affinity of *N. crassa* XD for NAD^+ (K_m 0.7 mM) was much lower than that reported from *C. shehatae* (K_m 0.1-0.24 mM) (Yang & Jeffries, 1990). Comparison of the K_m values for the substrates xylitol and sorbitol revealed that the enzyme has higher affinity for xylitol. The K_m for xylitol (K_m 28.5 mM) was higher than that of XD from *C. shehatae* (K_m 18.5 mM) (Yang & Jeffries, 1990) and much lower than that of *P. tannophilus* (K_m 70 mM) (Morimoto *et al*, 1986). The higher affinity of XD for xylitol probably plays a crucial role in the efficient conversion of xylose to ethanol by *N. crassa*, where 0.3 g of ethanol is produced per g of D-xylose which is a high efficiency of ethanol production. In case of *P. tannophilus* (Morimoto *et al*, 1986) the low affinity of XD for xylitol leads to accumulation of xylitol thus decreasing the efficiency of ethanol production.

Table 9. Kinetic constants of XD from *N. crassa*

Substrate	K_m (mM)	V_{max} (U. mg^{-1})
Xylitol	28.5	17
Sorbitol	100	30
NAD^+	0.7	21

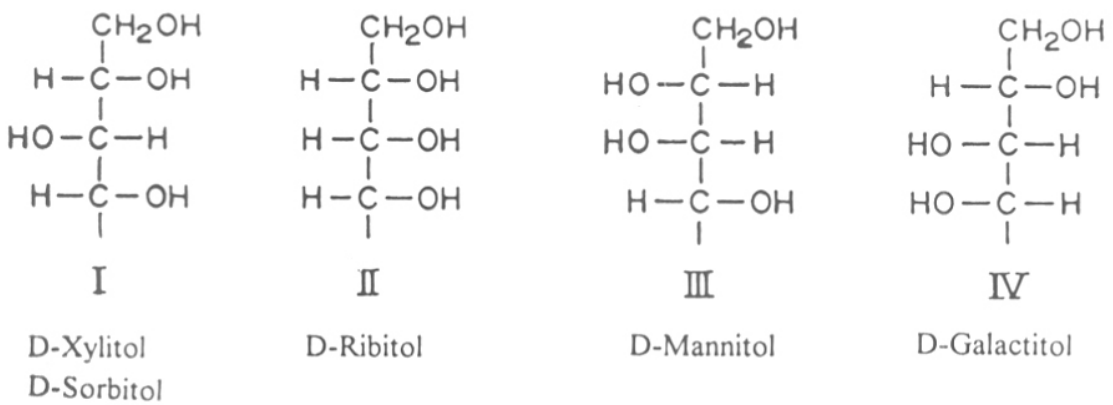

Fig. 11 Configuration of acyclic polyols

CHAPTER 4

Active Site Characterization of Xylose Reductase

Summary

The importance of various functional groups for the activity of XR was investigated by the use of chemical modifiers with restricted amino acid specificity, under the conditions which did not alter the enzyme conformation. XR was inactivated by *N*-bromo succinimide (NBS) suggesting the presence of an essential Trp in XR. NADPH afforded 90% protection against inactivation. Kinetic analysis of the NBS modified XR and acrylamide quenching studies confirmed the involvement of Trp at the coenzyme binding site of XR. Chemical modification studies in combination with ANS binding experiments revealed that the Trp residues of XR are essential for maintaining the hydrophobicity of the NADPH binding site and thus permit its efficient binding to the enzyme.

The inhibition of XR by the modifiers *p*-hydroxymercury benzoate (PHMB), *o*-phthalaldehyde (OPTA) and 2,4,6-trinitrobenzenesulfonic acid (TNBS) indicated the presence of essential Cys and Lys residues at the active site of XR. Double inhibition studies showed that Cys residues involved in the reaction with PHMB (SH_I) and OPTA (SH_{II}) are distinctly different and essential for XR activity. Experimental evidence has been presented that serves to implicate that SH_I located in a hydrophobic microenvironment at the high affinity NADPH binding site of XR plays a role in the binding of the coenzyme to XR; whereas, SH_{II} serves to maintain the conformation of the active site essential for catalysis by interacting with the NH_2 group of the Lys residue situated at a distance of 3 Å.

The k_{cat}/K_m profile of XR reaction at varying pH yielded pK_a values of 5.5 and 7.0 Comparison of the pH-k_{cat}/K_m profile of XR measured in water and 20% ethanol indicated that the pK_a values of 5.5 and 7.0 may be ascribed to an ionizable His and carboxyl group respectively. Further, the role of these residues in the mechanism of action of XR was delineated by chemical modification studies. The differential reactivity of native and diethyl pyrocarbonate (DEPC) modified XR towards xylose isomers indicated that the essential His in XR is involved in binding and directing the specificity of aldose substrates within the active site of the enzyme. The involvement of carboxyl group in the catalytic action of XR was investigated by using the modifier 1-ethyl-3[3-(dimethylamino)-propyl]-carbodiimide (EDC).

Introduction

Active site can be defined as the sum of the residues which together are involved in the binding of the substrate(s) and consequent make and break of a covalent bond. To learn about the catalytic mechanism of an enzyme, it is essential to study the structural elements and the 3-D conformation of this site. Chemical modification of reactive amino acid side chain helps to identify those residues in the active site essential for catalysis. Conditions for chemical modification are so adopted that it results in the quantitative covalent derivatization of the functional group of a single unique amino acid residue in a protein without any demonstratable effect on either any other functional groups or the conformation of the molecule.

A plethora of reports are available on the chemical modification of amino acid residues and their role in the structure-function of enzymes. Phenyl glyoxal, a dicarbonyl reagent which reacts with the highly basic guanidino groups of arginine was first used as an arginine specific reagent by Takahashi (1968). For the modification of cysteine residues the reagents *N*-ethylmaleimide (Ambrose, 1976), 5-5'-dithiobis-2-nitrobenzoic acid (Ellman, 1959) and organic mercurials such as *p*-hydroxymercurybenzoate (Bai, 1979) have been widely used. Johnson (1979) showed that 2,4,6-trinitrobenzene sulfonic acid is a useful reagent for the modification of lysine residues. Diethylpyrocarbonate which carboxyethylates the imidazole nitrogens has been used for modification of histidine residues (Miles, 1977). *N*-bromo succinimide, an oxidizing agent which oxidizes the indole residues to oxyindole derivative, and the reagent hydroxy-5-nitrobenzyl bromide have been used to probe the role of tryptophan in enzymes (Horton & Koshland, 1965). The reagents N-acetylimidazole and phenylmethyl sulfonylfluoride have been widely used for the modification of tyrosine and serine residues respectively (Riordan *et al*, 1965; Whitaker & Perez, 1968).

Although, reports are available on the purification and characterization of XR, virtually nothing is known about the amino acid residues constituting the active site or participating in the catalytic process. This chapter reports the presence of essential amino acids in XR and their role in structure-function.

Materials and Methods

Materials

ANS (8-anilinonapthalene-1-sulfonic acid), NBS (*N*-bromosuccinimide), β-mercaptoethanol, HNBB (2-hydroxy-5-nitrobenzyl bromide), PHMB (*p*-hydroxymercury benzoate), OPTA (*o*-phthalaldehyde), TNBS (2,4,6-trinitrobenzenesulfonic acid), DEPC (diethylpyro- carbonate) and EDC 1-ethyl-3[3-(dimethylamino)-propyl]-carbodiimide were obtained from Sigma Chemical Co., USA.

Methods

Reaction of XR with chemical modifiers

XR was incubated with the respective chemical modifiers under the specified conditions. Aliquots were withdrawn periodically for the measurement of residual enzyme activity. Substrate protection studies were performed by preincubating the enzyme with the substrates xylose or NADPH for 10 min prior to the addition of the modifier. Control tubes having only enzyme or only inhibitor or inhibitor and substrate were incubated under identical conditions. The inactivation data was then analyzed as described below.

According to Topham & Dalziel (1986), pseudo first-order rate constants for the fast (k_f) and slow phase (k_s) of inactivation were obtained by fitting data into the equation

$$a = C_1 \exp [-k_f t] + C_2 \exp [-k_s t]$$

where a is the fractional residual activity, C_1 and C_2 are the amplitude of the fast and slow phase of inactivation. The values of k_s and k_f were calculated from the slope of the line obtained by plotting $\ln a$ or $\ln(a-C_2 \exp [-k_s t])$ versus time (t) while the vertical intercepts yielded the values of C_2 and C_1 respectively. The second-order rate constants for the fast and slow phase of inactivation were obtained from slope of plots of k_f or k_s against varying concentrations of the inhibitor.

As described by Levy *et al* (1963), the apparent first-order rate constant of inactivation depends on the concentration of the modifier and can be expressed as

$$K_{app} = K (M)^n$$

where K_{app} is the apparent first order rate constant, K is the second order rate constant, M is the concentration of the modifier and n is the number equal to the average order of the reaction with respect to the concentration of modifier.

$$\log K_{app} = \log K + n \log (M)$$

K_{app} can be calculated as a slope from a semilogarithmic plot of residual activity as a function of time. The second-order rate constant for inactivation was determined from the slope of the plot of pseudo-first order rate constant against inhibitor concentration. The order of reaction (n) was estimated by determining K_{app} at different concentrations of the modifier. A plot of log K_{app} against log M gives a straight line with the slope equal to n where n is the number of the molecules of the modifier reacting with each active unit of the enzyme to produce E-inhibitor complex.

Kinetic parametrs

The primary and secondary plots of bisubstrate reaction kinetics (*described in chapter 3*) were used to determine the kinetic parameters of the chemically modified XR.

Fluorescence measurements

The fluorescence spectra of the native and modified XR (each 0.5 μM) were recorded on an AMINCO SPF-500 spectrofluorometer at 25 °C. The fluorescence signal was corrected for dilution background and inner filter effect (Lakowicz, 1983). Corrections due to inner filter effect were done according to the formula

$$F_c = F \text{ antilog } [(A_{ex} + A_{em})/2]$$

where, F_c and F are the corrected and uncorrected fluorescence intensities respectively and A_{ex} and A_{em} are the absorbances at excitation and emission wavelengths respectively.

Circular dichroism measurements

The CD spectra of native and modified XR (each 1.5 μM) were recorded in the far-UV region (200-250 nm) at 25 °C using a JASCO J600 model spectropolarimeter. All measurements were made with cylindrical quartz cells with a path length of 0.1 cm. Spectra of the solutions containing all components except the protein were obtained and subtracted from the spectra of appropriate samples.

Acrylamide quenching studies

The sample was titrated with small aliquots of the quencher acrylamide (8 M stock solution) and the fluorescence intensities were determined (λ_{ex} 295 nm; λ_{em} 326 nm). The spectra were corrected for inner filter effects due to the quencher. The quenching data was analyzed according to Stern-Volmer relationship

$$F_o / F = 1 + K_{sv} [Q]$$

where, F_o and F are the fluorescence intensities at an appropriate emission wavelength in the absence and presence of the quencher respectively, $[Q]$ is the molar quencher concentration and K_{sv} is the Stern-Volmer quenching constant obtained from the plot of F_o / F versus $[Q]$ (Stern-Volmer, 1919). For proteins containing more than one fluorescing tryptophan residue differing in their accessiblity to the quencher, the Stern-Volmer plot will be non-linear and hence a modified Stern-Volmer equation has been applied

$$F_o / F_o - F = 1/ f_{a(eff)} + 1/ f_{a(eff)} K_{Q(eff)} [Q]$$

Graphical analysis of the plot of $F_o / F_o - F$ versus $[Q]^{-1}$ yields the values of $f_{a(eff)}$, the maximum fractional accessible fluorescence (intercept)$^{-1}$ and $K_{Q(eff)}$, the effective quenching constant (intercept.slope^{-1}) (Lehrer, 1971).

Chemical modification of XR by NBS

Reaction with NBS

XR (15 µg) was incubated with varying concentrations of NBS (4-10 µM) in 0.05M sodium acetate buffer pH 6.0, at 25 °C in a reaction mixture volume of 500 µl. At varying time intervals the residual activity was measured. Pseudo first-order and second-order rate constants were determined according to Topham and Dalziel (1986). Substrate protection studies were performed under the conditions described above by preincubating the enzyme with the substrates xylose or NADPH for 10 min prior to the addition of NBS. Protection studies were also used to calculate the dissociation constant of E-NADPH complex applying the following equation:

$$1 /(k_o - k_{app}) = 1 /(k_o - k_{min}) + K_d /(k_o - k_{min})[\text{NADPH}]$$

where, k_o and k_{app} are the second-order rate constants in the absence and presence of varying concentrations of NADPH respectively. These values were determined as described earlier. Graphical analysis of the plot of $1/(k_o - k_{app})$ versus $[\text{NADPH}]^{-1}$ yielded the values of K_d,

dissociation constant of XR-NADPH complex (slope.intercept^{-1}) and k_{min}, the second-order rate constant in the presence of saturating amount of NADPH.

Titration of XR with NBS

Oxidation of tryptophan residues by NBS was carried out into cuvettes, one containing XR (0.92 μM) in 0.05 M (pH 6.0) and another containing buffer. Successive 10 μl aliquots of NBS (5.0 mM) were added to the sample and reference cuvette and the progress of the oxidation reaction was monitored at 280 nm. Simultaneously aliquots of the reaction mixture were withdrawn to assay the residual enzyme activity. The number of tryptophans oxidized were determined by the method of Spande and Witkop (1967).

ANS binding studies

Binding of the hydrophobic probe ANS to XR was monitored fluorometrically. In a typical experiment XR (0.5 μM) in 0.05 M sodium phosphate buffer pH 7.2, was titrated with increasing concentrations of ANS and the fluorescence intensities were determined on excitation of the sample at 375 nm. The emission spectra were obtained by scanning from 400 to 500 nm. The displacement of ANS from XR-ANS complex was studied fluorometrically by titration of the complex with varying concentrations of NADPH or xylose. The dissociation constant of XR-ANS complex was calculated from a plot of 1/ % F versus [ANS]$^{-1}$ where F is the fluorescence intensity in the presence of ANS. To investigate the energy transfer process from the tryptophanyl groups of XR to the bound ANS, 0.2 μM of the enzyme in 0.05 M phosphate buffer pH 7.2, was titrated with varying concentrations of NBS and the change in the tryptophanyl and ANS fluorescence was monitored. The excitation wavelength was fixed at 295 nm to ensure that the light was absorbed entirely by the tryptophanyl groups.

Titration of XR and XR-NADPH complex by acrylamide

XR (0.42 μM) in the presence and absence of NADPH (0.1 mM) was titrated with varying concentrations of acrylamide and the change in the fluorescence intensity at 326 nm was studied with the excitation wavelength fixed at 295 nm. Quenching data was analyzed according to Stern-Volmer and modified Stern-Volmer equation as described earlier.

Chemical modification of XR by PHMB

Reaction with PHMB

XR (20 μg) was incubated with varying concentrations of PHMB in 0.05 M phosphate buffer pH 7.0, at 25 °C. The loss in activity at different time intervals was measured and the inactivation data was analyzed according to Topham and Dalziel (1986).

Titration of XR with PHMB

XR (1.5×10^{-5} M) in 50 mM phosphate buffer pH 7.0, was titrated with 10 μl volumes of PHMB (1 mM) and the progress of the reaction was monitored spectrophotometrically at 250 nm. Simultaneously aliquots of the reaction mixture were withdrawn to assay the residual activity. The number of Cys residues modified were determined by the method of Riordan and Vallee (1972).

NADPH binding studies

PHMB and NEM modified XR each 0.15 μM in 0.05 M phosphate buffer pH 6.3, were titrated with varying concentrations of NADPH and the changes in the tryptophanyl fluorescence at 326 nm were recorded with the excitation wavelength fixed at 295 nm. The dissociation constant of XR-NADPH complex was obtained on analysis of the quenching data according to Stinson and Holbrook (1973) (*refer chapter 3*).

Chemical modification of XR by OPTA

Re*action with OPTA*

XR (150 μg) in 1 ml 0.05 M sodium phosphate pH 7.0, was incubated with 15 μl of 10 mM OPTA in methanol at 25 °C. Aliquots were withdrawn periodically and the residual activity was measured on termination of the reaction by adding 5 μl of cysteine (10 mM). In control experiments 20 μl of methanol was added; however, it had no effect on the enzyme activity. Simultaneously the formation of XR-isoindole derivative was followed spectrophotometrically at 337 nm. The extent of inactivation in the presence of substrates xylose and NADPH was also investigated. The ability of reagents containing SH and NH_2 groups to terminate the reaction between XR and OPTA was investigated. XR (1.8 μM) was incubated with 15 μl of 10 mM OPTA in 0.05 M phosphate buffer pH 7.0, at 25 °C for 5 min at which time 3 mM each of cysteine, homocysteine, glutathione or cystine was added to the reaction mixture and the residual activity measured

Modification of XR by TNBS

Reaction with TNBS

XR (30 μg) in 0.25 ml of 4% sodium bicarbonate was incubated with varying concentrations of TNBS a Lys group specific modifier at 37 °C in a reaction mixture volume of 0.5 ml. Aliquots were withdrawn at suitable time intervals and the reaction was terminated by adjusting the pH to 4.6. The inactivation data was analyzed according to Topham and Dalziel (1986).

Chemical modification of XR by DEPC

Carbethoxylation

XR (1.2 μM) in 0.05M phosphate buffer pH 7.0 was incubated at 37 °C with the indicated concentrations of DEPC, freshly diluted in absolute alcohol. The final concentration of ethanol in the reaction mixture never exceeded 5% v/v and had no effect on the activity and stability. Samples were withdrawn at varying time intervals and the residual activity was determined. To determine the number of His residues essential for XR activity the enzyme (6 μM) was incubated with 5 mM DEPC and the loss in enzyme activity was measured, simultaneously the amount of N-ethoxycarbamyl histidyl derivative per XR dimer was calculated by using 3200 M^{-1} cm^{-1} as the molar absorption coefficient. (Ovadi et al, 1967). To study the pH dependence of the rate of reaction of essential His residue in the enzyme (1.2 μM) was incubated with DEPC in the presence of phosphate buffer (6-7). and acetate buffer (pH 5 - 5.8)

Modification of XR by EDC

XR (2 μM) in 0.05 M Mes buffer, pH 6.0 was incubated with varying concentrations of EDC at 25 °C. Samples were withdrawn from the reaction mixture at the indicated time quenched in 0.1 M sodium acetate pH 5.0 and assayed for residual activity. To study the influence of pH on the inactivation process the experiments were performed as described above in the presence of Mes (pH 5-5.6) and Mops (7-7.5) buffer.

Results and Discussion

Involvement of Trp residue at the NADPH binding site of XR

Kinetics of inactivation of XR by NBS

Fig. 1 shows a plot of ln*a* versus time for inactivation of XR at a fixed concentration of NBS. The inactivation of the enzyme by varying concentrations of NBS was found to be biphasic which may be due to the dimeric form of the enzyme. Applying the analysis described by Topham and Dalziel (1986) the pseudo-first order rate constants for the slow phase (k_s) and fast phase (k_f) of inactivation were calculated to be 7.5×10^{-4} s^{-1} and 3.4×10^{-3} s^{-1} respectively. A value of 0.76 was obtained for the amplitude of slow phase of inactivation (C_2). Second-order rate constant values of 2.5×10^{-2} and 80 $M^{-1}s^{-1}$ were obtained for slow and fast phase of inactivation respectively.

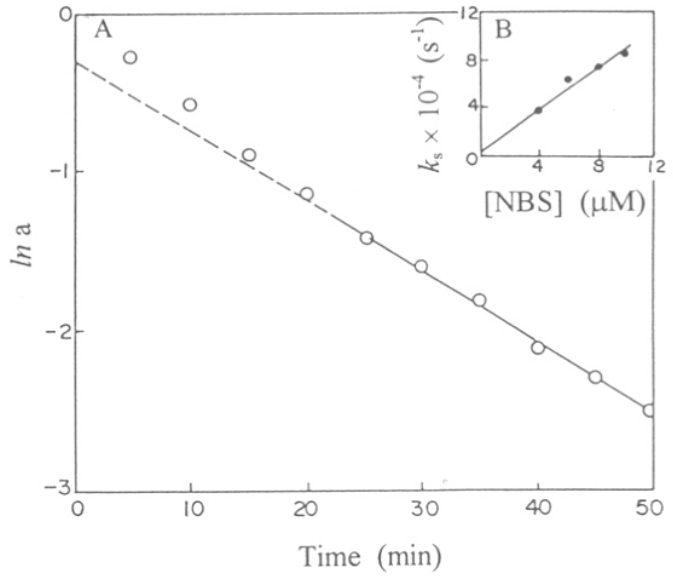

Fig. 1 **Inactivation of XR by NBS**

A. Plot of ln *a versus t* (o) for the inactivation of XR by NBS .

B. Plot of pseudo-first order rate constants for the slow phase of inactivation (k_s) against varying concentrations of NBS (•).

Titration of XR by NBS

The possibility that the inhibition of XR by NBS is solely due to oxidation of Trp was supported by the inhibition of the enzyme by HNBB (2 mM) a Trp specific reagent at neutral pH. The reaction of proteins with NBS is accompanied by a decrease in absorbance at 280 nm. This is attributed to the NBS induced oxidation of indole chromophore of Trp which absorbs strongly at 280 nm to oxyindole a much weaker chromophore at this wavelength (Eyzaguirre, 1986). As shown in Fig. 2, the titration of XR by NBS resulted in a linear decrease in absorbance at 280 nm with a concomitant loss in enzyme activity. Modification of total 3.5 Trp residues per molecule of XR lead to a complete inactivation of the enzyme. Altogether these studies reinforced the evidence for Trp modification at the active site of XR.

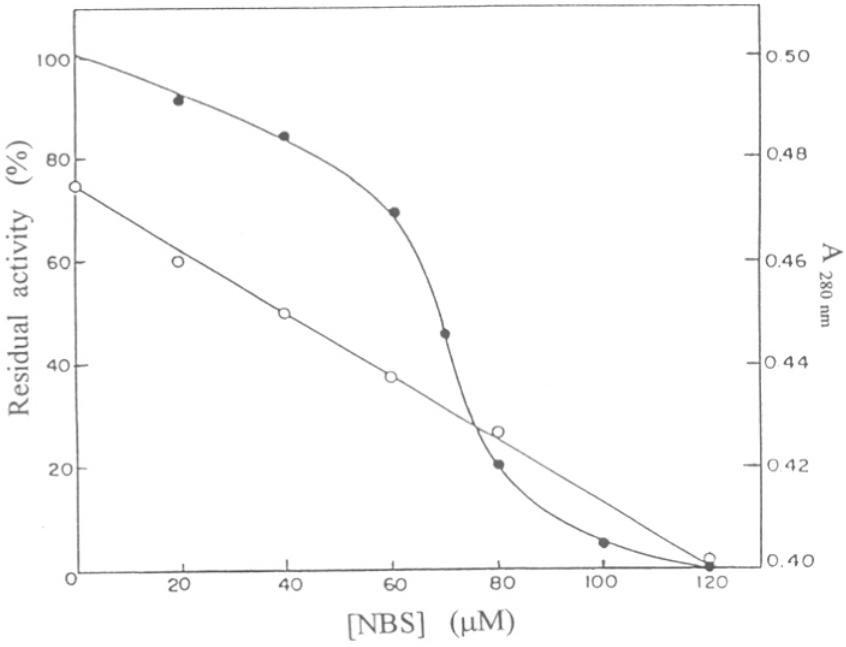

Fig. 2 **Titration of XR by NBS**

Residual activity of XR (•) and A_{280} nm (o) on titration with NBS.

Fluorescence and circular dichroism studies

XR (0.42 μM) in 0.05 M acetate buffer pH 6.0, when titrated with increasing concentrations of NBS led to the progressive quenching of the tryptophanyl fluorescence due to oxidation by NBS (Fig. 3A). However no blue or red shift in the emission maximum at 326 nm was observed suggesting no change in conformation due to shift of Trp residues from polar to nonpolar environment and vice versa. The CD spectra of native and NBS modified XR (Fig. 3B) were similar indicating negligible effect on the α-helix and β-sheet of XR. The analysis of fluorescence and CD spectra of the native and modified enzyme indicated that inactivation by NBS was not due to gross conformational change but due to oxidation of essential tryptophans(s) involved in substrate binding or in catalysis.

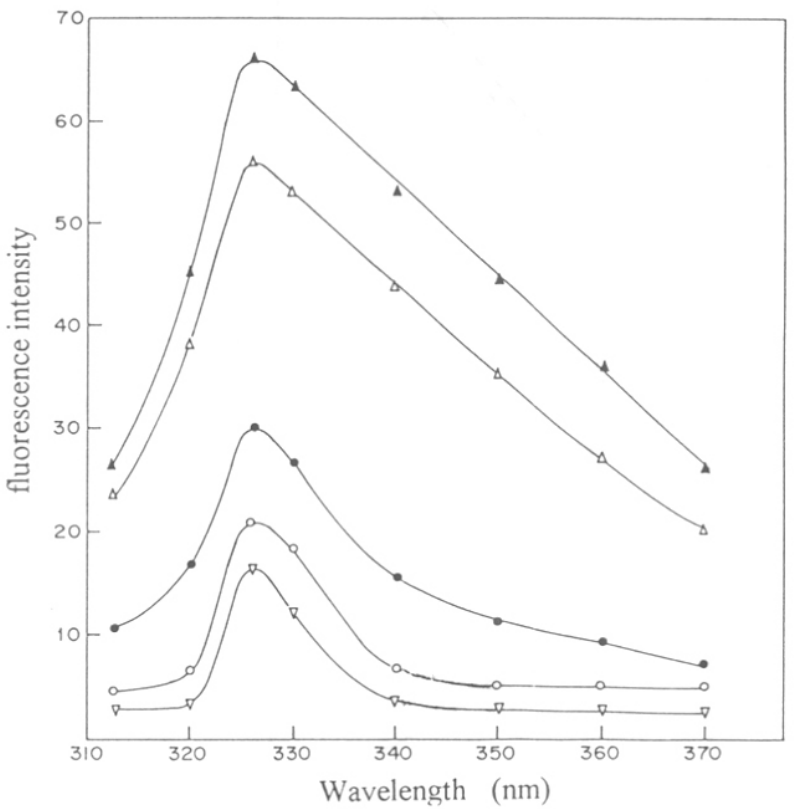

Fig. 3A **Fluorescence spectra of native and NBS modified XR**

XR fluorescence (λ_{ex} 295 nm; λ_{em} 326 nm) on incubation with 0 μM (▲), 2 μM (Δ), 6 μM (•), 12 μM (o) and 20 μM (▽) NBS.

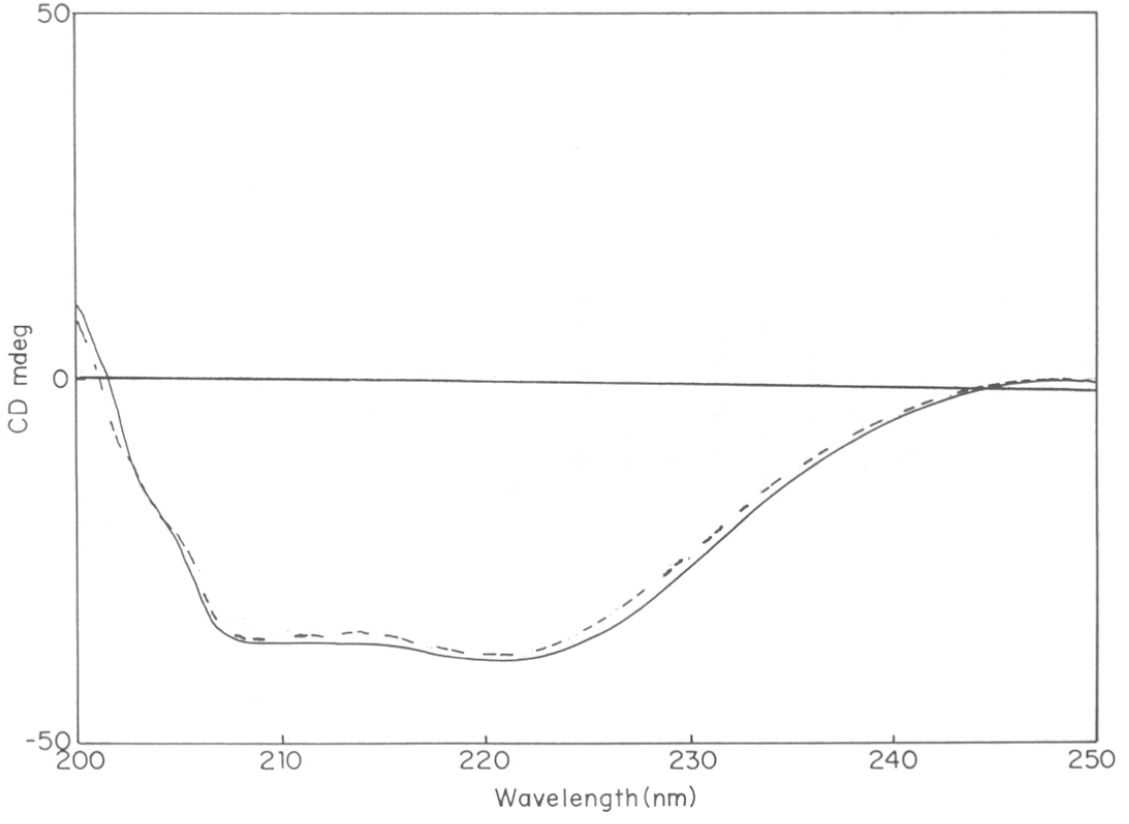

Fig. 3B CD spectra of Native (–) and NBS modified XR (– –)

Protection by NADPH against inactivation of XR by NBS

Xylose or Glucose (0.3 M) and $NADP^+$ (100 μM) afforded no protection against inactivation by NBS which may be due to the fact that the enzyme follows an *iso-ordered bi bi mechanism* wherein xylose binds to XR-NADPH complex and $NADP^+$ to E' form of the enzyme. The coenzyme NADPH at a concentration of 100 and 250 μM protected 50 and 90% of XR activity respectively. Considering a K_d value of 1.05 μM for NADPH (*refer chapter 3*) 99% of the enzyme may be assumed to be in the XR-NADPH form at a NADPH concentration of 100 μM. However, NADPH (100 μM) protected only 50% loss in activity. These results indicated that the NBS induced inactivation of XR may be due to the modification of tryptophan(s) at another NADPH binding site of XR which has a low affinity for the coenzyme. To determine the dissociation constant of XR-NADPH complex at this site, the NBS induced inactivation of XR in the absence and presence of varying concentrations of NADPH was studied. Double reciprocal plot of second-order rate constants for the slow phase of inactivation against varying concentrations of NADPH yielded a dissociation constant (K_d) value of 72 x 10^{-6} M for XR-NADPH complex at the low affinity NADPH binding site of XR (Fig. 4).

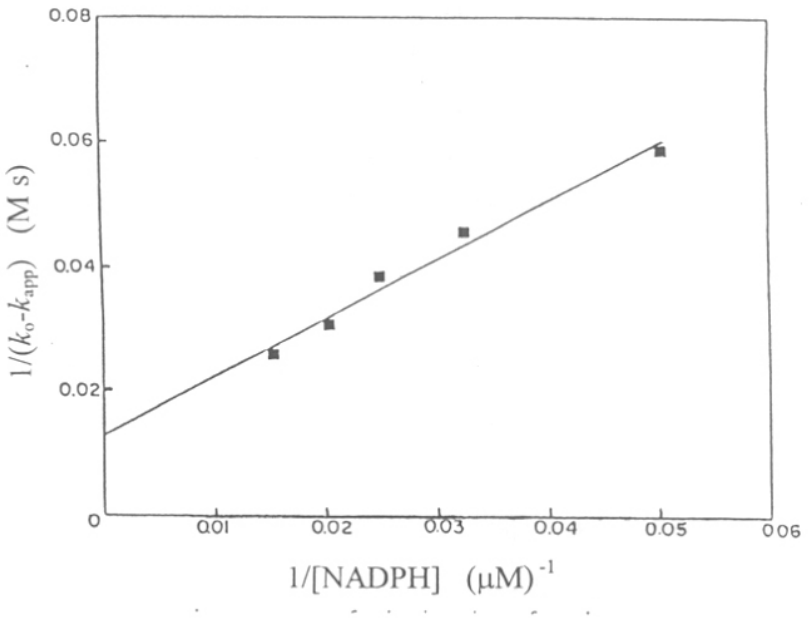

Fig. 4 Double reciprocal plot of second-order rate constants for the slow phase of inactivation against varying NADPH concentration

Kinetic parameters of the native and NBS modified XR

The primary and secondary plots of bisubstrate reaction kinetics (*described in chapter 3*) were used to determine the various kinetic constants of the NBS modified XR which are compared with that of the native enzyme and tabulated in (Table 1). The results revealed that the modification of the enzyme by NBS was accompanied by a significant increase in K_m value for NADPH (K_A) and decrease in k_{cat}, however K_m for xylose (K_B) was not affected. The inactivation affected the binding of NADPH which is also supported by an increase in K_{iA}, the dissociation constant for XR-NADPH complex and decrease in *on* velocity for NADPH (k_1) by a factor of 150 and 5 respectively.

Table 1. Kinetic parameters of native and NBS modified XR

Kinetic parameters	Native	Modified
V_{max} (U mg^{-1})	77	51.2
k_{cat} (min)	4638	3084
K_A (μM)	9	28.4
K_B (mM)	22	21.2
K_{iA} (μM)	1.05	157
k_1 ($M^{-1}min^{-1}$)	515	108.6

For preparation of modified enzyme, XR (30 μg) was treated with NBS (10 μM) at 25 °C for 5 min in 0.05 M sodium acetate buffer pH 6.0, total volume 1 ml. 10 μl of Trp (10 $mg.ml^{-1}$) was used to terminate the reaction.

Assessment of the microenvironment of Trp residues

To investigate the environment of the tryptophans in XR and the changes associated with the binding of NADPH, quenching studies were performed in the absence and presence of NADPH using acrylamide. Acrylamide is a polar uncharged quencher with the ability to quench the fluorescence of indole derivatives predominantly by the collisional process (Eftink & Ghiron, 1976). It was observed that acrylamide had no effect on the activity and emission maximum of XR indicating that the quenching was an entirely physical process. The quenching of XR with increasing concentrations of acrylamide resulted in a Stern-Volmer plot with downward curvature (Fig. 5A) which suggested that the fluorescence of

certain tryptophans is selectively quenched before others and thus the microenvironment of the Trp residues contributing to fluorescence emission is heterogeneous (Lehrer, 1971). The quenching parameters $f_{a(eff)}$, maximum fractional accessible fluorescence and $K_{Q(eff)}$, effective quenching constant were derived for XR from a replot of quenching data according to modified Stern-Volmer equation (Fig. 5B) and values of 0.49 and 5.7 M^{-1} respectively were obtained, indicating that nearly 49% of the tryptophanyl fluorescence was accessible to quenching by acrylamide. However, in the presence of NADPH, the quenching of XR fluorescence was completely abolished (Fig. 5A) confirming the involvement of certain tryptophans at NADPH binding site of XR.

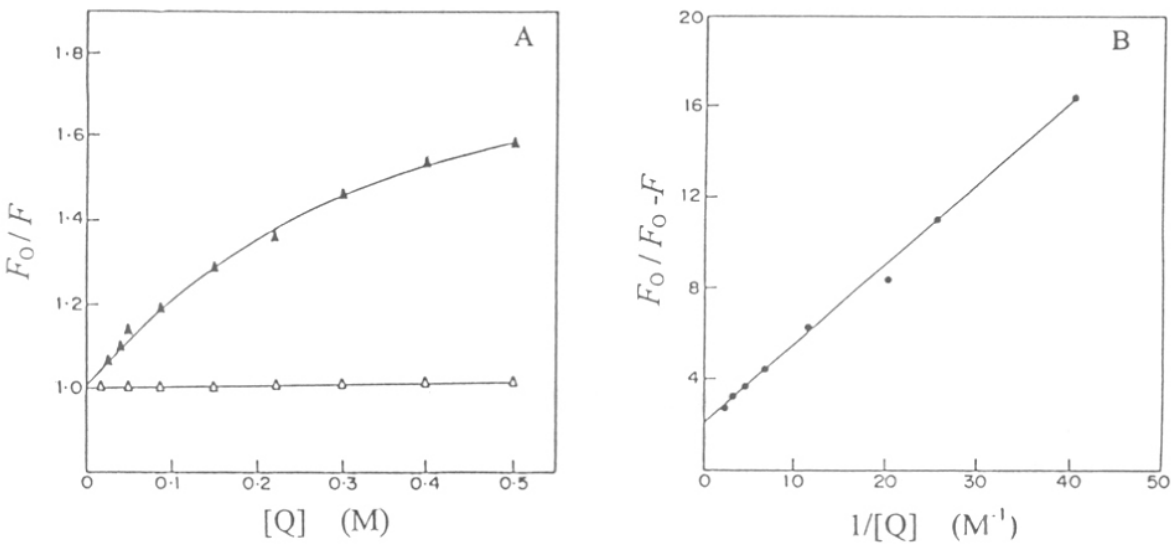

Fig. 5 **Acrylamide quenching of XR and XR-NADPH complex**

A. Stern-Volmer plots of fluorescence quenching of XR (▲) and XR-NADPH complex (Δ).

B. Modified Stern-Volmer plot of quenching of XR.

Assessment of the polarity of NADPH binding site

The polarity of the pyridine nucleotide binding region was assessed using the hydrophobic probe ANS. The fluorescence property of the sulfonate group of ANS depends on the polarity of its environment. ANS has been widely used to detect the exposure of hydrophobic surfaces in the folding intermediates of proteins (Ptitsyn, 1990). As shown in Fig. 6, the aqueous solution of ANS when excited at 375 nm had a low quantum yield and an emission maximum at 510 nm. However, when bound to XR an

enhancement of the dye fluorescence (λ_{em} 465 nm) was observed indicating that the microenvironment in XR that binds ANS is hydrophobic in nature. A value of 90 μM was obtained for the dissociation constant of ANS.

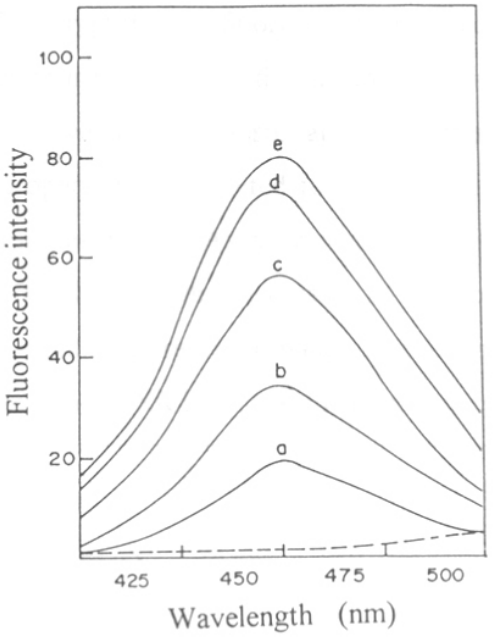

Fig. 6 **Fluorescence spectra of ANS bound to XR**
XR was titrated with varying concentrations of ANS (a) 15 μM, (b) 30 μM, (c) 55 μM, (d) 90 μM and (e) 125 μM and the fluorescence spectra recorded with the excitation wavelength fixed at 375 nm.

Addition of NADPH (250 μM) to XR-ANS complex led to a significant blue-shift in emission maximum from 465 to 445 nm indicating formation of E-NADPH complex by replacement of ANS by the coenzyme. ANS and NADPH occupy the same site and the displacement is not due to conformational changes induced on binding of NADPH to XR was also supported by the analysis of the fluorescence and CD spectra. However, minor conformational changes induced to allow binding of xylose to XR-NADPH complex would not be detected. In contrast to the above observation, ANS could not be displaced by the substrate xylose (0.25 M) and low concentration of NADPH (20 μM). These results revealed that the microenvironment at the low-affinity NADPH binding site of XR is hydrophobic in nature. Modification of XR tryptophans by NBS was accompanied by loss in enzyme activity (Fig. 1) and ANS fluorescence (λ_{ex} 375 nm; λ_{em} 465 nm). These studies

indicated that the essential Trps in XR are involved in maintaining the hydrophobicity at the low-affinity NADPH binding of the enzyme.

Proximity of Trp residues to the ANS binding site

The quenching of the tryptophanyl fluorescence of a protein by its prosthetic group is due to resonance energy transfer provided the group is within a limited distance and the emission spectrum of Trp overlaps the absorbance spectrum of the prosthetic group (Guilbault, 1973). This property was exploited to confirm the proximity of ANS binding site to the essential Trp residues in XR. As shown in Fig. 7, titration of XR by increasing concentrations of ANS, resulted in the decrease in tryptophanyl fluorescence and enhancement in the ANS-specific fluorescence which may be attributed to energy transfer from the aromatic amino acid to the XR bound ANS situated in close proximity.

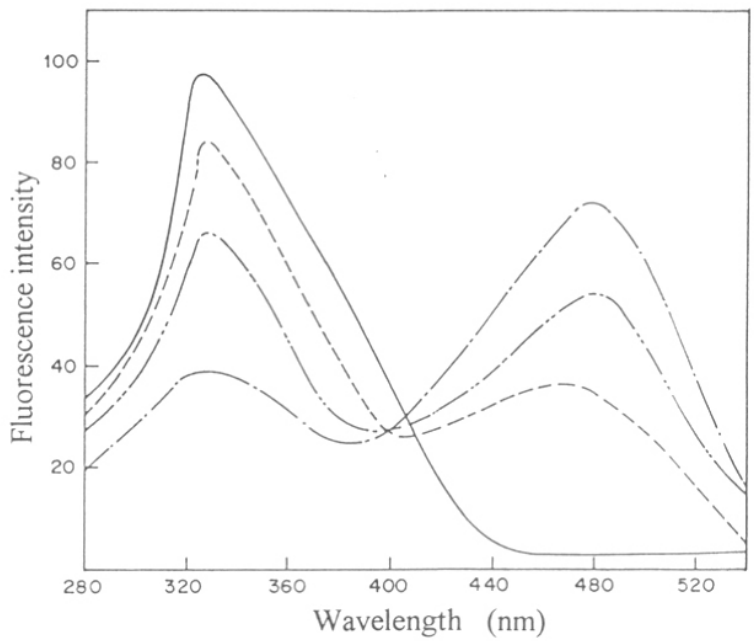

Fig. 7 **Fluorescence energy transfer from XR to bound ANS**

Tryptophanyl (λ_{ex} 292 nm; λ_{em} 326 nm) and ANS (λ_{ex} 292 nm; λ_{em} 475 nm) fluorescence on titration of XR with 0 μM (—) , 30 μM (– –) , 60 μM (– · · –) and 120 μM (– · –) ANS.

Site and significance of Cys and Lys residues in XR

Inactivation of XR by PHMB

Fig. 8A shows a plot of ln*a* versus time for inactivation of XR at a fixed concentration of PHMB. The inactivation of XR by varying concentrations of PHMB was found to be biphasic. Applying the analysis described by Topham and Dalziel (1986) the pseudo first-order rate constant values of 5.8×10^{-3} and 4.15×10^{-4} s^{-1} and second-order rate constant values of 80 and 6 M^{-1} s^{-1} were obtained for the fast (k_f) and slow (k_s) phases of inactivation (Fig. 8B). Values of 0.27 and 0.72 were obtained for the amplitude of fast (C_1) and slow phase (C_2) of inactivation. Plot of residual activity against number of Cys residues (Fig. 9) revealed that the inactivation was a result of modification of 0.90 Cys residues (SH_I) per molecule of XR.

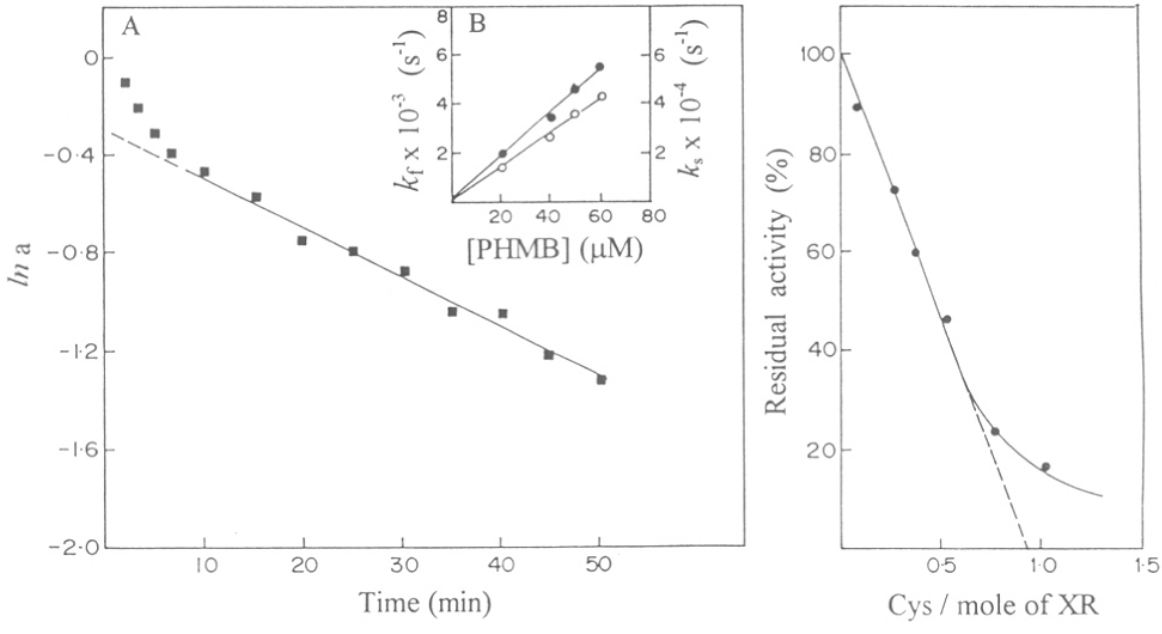

Fig. 8 **Inactivation of XR by PHMB**

A. Plot of ln *a versus t* (■) for inactivation of XR by PHMB.

B. Plot of pseudo-first order rate constants for fast, k_f (•) and slow, k_s (o) phase of inactivation *versus* varying concentrations of PHMB.

Fig. 9 **Correlation of residual activity and number of Cys residues modified/mole of XR**

Reactivation of PHMB modified XR

The recovery of XR activity on complete inactivation by PHMB was determined by transferring aliquots of the inactivated enzyme in different concentrations of β-ME at 25 °C. A maximum 85-90% of the initial activity of the PHMB-modified XR was restored in the presence of 5 mM β-ME in 15 min.

Conformational changes on inactivation of XR by PHMB

The inactivation of XR by PHMB did not alter the fluorescence profile (λ_{ex} 295 nm; λ_{em} 326 nm) of the enzyme indicating no shift of Trp residues from polar to nonpolar environment and vice versa. The circular dichroism measurements revealed no effect on the α-helix and β-sheet content of XR (Fig. 10). Hence the PHMB induced inactivation of XR is a result of direct chemical modification of an essential Cys and cannot be attributed to subsequent disruption of the quaternary structure.

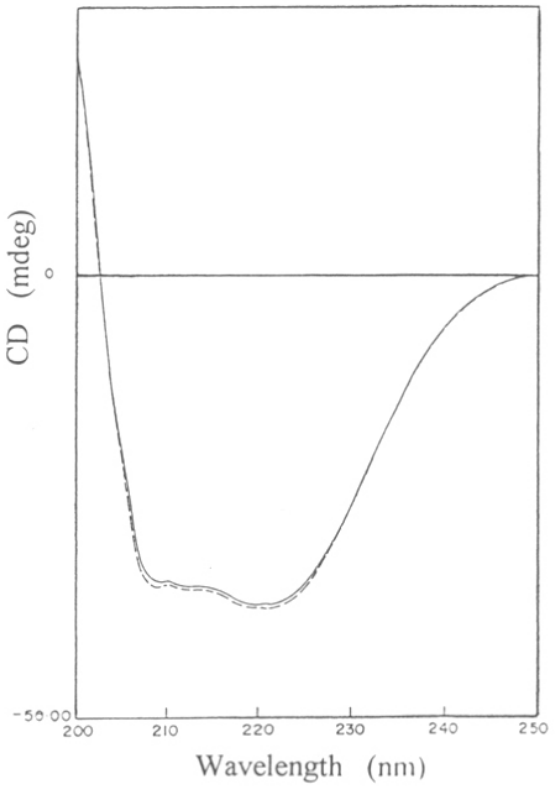

Fig. 10 CD spectra of native and PHMB modified XR

Far-UV CD (200-300 nm) spectras of native (—) and PHMB modified XR (---).

Substrate protection and NADPH binding studies

Xylose (0.3 M) afforded no protection against inactivation of XR by PHMB. This may be due to the fact that the enzyme follows an *iso-ordered bi bi* mechanism. NADPH (20 μM) protected maximum 90% of XR activity. Thus the inactivation may be due to modification of Cys residue (SH_I) situated at or near the NADPH binding site of XR. Further, investigations were carried out to study the influence of SH_I modification on the formation of XR-NADPH complex. The native and PHMB modified XR were titrated with varying concentrations of NADPH and the formation of E-coenzyme complex was studied by monitoring the quenching of the XR fluorescence (Fig. 11A). Applying the analysis described by Stinson and Holbrook (1973) the dissociation constant for XR-NADPH complex was calculated and values of 0.9 μM and 2.3 μM were obtained for the native and modified XR respectively (Fig. 11B). These results revealed that the PHMB induced inactivation of XR was accompanied by a decrease in the ability of XR to bind the phosphorylated coenzyme.

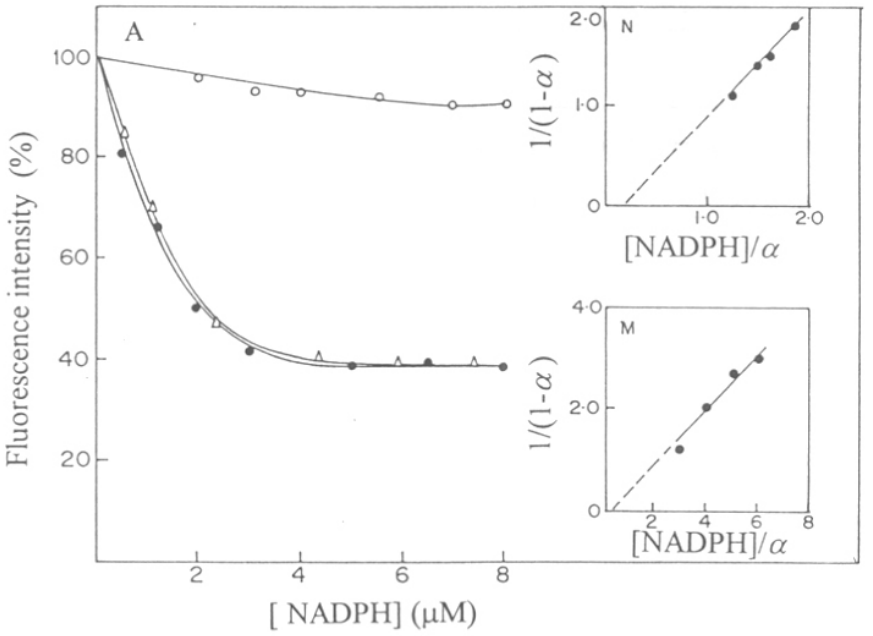

Fig. 11 **Titration of XR with NADPH**

A. Tryptophanyl fluorescence intensity (λ_{ex} 295 nm; λ_{em} 326 nm) of native (•), PHMB (o) and NEM (Δ) modified XR on titration with NADPH.

B. Plot of 1/1-α *versus* NADPH/α for native (N) and PHMB modified XR (M).

Coenzyme binding (*chapter 3*) and substrate protection studies (*present chapter*) revealed the presence of a high (K_d 0.85 μM) and low (K_d 72 μM) affinity NADPH binding site per dimer of XR. In the present study it was observed that NADPH at a concentration of 20 μM afforded complete protection against inactivation by PHMB. Considering a K_d value of 0.9 μM for NADPH (Fig. 11B), 99% of the enzyme may be assumed to be in XR-NADPH form at this coenzyme concentration. Altogether, these results indicated that the PHMB induced inactivation of XR is due to the modification of SH_I located at the high-affinity coenzyme binding site of XR.

Microenvironment of SH_I in XR

To probe the microenvironment of SH_I in XR the inactivation of the enzyme by PHMB in dilute aqueous solutions of various alcohols was studied. The pseudo first-order rate constant for the fast (k_f) and slow phase (k_s) of inactivation increased in the order methanol, *t*-butanol, ethanol, *n*-propanol and *n*-butanol, despite the fact that with an increase in chain length the molar concentration of each alcohol decreased (Table 2).

Table 2. Dependence of PHMB induced inactivation of XR on the presence of dilute aqueous solutions of alcohols

Alcohol	Pseudo-first order rate constants	
	$k_f x10^{-3}$ s^{-1}	k_s $x10^{-3}$ s^{-1}
control	2.1	2.5
methanol (1.23 M)	5.7	2.6
***t*-butanol (0.27 M)**	5.74	2.65
ethanol (0.85 M)	6.5	3.16
***n*-propanol (0.67 M)**	6.68	6.2
***n*-butanol (0.27 M)**	6.82	7.1

XR (20 μg) in 0.05 M phosphate buffer pH 7.0, was incubated with PHMB (20 μM) at 25 °C in the presence of various alcohols listed above. The extent of inactivation at different time intervals was measured and the values of pseudo-first order rate constants were determined according to Topham and Dalziel (1986).

Addition of alcohol to aqueous solution results in the decrease in the dielectric constant. This would cause an increase in the strength of electrostatic interactions and hydrogen bonds, the strength of the latter is increased by the reduced competition of water molecules. An increase in XR inactivation in presence of alcohols (Table 2) revealed that neither of these types of bonding are responsible for the reduced reactivity of XR. With the increase in the length of the carbon chain the alcohols become more hydrophobic. It was evident from our results that the various alcohols act by reducing the hydrophobic interactions to varying extents which otherwise hinder the reaction of SH_I. The rate of inactivation of XR by PHMB was greater in *n*-butanol than *t*-butanol. Both these isomers have same dielectric constant and molecular weight; however, *t*-butanol is completely miscible in water and hence disrupts hydrophobic bonds to a lesser extent than *n*-butanol resulting in the differential rate of inactivation. Increase in inactivation is not a result of action of alcohol on the other groups of the enzyme, this possibility was ruled out as the concentration of alcohols used in these experiments had no effect on the XR activity.

The temperature dependence of hydrophobic interactions in proteins has been studied by Baldwin (1986). Maximum stabilization of these interactions is observed at higher temperatures and as the temperature is decreased the interactions weaken. The effect of temperature on the PHMB induced inactivation of XR was studied. It was observed that the pseudo first-order rate constant values for the fast (k_f) and slow phase (k_s) of inactivation at 18 °C (k_f, 2.31 x 10^{-3} s^{-1} ; k_s 3.5 x 10^{-3} s^{-1}) were 1.1 and 1.4 fold higher than that observed at 25 °C (k_f, 2.1 x 10^{-3} s^{-1}; k_s 2.5 x 10^{-3} s^{-1}). Thus the decrease in temperature was accompanied by a concomitant increase in the availability of SH_I for reaction with PHMB. Altogether these results supported the notion that the microenvironment of SH_I in XR is hydrophobic and this residue is involved in permitting the efficient binding of the NADPH to XR by maintaining the hydrophobicity of the coenzyme binding site.

Inactivation of XR by OPTA

OPTA is a bifunctional agent with absolute specificity for SH and NH_2 groups of the proteins (Simons & Johnson, 1978b; Palczewski *et al*, 1983). Incubation of XR with OPTA resulted in complete inactivation of the enzyme indicating that the SH and NH_2 groups of XR involved in the reaction with OPTA are situated at or close to the active site of XR. The inactivation was accompanied by a concomitant increase in fluorescence at 410 nm characteristic of an isoindole derivative (Fig. 12). No change in the emission (λ_{em} 410 nm) was observed in the presence of excess OPTA ruling out the possibility of slow side reactions. A plot of percent residual activity against number of isoindole derivatives formed (Fig. 13) revealed that the formation of a single isoindole derivative/dimer of XR resulted in the inactivation of the enzyme.

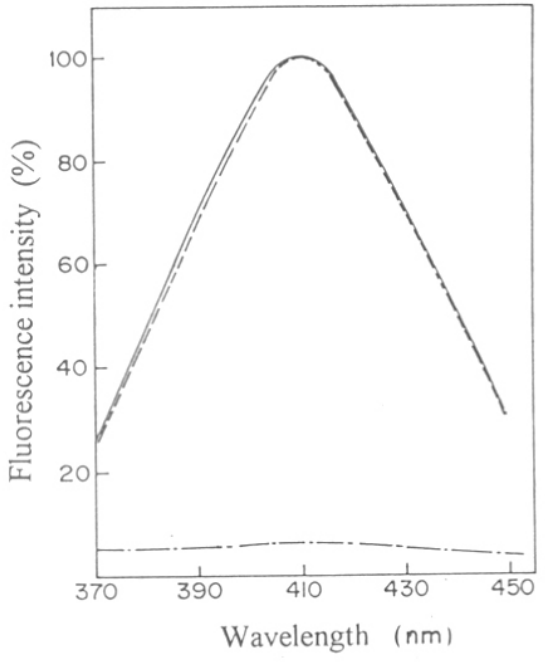

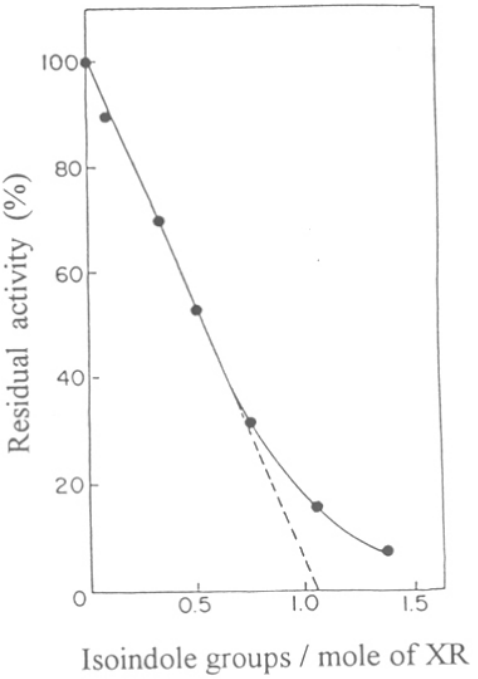

Fig. 12 **Isoindole fluorescence of XR**
Fluorescence spectra of native (—), PHMB (---) and NEM (- • -) inactivated XR on incubation with OPTA.

Fig. 13 **Plot of residual activity *versus* number of isoindole groups/mole of XR**

Double inhibition studies

Double inhibition studies were performed to ascertain whether reactive Cys binding to PHMB is also involved in OPTA reaction. Two sets of experiments were performed, wherein XR was treated with PHMB prior to OPTA modification or vice versa followed by cysteine, a terminator of OPTA reaction and β-ME that reverses the inhibition due to PHMB. As shown in Table 3, the enzyme was inactivated in both cases indicating that the Cys residues reacting with PHMB (SH_I) and OPTA (SH_{II}) are distinctly different. If they were same then reactivation would have been observed in the case where the enzyme was modified with PHMB prior to OPTA. This was also confirmed by the observation that the PHMB-modified XR (0.5 μM) retained its ability to form the XR-isoindole derivative on reaction with 20 μM OPTA (Fig. 12). Modification of XR with 5 mM NEM (2h) a Cys modifier, at pH 7.5 resulted in inactivation of XR. Addition of NADPH to NEM-modified XR resulted in the quenching of XR fluorescence indicating that the inactivation did not alter the formation of XR-NADPH complex (Fig. 11). However, the modified enzyme (0.5 μM) failed to form the XR-isoindole derivative on reaction with 20 μM OPTA (Fig. 12) indicating that the Cys residue involved in the reaction with NEM and OPTA is the same (SH_{II}). These results indicated that SH_{II} plays no role in the binding of NADPH to XR but its integrity is essential for the catalytic mechanism of the enzyme.

Table 3. Effect of β-ME and Cys on the XR inactivated by PHMB and OPTA

Inhibitor	Cys+β-ME	Residual activity (%)
Control	-	100
PHMB	+	74
OPTA	+	4
PHMB/OPTA	-	21/22
OPTA →PHMB	-/+	3
PHMB → OPTA	-/+	2

XR (0.16 μM) was incubated with PHMB (50 μM) and OPTA (50 μM) each for 5 min. The reaction mixture was further incubated with 1 mM Cys and 5 mM β-ME and the XR activity was measured.

Characterization of the Lys residue involved in OPTA reaction

Inactivation of XR with varying concentrations of TNBS, a Lys modifier was found to be biphasic. Fig. 14 shows a plot of ln*a versus* time for inactivation of XR at a fixed concentration of TNBS. The pseudo first-order rate values of 3.3×10^{-3} and $1.25 \times 10^{-3} s^{-1}$ and second-order rate constant values of 60 and 21 $M^{-1} s^{-1}$ were obtained for the fast (k_f) and slow phase (k_s) of inactivation respectively. A value of 0.35 and 0.68 was obtained for the amplitude of fast (C_1) and slow phase (C_2) of inactivation. NADPH (250 μM) and xylose (0.3 M) afforded no protection against inactivation implicating that the Lys residue is not involved in the binding of the substrates. Inactivation of XR by TNBS was accompanied by a loss in ability to form the fluorescent XR-isoindole derivative (λ_{ex} 338 nm; λ_{em} 410 nm), indicating that the Lys residue involved in the reaction with TNBS and OPTA is the same and is essential for XR activity.

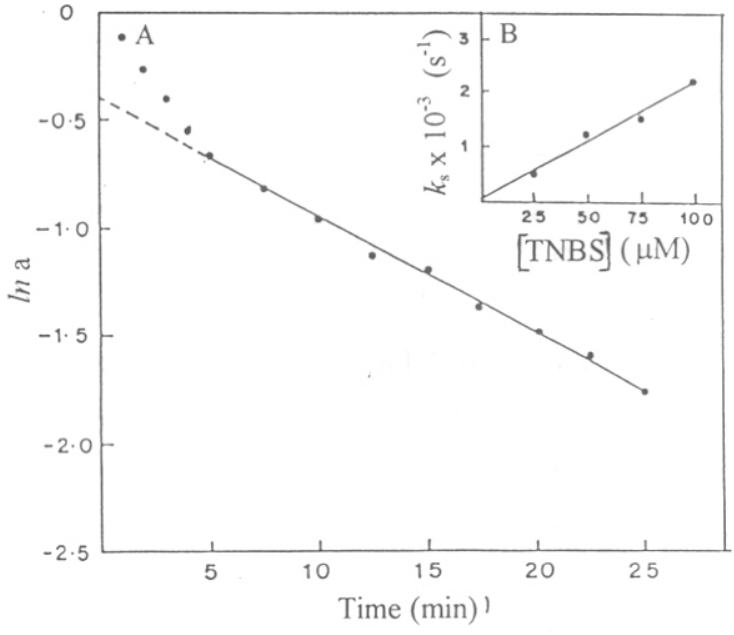

Fig. 14 Inactivation of XR by TNBS

A. Plot of ln *a versus t* (•) for the inactivation of XR by TNBS.

B. Plot of pseudo-first order rate constants for the slow phase of inactivation *versus* varying concentrations of TNBS.

Kinetic parameters of native and TNBS modified XR

The primary and secondary plots of bisubstrate reaction kinetics (*described in chapter 3*) were used to determine the kinetic parameters of the native and TNBS modified XR which are tabulated in Table 4. The modification of XR by TNBS resulted in a 2.5 fold decrease in k_{cat}. However, K_m for xylose and NADPH was not affected thus indicating the involvement of Lys residue in the catalysis of XR. Several nicotinamide nucleotide-linked dehydrogenases are also inactivated on modification of a Lys residue suggesting a possible common role for Lys in these enzymes. In glutamate dehydrogenase the binding of coenzymes and substrates does not depend on the integrity of Lys126 but plays a direct role either in the orientation of the reactants or in the catalytic process (Chen & Engel, 1975).

Table 4. Kinetic parameters of native and TNBS modified XR

XR	k_{cat} (min^{-1})	$K_{m(NADPH)}$ (μM)	$K_{m(xylose)}$ (mM)
Native	4680	9	22
Modified	1872	8.1	23

For the preparation of TNBS-modified enzyme 50 μg of XR was incubated with 110 μM TNBS at 25 °C for 10 min in 4% of $NaHCO_3$ in a total volume of 1 ml. The reaction was terminated by adjusting the pH to 4.6.

Proximity of Cys and Lys residues in XR-isoindole derivative

Investigations were carried out to assess the distance between the essential SH and NH_2 groups of XR involved in the reaction with OPTA. Several reagents that contain SH and NH_2 functions in varying distance (Fig. 15) were examined for their ability to terminate the reaction between XR and OPTA. It was observed that on addition of excess cysteine a residual activity of 68% was obtained. This indicated that cysteine effectively terminated the reaction and the proximity of SH and NH_2 functions of the participating Cys and Lys residues in the XR molecule and that of cysteine are comparable to that between the two -CHO functions in OPTA. Based on the bond distances and bond angles of the two -CHO functions in OPTA (March, 1977), the present studies revealed that the SH and NH_2 functions in XR involved in the formation of XR-isoindole derivative and cysteine are probably 3 Å apart. Homocysteine and glutathione were not efficient terminators with a

residual activity of 35%. This can be explained by the fact that the SH and NH_2 functions in these reagents do not assume the 3 Å distance with respect to each other as in cysteine. Glycine and Cystine completely lacked the ability to terminate the reaction because of the absence of a free SH function.

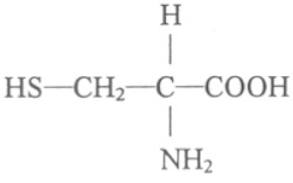

Cysteine

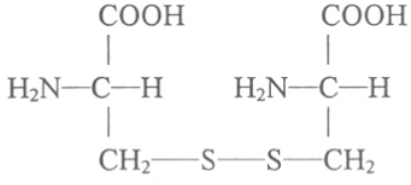

Cystine

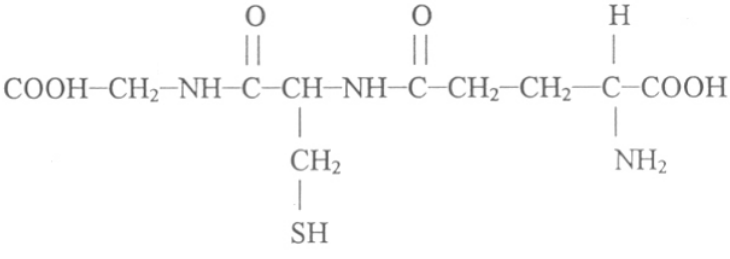

Glutathione

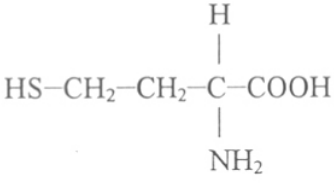

Homocysteine

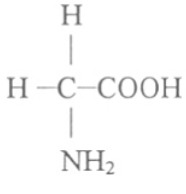

Glycine

Fig. 15 Reagents with SH and NH_2 functions at varying distance

Role of His and carboxyl group in the catalytic mechanism of XR

Kinetic parameters of XR as a function of pH

The pH dependence of the kinetic parameters of XR for the reduction of D-xylose was studied in the pH range 5-8. As shown in Fig. 16 the k_{cat}/K_m profile at varying pH displayed a bell shaped profile and pK_a values of 5.5 and 7.0 were obtained from the acidic and basic limb of the curve (Fig. 16) which are consistent with the participation of a carboxyl and His group respectively in the catalytic function of XR. However the results of these studies are not conclusive since the pK_a value of an amino acid observed is greatly influenced by its microenvironment in the protein molecule. The kinetic parameters of XR in the presence of 20% ethanol was also investigated . The plot of pH *versus* k_{cat}/K_m yielded two pK_a values of 5.25 and 7.45 (Fig. 16). These results indicated that the presence of ethanol resulted in a 0.25 log unit decrease and a 0.45 log unit increase in the pK_a values obtained from the acidic and basic limb of the curve respectively. Presence of ethanol failed to alter the fluorescence of XR indicating that the influence of ethanol on the pK_a values cannot be attributed to disruption of the quaternary structure of the enzyme.

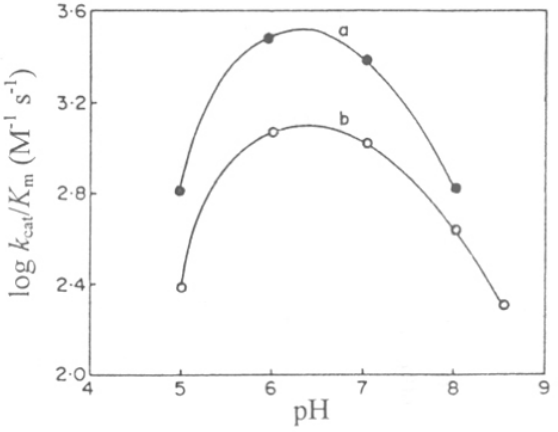

Fig. 16 Influence of pH on the k_{cat}/K_m for the reduction of D-xylose by XR
pH- k_{cat}/K_m profile of XR in the absence (•) and presence (o) of 20% ethanol

It has been reported that the pK_a values of cationic acids such as imidazolium ion decreases as the proportion of ethanol in a water-ethanol solvent is increased whereas the pK_a values

of uncharged acids such as acetic acid increases under the same conditions. In presence of 20% ethanol the measured pK_a of imidazolium ion decreases 0.2 log unit whereas the pK_a of acetic acid increases 0.17 log unit as compared to the value obtained in water (Mizutani, 1935). The difference in the effect of ethanol on uncharged and cationic acids was exploited to determine the charge type of the ionizable groups involved in the catalytic mechanism of XR. The studies revealed that in XR the pK_a of 5.5 and 7.0 represents the ionization of an abnormal His and carboxyl group respectively. This observation stimulated the chemical modification studies to further probe the role of these residues.

Kinetics of inactivation of XR by DEPC

Incubation of *N. crassa* XR with DEPC resulted in a rapid loss of enzyme activity indicating the presence of an essential His residue at or near the active site of XR. Plots of log of residual activity *versus* time at all concentrations of the reagent (Fig. 17A) were linear indicating that the process of DEPC induced inactivation of XR followed first-order kinetics.

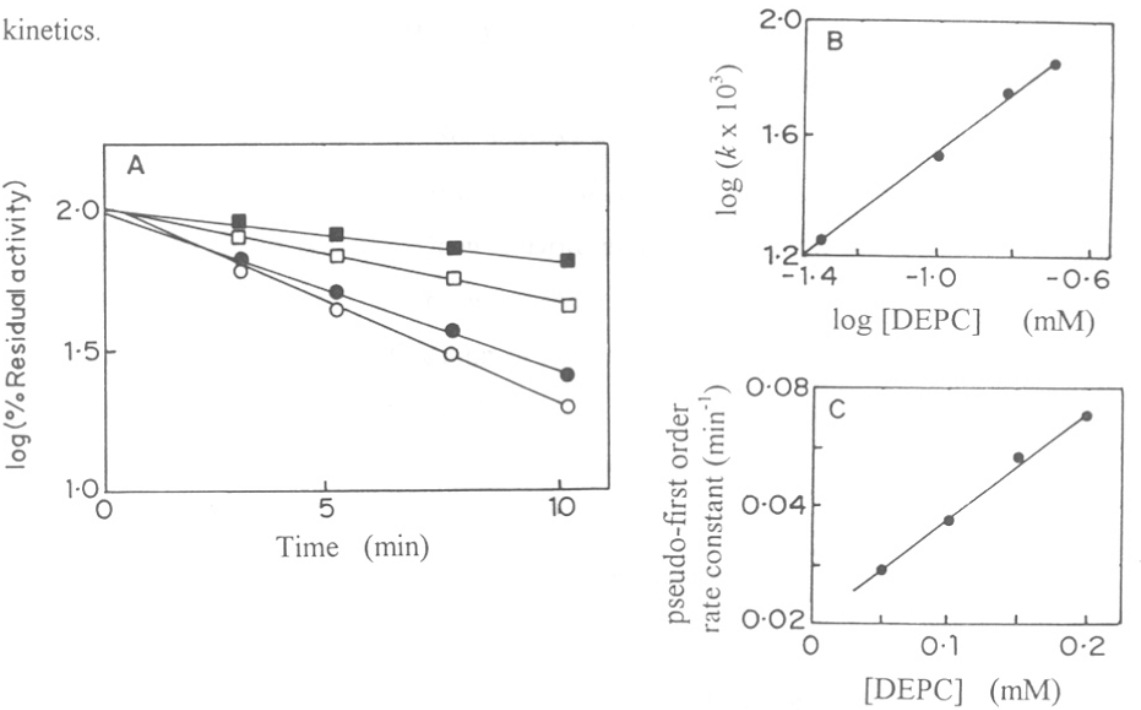

Fig. 17 Kinetics of inactivation of XR by DEPC

A. Plot of residual activity *versus* time for the inactivation of XR by DEPC 0.05 mM (■), 0.1 mM (□), 0.15 mM (•) and 0.2 mM (o).

B. Double logarithmic plot of pseudo-first order rate constant *versus* [DEPC]

C. Plot of pseudo-first order rate constant *versus* [DEPC]

Applying the analysis described by Levy *et al* (1963), the pseudo-first order rate constants were calculated from the slope of the plots of Fig. 17A. A double logarithmic plot of the observed pseudo-first order rate constants against reagent concentration (Fig. 17B) yielded a reaction order of one indicating that the modification of one residue/dimer resulted in the loss of XR activity. The second-order rate constant for the inactivation process was calculated to be 364 $M^{-1}min^{-1}$ (Fig. 17C)

Monitoring conformational change

The treatment of XR with DEPC did not result in any significant change in the intrinsic fluorescence of the enzyme (λ_{ex} 295 nm; λ_{em} 326 nm) which ruled out the possibility that the DEPC induced inactivation of XR was a result of gross conformational change. This view was also supported by the fact that the treatment of DEPC inactivated XR by hydroxylamine resulted in complete restoration of the original activity.

Identification of His as the DEPC modified amino acid

Although DEPC can be expected to react fairly specifically with the side chains of His other residues such as Tyr, Ser and Lys may be modified in neutral or weakly alkaline media (Pradel & Kassab, 1968; Burstein *et al*, 1974). Cys residues have not been modified in a wide variety of proteins (Dann & Britton, 1974) although the modification of model sulfhydryl compounds has been observed (Mühlrad *et al*, 1967). Keeping in view the varied reactivity of DEPC, the identification of the amino acid whose modification resulted in the loss of XR activity was investigated by

a) Treatment of the inactivated enzyme with hydroxylamine

b) Monitoring changes in the absorbance at 240 and 280 nm

c) Investigating the effect of pH on the rate of inactivation

Hydroxylamine treatment

Incubation of DEPC inactivated XR with 0.5 M hydroxylamine at pH 25 °C resulted in 80-85 % restoration of enzyme activity in 1h. However, dilution of the modified enzyme in the buffer alone did not cause any restoration. Since hydroxylamine deacylates only ethoxyformylated His and Tyr residues (Melchior & Fahrney, 1970) these results suggested that the inactivation of XR by DEPC may be due to modification of essential His and Tyr

residues and ruled out the possibility of its reaction with Cys, Lys and Ser residues. Further investigations were undertaken to probe the possibility of modification of tyrosyl residues.

Comparison of the absorbance of native and DEPC modified XR at 240 and 280 nm

The reaction of His with DEPC leads to the formation of N-carbethoxyhistidine which causes an increase in absorbance at 240 nm (Ovadi *et al*, 1967). Whereas, modification of tyrosyl residues leads to the formation of 2-O-carbethoxytyrosyl which causes a large decrease in the absorbance of the enzyme at 278 nm (Burstein *et al*, 1974). The difference spectrum of native and DEPC modified XR exhibited maximum near 242 nm. The absence of any appreciable difference in the region 280 nm indicated that DEPC did not react with Tyr residues in XR. These studies reinforced the evidence for His modification at the active site of XR. The number of His residues modified were calculated from the change in absorbance at 242 nm. Data in Fig. 18 indicated that the modification of a single His residue per dimer of XR resulted in complete inactivation of the enzyme.

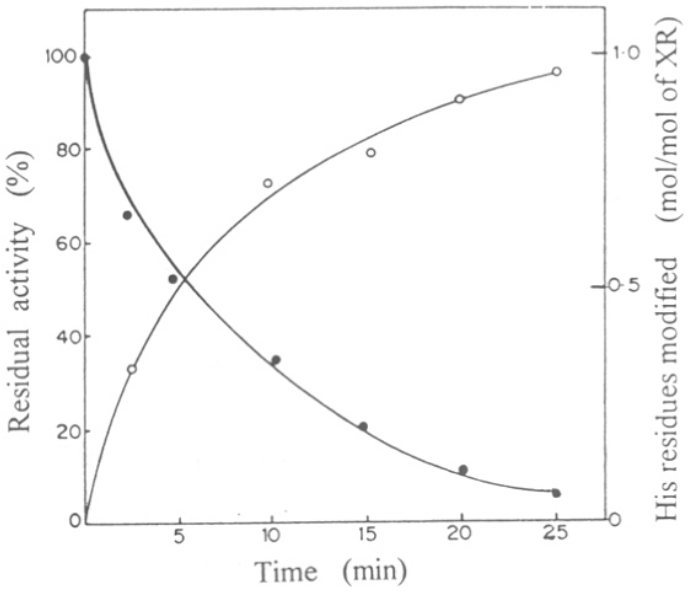

Fig. 18 **Correlation between the residual XR activity and the number of His groups modified by DEPC.**

Influence of pH on the rate of inactivation of XR by DEPC

DEPC induced inactivation of XR was measured in a series of buffers (pH 5-7) of constant ionic strength and under identical experimental conditions. It was observed that the rate of inactivation increased with the decrease in $[H^+]$ which may be attributed to an increase in the availibility of unprotonated His, the species that reacts with the inhibitor. Plot of k_{app} $[H^+]$ versus k_{app} (Fig. 19) yielded a value of 5.5 for the apparent pK_a of the His residue which represents a 1.5 pK_a unit shift from the pK_a of 7.0 seen for a free histidyl group in solution. The abnormal pK_a value of His in XR may be attributed to its location in a hydrophobic environment.

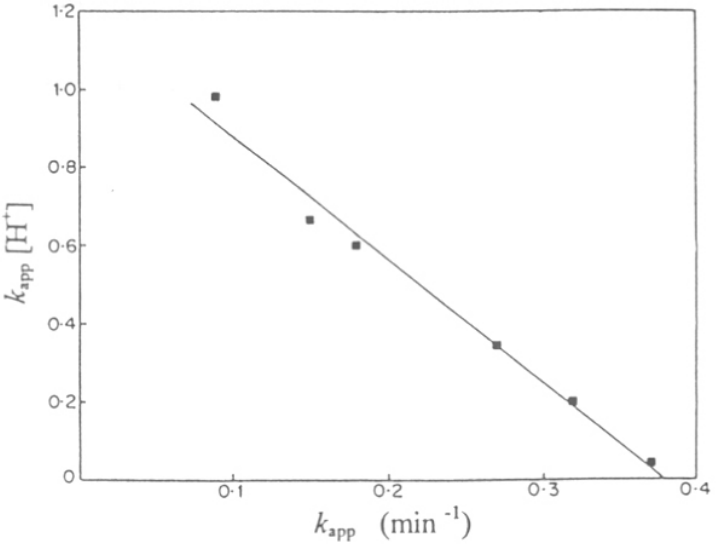

Fig. 19 pH dependence of the rate of reaction of XR His with DEPC

Kinetics of reduction of D-xylose by native and DEPC modified XR

The kinetic parameters for the reduction of D-xylose by native and DEPC modified XR are summarized in Table 5. It was observed that the modified enzyme showed a minimal increase in the K_m of the enzyme for NADPH. However, it had a drastic effect on the affinity of the enzyme for D-xylose with K_m increasing from 0.023 to 1.05 M while the catalytic constant k_{cat} decreased by a factor of 3.1. These findings suggested that His possibly plays an important role in the efficient binding of the substrate xylose to XR This view was also supported by the fact that the catalytic efficiency of XR drastically decreased

at pH 5.0 (Fig. 16) which may be attributed to the protonation of His residue that affects xylose interaction increasing its K_m .

Table 5. Kinetic parameters of native and DEPC modified XR

XR	k_{cat} (min^{-1})	$K_{m(NADPH)}$ (μM)	$K_{m(xylose)}$ (M)
Native	4486	9.2	0.023
Modified	1451	10.04	1.05

For the preparation of DEPC-modified enzyme, XR (1.2 μM) in 0.05 M phosphate buffer pH 7.0, was incubated with 0.18 mM DEPC. After 5 min the reaction was terminated by the addition of 2 mM His.

Reactivity of native and DEPC modified XR towards xylose isomers

Investigations were undertaken to probe the interaction of His with the substrate D-xylose by studying the reactivity of native and DEPC modified XR towards D-xylose and its stereoisomer D-lyxose as substrates. L-Lyxose is an isomer of D-xylose which differs only in the steric configuration of the hydroxyl group on C2.

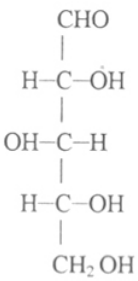

D-Xylose

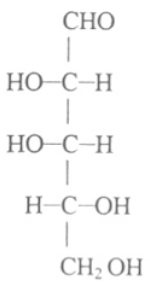

D-Lyxose

The kinetic constants of the native and DEPC modified XR for the sugar substrates are shown in Table 6. It was observed that the catalytic efficiency of the native enzyme for the substrate D-xylose was 1035 fold higher than that observed for D-lyxose. These results indicated the ability of XR to differentiate between D-xylose and its isomer further suggesting the importance of C2 (D-xylose vs D-lyxose) hydroxyl group in allowing the binding of the aldose substrate to XR. As shown in Table 6, the modification of essential

His residue in XR drastically decreased the catalytic efficiency for D-xylose and its stereoisomer. The catalytic efficiency for D-xylose was 187 fold higher than that for D-lyxose. Comparison of the data with that observed for the native enzyme revealed that the modification of essential His residue in XR was accompanied by a concomitant decrease in the ability to differentiate between D-xylose and its isomer. Altogether the studies revealed that the essential His in XR may be involved in directing the specificity of aldose substrates within the active site of the enzyme.

Table 6. Kinetic parameters of native and DEPC modified XR for xylose isomers

XR	D-xylose	D-lyxose
Native		
K_m (M)	0.023	2.1
k_{cat} / K_m ($M^{-1} s^{-1}$)	3250	3.14
Modified		
K_m (M)	1.05	2.25
k_{cat} / K_m ($M^{-1} s^{-1}$)	36	0.19

For the preparation of DEPC-modified enzyme, XR (1.2 μM) in 0.05 M phosphate buffer pH 7.0 was incubated with 0.18 mM DEPC. After 5 min the reaction was terminated by the addition of 2 mM His

Kinetics of inactivation of XR by EDC

The involvement of carboxyl groups in the catalytic mechanism of XR was investigated using the water soluble carbodiimmide EDC. Fig. 20 A shows a plot of residual activity as a function of time for inactivation of XR at a fixed concentration of EDC. The inactivation of the enzyme by varying concentrations of EDC was found to be linear signifying that in all cases the process obeyed pseudo-first order kinetics. Analysis of the order of the reaction by the method of Levy *et al* (1963) yielded a slope of 1.2 (Fig. 20 B) indicating that the loss of enzyme activity resulted from the reaction of atleast one molecule of the inhibitor per molecule of XR. The second-order rate constant for the inactivation process was calculated to be 1.6×10^{-2} M^{-1} s^{-1}. NADPH (250 μM) and xylose

(0.3 M) afforded no protection against inactivation implicating that the essential carboxyl group in XR is not involved in the binding of the substrates.

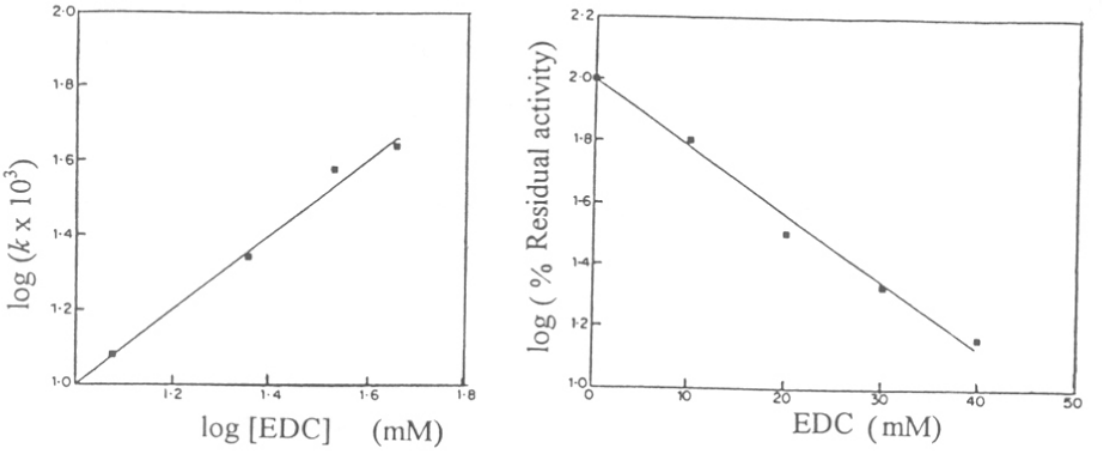

Fig. 20 Inactivation of XR by EDC

A. Plot of residual activity *versus* time for the inactivation of XR by 23 mM EDC

B. Double logarithmic plot of pseudo-first order rate constant *versus* [EDC]

Identification of carboxyl as the EDC modified group in XR

Although carbodiimides are highly selective for the modification of carboxyl groups in proteins, at slightly acidic pH Tyr can also be modified. Hence the following investigations were undertaken for the identification of the amino acid whose modification by EDC resulted in the loss of XR activity.

Hydroxylamine treatment

It has been shown by Carraway and Koshland (1969) that if the inactivation of an enzyme by EDC is due to modification of Tyr residues then treatment of the enzyme with hydroxylamine results in the liberation of the carbodiimide and restoration of enzyme activity. However, when EDC modified XR was incubated with 0.5 M hydroxylamine for various times upto 5h no regain in activity was observed. These results suggest that the EDC induced inactivation of XR may be attributed to the modification of essential carboxyl group in XR.

pH dependence of the rate of reaction of carboxyl group of XR with EDC

The influence of pH on the inactivation of XR by EDC was investigated. As shown in Fig. 21 the apparent rate of inactivation increased with the increase in $[H^+]$. Earlier Hoare and Koshland (1967) have reported that the reactivity of carbodiimides depends on the availibility of protonated carboxyl groups and thus the observed increase in the apparent rate of inactivation between pH 5 to 7.5. (Fig. 21) may be attributed to the ionization of the essential carboxyl groups. A value of 6.97 was obtained for the apparent pK_a of the carboxyl group in XR which is higher than that observed in free solution. The pK_a value of 6.97 derived from the chemical modification studies towards carboxyl group is in agreement with the pK_a value of 7.0 obtained from the pH dependence of k_{cat}/K_m (Fig. 16). The abnormally high pK_a value may be attributed to its location in a hydrophobic microenvironment. The aforementioned observations reinforced the evidence for carboxyl group modification at the active site of XR.

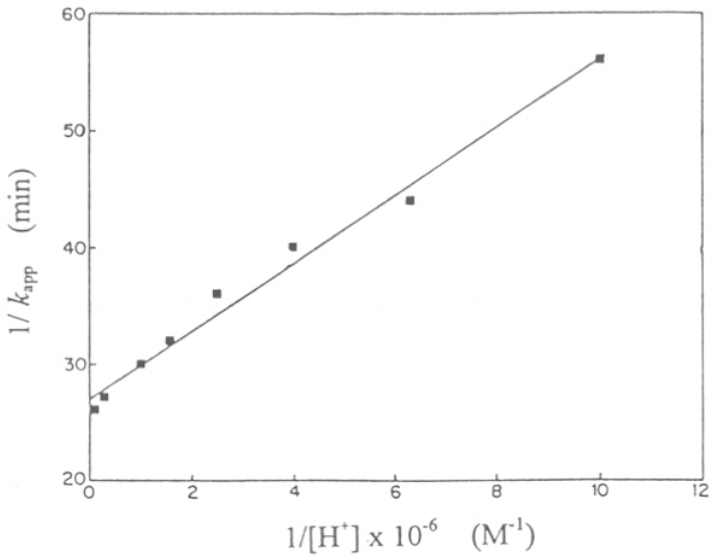

Fig. 21 Influence of pH on the pseudo-first order rate constants for the inactivation of XR by EDC

Effect of carboxyl modification on the kinetics of reduction of D-xylose

The kinetic parameters for the reduction of D-xylose by native and EDC modified XR is shown in Table 7. It was observed that the modification of XR by EDC was accompanied by a modest change in the affinity of the enzyme for D-xylose and NADPH.

This observation ruled out the possibility of involvement of a carboxyl group in the binding of substrates to XR. However the modification had a drastic effect on the enzyme activity of the enzyme with its k_{cat} value decreasing from 4725 to 1507 min^{-1}. These studies further confirmed the involvement of carboxyl group in the catalytic mechanism of XR.

Table 7. Kinetic parameters of native and EDC modified XR

XR	k_{cat} (min^{-1})	$K_{m(NADPH)}$ (μM)	$K_{m(xylose)}$ (mM)
Native	4725	8.8	21.4
Modified	1507	8.1	23

For the preparation of EDC-modified enzyme 70 μg of XR in 0.05 M Mes buffer pH 6.0 was incubated with 34 mM EDC at 25 °C. After 10 min the reaction was quenched by the addition of 0.1 M sodium acetate pH 5.0.

The investigations described in this chapter shed light on the essential amino acid residues in XR and their role in structure-function. Studies using the Trp modifier NBS and the hydrophobic probe ANS revealed that the Trp residues of XR play a role in maintaining the hydrophobicity of the NADPH binding site and permitting its efficient binding to the enzyme. Involvement of a Trp residue at the NADPH binding site of dihydrofolate reductase has also been reported and Trp21 has been identified as the crucial residue which is conserved in all bacterial and mammalian dihydrofolate reductases (Peterson *et al*, 1975; Freisheim *et al*, 1977).

Cys residues are known to play a crucial role in enzyme catalysis. Investigations that shed light on their location are of importance in the crystallographic context of locating binding sites for Hg atoms in heavy metal derivatives. Earlier, based on chemical modification studies Webb and Lee (1992) reported the presence of Cys residue at the NADPH binding site of XR from *P. stipitis*. The sensitivity of this enzyme to thiol-specific reagents was attributed to both Cys 27 and Cys 130 residues as substitution of either residues with Ser resulted in a significant but incomplete loss of senstivity to *p*-chloromercury benzenesulfonic acid (PCMBS) (Zhang & Lee, 1997). Several nicotinamide nucleotide-linked dehydrogenases are also inactivated on modification of a Lys residue suggesting a possible common role for Lys in these enzymes. In glutamate dehydrogenase

the binding of coenzymes and substrates does not depend on the integrity of Lys126 but plays a direct role either in the orientation of the reactants or in the catalytic process (Chen & Engel, 1975). The present investigation revealed the presence of two Cys and one Lys residue at the active site of XR. SH_I located at the high-affinity coenzyme binding site is involved in maintaining the hydrophobicity of the NADPH binding site and permitting its effficient binding to the enzyme. Using the bifunctional reagent OPTA as the chemical initiator for fluorescent chemoaffinity labeling we have also identified a Cys residue (SH_{II}) at the active site of XR. SH_{II} probably interacts with the NH_2 group of the essential Lys residue situated at a distance of 3 Å and thus serves to maintain the conformation of the active site essential for catalysis.

The k_{cat}/K_m profile at varying pH displayed a bell shaped profile with optimal catalysis and/or binding when an enzymic group with pK_a 5.5 is unprotonated and a second group with pK_a. 7.0 is protonated. Based on the various studies conducted using DEPC and EDC as chemical modifiers for His and carboxyl groups respectively we would ascribe the pK_a value of 5.5 seen in the k_{cat}/K_m profile to His and the pK_a vaue of 7.0 to carboxyl group. The abnormal pK_a values observed for these residues may be attributed to their location in a hydrophobic microenvironment at the active site of XR. The differential reactivity of the native and DEPC modified XR at varying pH and towards xylose isomers indicated that the His residue in XR plays a crucial role in binding and directing the specificity of aldose substrates within the active site of XR by acting as a hydrogen bond acceptor. The XR from *N. crassa* follows an *iso ordered bi bi mechanism* that involves binding of the substrate xylose to the active site pocket of the XR-NADPH complex (*refer chapter 3*). The reduction of aldehyde to alcohol involves a nucleophilic attack on an aldehyde carbonyl by a hydride from the nicotinamide ring followed by subsequent protonation of the negatively charged oxygen of the resulting alkoxide ion (Fig. 22). (Walsh,1979). In XR the positively charged Lys residue at the active site of XR may be involved in imparting stability to the alkoxyl intermediate formed during the reduction of xylose to xylitol. The His residue has an abnormally low pK_a value and hence it would be predominantly unprotonated at about pH 6.3 where XR exhibits maximum activity rendering its role in proton donation improbable. The pK_a value of carboxyl groups in proteins has been reported to be in the

range 3.5-5.0. The present studies revealed a abnormally high pK_a for the carboxyl group in XR indicating that the residue would be predominantly protonated at the optimum pH of XR and hence is likely to act as a proton donor. A similar role for the carboxyl group has also been reported in dihydrofolate reductase and aspartic/glutamic acid has been shown to be conserved at the active site (Basran *et al.* 1995).

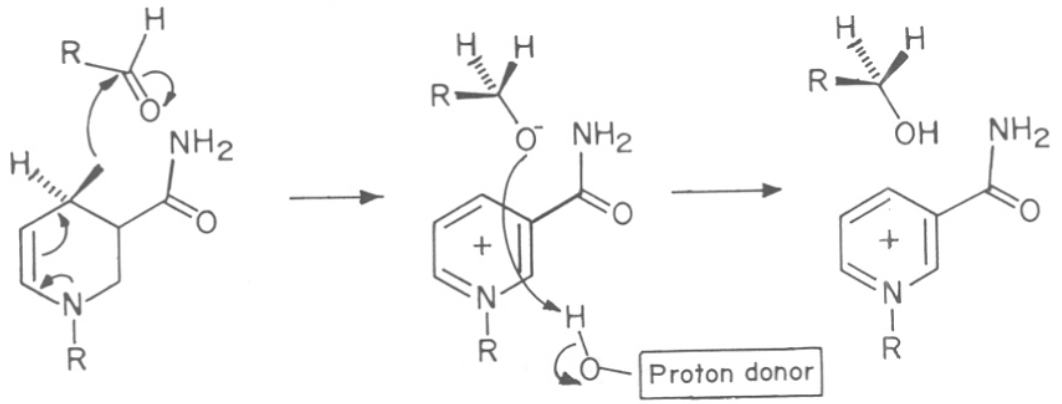

Fig. 22 Schematic representation of the reduction of an aldehyde to an alcohol

CHAPTER 5

Conformation and Microenvironment of the Active Site of Xylose Reductase

Summary

In the present investigation the conformation and microenvironment of the active site of XR from *N. crassa* has been probed. XR was completely inactivated by low concentrations of Gdn/HCl which was used as a active site perturbant. Fluorescence studies revealed that the inactivation of XR by Gdn/HCl precedes gross conformational change and the possibility of secondary conformational change was eliminated by acrylamide quenching studies. The change in the active site conformation was monitored by fluorescent chemoaffinity labeling (FCAL) using *o*-phthalaldehyde (OPTA) as a chemical initiator. OPTA reacts with XR at the active site resulting in the formation of a fluorescent XR-isoindole derivative. The enzyme inactivated by low concentrations of Gdn/HCl retained its ability to form the isoindole derivative indicating that inactivation was not due to conformational changes at or near the active site of XR. Gdn/HCl also had no effect on the binding of NADPH to XR. Energy transfer experiments further revealed the structural integrity at the active site of the Gdn/HCl-inactivated XR. Changes in the fluorescence emission maximum of 1-(β-hydroxyethylthio)-2-β hydroxyethylisoindole (EA adduct) in solvents of varying polarity was studied. The data obtained was utilized to interpret the fluorescence behaviour of XR-isoindole derivative and assess the polarity at the active site. Experimental evidence presented in this work serves to implicate that the active site of XR is less fragile and is located in a microenvironment of low polarity.

Introduction

Structure/function relationships are one of the central issues in the investigation of biological macromolecules. The conformational integrity of an enzyme is essential for its activity; however, few attempts have been made to correlate the conformational changes of an enzyme to changes in its catalytic activity. The present study reports on the conformation and microenvironment at the active site of XR using the technique of fluorescent chemoaffinity labeling. Affinity labeling is a powerful technique for studying the binding sites of ligand macromolecule complexes. Electrophilic affinity labeling (EAL) relies on the presence of a nucleophile (HNuc) in the binding cavity of the macromolecule (B) which can attack a chemically reactive functional group (X) attached to the ligand (A). These reactions are reasonably specific for a given X-HNuc combination; however, no control over the reaction is possible since covalent bond formation occurs upon approximation of two groups. In photo- or photoactivated affinity labeling (PAL), photolysis converts a suitable group Z to a highly reactive Z* with the ability to react with any substituent of B to form the product A-Z*-B. The reaction is almost instantaneous but occurs only after irradiation. In chemo- or chemically activated affinity labeling (CAL) the addition of a chemical is required to activate the formation of a covalent linkage between groups M on the ligand (A) and N on the macromolecule (B). Chemoaffinity labeling combines control over the timing of covalent bond formation with the advantage of the relatively stable and specific reactive functional groups found in electrophilic affinity labeling. OPTA the chemical initiator for CAL reacts with the SH and NH_2 groups to form isoindole derivatives in high yields. Since the isoindoles are intensely fluorescent this CAL reaction is referred to as fluorescent chemoaffinity labeling (FCAL). The variations in the thiol and amino substituents and solvent polarity and pH have large effects on the position of the emission maximum of the fluorescent isoindole derivative (Simon *et al*, 1979) which enables to assess the microenvironment of its binding cavity.

Materials and Methods

Materials

Gdn/HCl (guanidine hydrochloride)and *o*-phthalaldehyde (OPTA) were purchased from Sigma., 1-(*β*-hydroxyethylthio)-2-*β* hydroxyethylisoindole (EA adduct) an isoindole derivative of OPTA was synthesized by the procedure described earlier by Simons and Johnson, (1978a; 1979) for 1-(*β*-hydroxy ethylthio)-2-propylisoindole except that *n*-propyl-amine was substituted for ethanolamine.

Methods

Effect of Gdn/HCl on XR

The tryptophanyl fluorescence (λ_{ex} 295 nm; λ_{em} 326 nm) and activity of XR (0.5 μM) was measured in 0.05 M phosphate buffer pH 7.0, with varying concentrations of Gdn/HCl. OPTA-labeled XR was prepared by incubating XR (0.5 μM) with OPTA (20 μM) for 15 min at 25 °C in the same buffer and changes in the isoindole fluorescence (λ_{ex} 338 nm; λ_{em} 410 nm) on exposure to varying concentrations of Gdn/HCl was monitored.

Binding of NADPH to XR in presence of Gdn/HCl

XR (0.15 μM) in 0.05 M sodium phosphate buffer pH 7.0, was titrated with varying concentrations of NADPH in the absence or presence of Gdn/HCl and the tryptophanyl fluorescence was monitored at 326 nm with the excitation wavelength fixed at 295 nm. The quenching data was analyzed according to Stinson and Holbrook (1973) and the dissociation constant for the XR-NADPH complex was obtained (*refer chapter 3*).

Quenching studies using acrylamide

XR (0.42 μM) in 0.05 M sodium phosphate buffer pH 7.0, was titrated with varying concentrations of acrylamide in the absence and presence of Gdn/HCl and the changes in the protein fluorescence (λ_{ex} 295 nm; λ_{em} 326 nm) were monitored. The spectra were corrected for inner filter effects due to the addition of the quencher and the data was analyzed by the Stern-Volmer and modified Stern-Volmer plots (*refer chapter 4*).

Probing of active site polarity

To study the microenvironment of the isoindole derivative in XR, 12 μM of 1-(β-hydroxy ethylthio)-2-β-hydroxyethylisoindole (EA adduct) an isoindole derivative model compound was dissolved in solvents of varying polarity and its fluorescence emission maximum determined with the excitation wavelength fixed at 338 nm. The data obtained were correlated to betaine iodide transition energies (E_T) in different solvents and further utilized to study the fluorescence behaviour of XR-isoindole derivative. For solvents such as water, ketone, hydrocarbons etc., the correlation between E_T and emission maximum is given by the equation $E_T = 2.985\ \lambda_{em} - 1087.28$ (Dimorth *et al*, 1963).

Results and Discussion

Monitoring conformational changes in XR on inactivation by Gdn/HCl

Conformation at the active site of XR was studied using lower concentrations of Gdn/HCl as the active site perturbant. Fig. 1 shows the effect of Gdn/HCl on the activity of XR. The inactivation of the enzyme by Gdn/HCl was not due to gross conformational change as no change in the intensity or shift in the tryptophanyl fluorescence of XR (λ_{em} 295 nm; λ_{ex} 326 nm) was observed. Changes at the active site were monitored using fluorescent XR-isoindole probe (λ_{em} 338 nm; λ_{ex} 410 nm). Fig. 1 shows the effect of Gdn/HCl on the isoindole fluorescence of OPTA-labeled active site. Gdn/HCl (0-0.5 M) had no effect on the XR-isoindole fluorescence indicating that the microenvironment of the active site is not perturbed and hence the inactivation of XR by lower concentrations of Gdn/HCl is not due to conformational change at the active site. However, Gdn/HCl concentrations beyond 0.5 M did perturb the conformation at the active site before a change in gross conformation, as indicated by a rather sharp variation in the fluorescence of isoindole (Fig. 1).

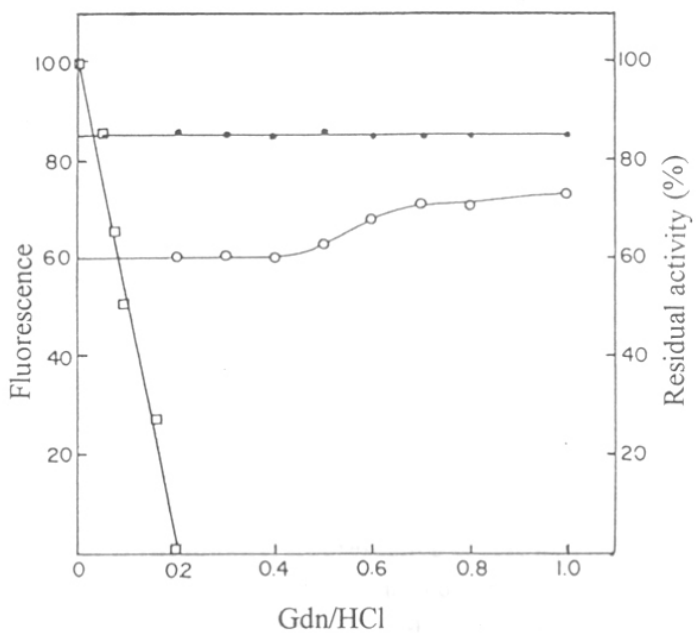

Fig. 1 Influence of Gdn/HCl on the activity and conformation of XR

Tryptophanyl (λ_{ex} 295 nm; λ_{em} 326 nm) (•), XR-isoindole (λ_{ex} 338 nm; λ_{em} 410 nm) (o) fluorescence and activity (□) of XR.

Binding of NADPH to XR in the presence of Gdn/HCl

The quenching of intrinsic fluorescence of XR by NADPH after inactivation of the enzyme by 0.2 M and 1 M Gdn/HCl is shown in Fig. 2. It was observed that NADPH quenched the XR fluorescence (λ_{ex} 295 nm; λ_{em} 326 nm) to the same extent in the presence and absence of 0.2 M Gdn/HCl. Applying the analysis described by Stinson and Holbrook (1973) (*refer chapter 3*) a K_d value of 0.97 was obtained for NADPH indicating that the inactivation of the enzyme by Gdn/HCl had no effect on the formation of XR-NADPH complex at the high affinity site. However, only 3 % of the tryptophanyl fluorescence of 1 M Gdn/HCl treated enzyme was quenched by higher concentration of NADPH (50 μM), indicating that NADPH is no longer bound. Binding of NADPH to the native XR resulted in the quenching of tryptophanyl fluorescence (λ_{em} 326 nm) and enhancement of NADPH fluorescence with a concomitant shift in the λ_{em} maximum from 465 to 445 nm. Gdn/HCl-inactivated enzyme also exhibited similar fluorescence.

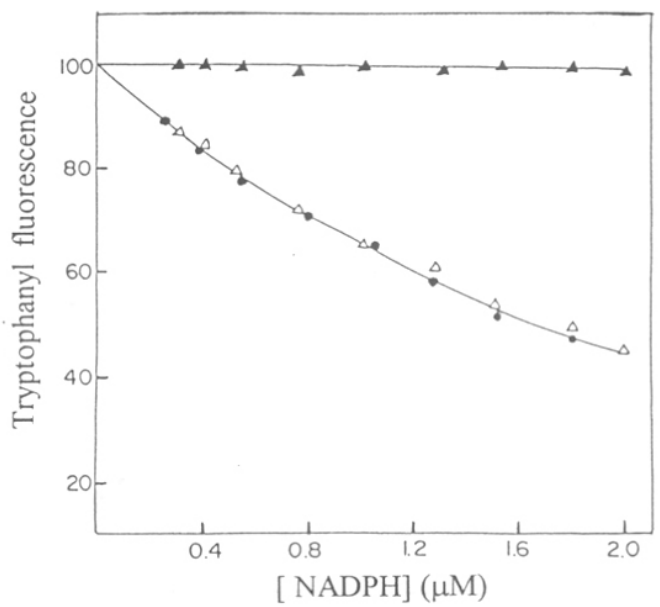

Fig. 2 **Quenching of tryptophanyl fluorescence of XR by NADPH**
XR fluorescence (λ_{ex} 295 nm; λ_{em} 326 nm) on titration with NADPH in the presence of following concentrations of Gdn/HCl 0 M (Δ); 0.2 M (•) and 1 M (▲).

Acrylamide quenching of XR fluorescence in the presence of Gdn/HCl

Fluorescence quenching studies were performed using acrylamide as the probing molecule, to detect any minor conformational change which accompanied inactivation of XR by Gdn/HCl. Acrylamide is a polar uncharged quencher, very sensitive to the exposure of the tryptophans in a protein molecule and decreases their fluorescence *via* physical contact with the excited indole group (Eftink & Ghiron, 1976). It was observed that acrylamide had no effect on the activity and emission maximum of the enzyme indicating that the quenching is an entirely physical process. The quenching of Gdn/HCl inactivated enzyme with increasing concentrations of acrylamide resulted in a Stern-Volmer plot with a downward curvature similar to that observed in case of native XR, thus indicating no change in the heterogeneous microenvironment of the tryptophans of the enzyme. The $K_{Q(eff)}$ (effective quenching constant) values of 5.68 and 5.66 M^{-1} and $f_{a\ (eff)}$ (maximum fractional accessible fluorescence) values of 0.50 were obtained from the modified Stern-Volmer plots (Fig. 3) for XR in the absence and presence of Gdn/HCl respectively.

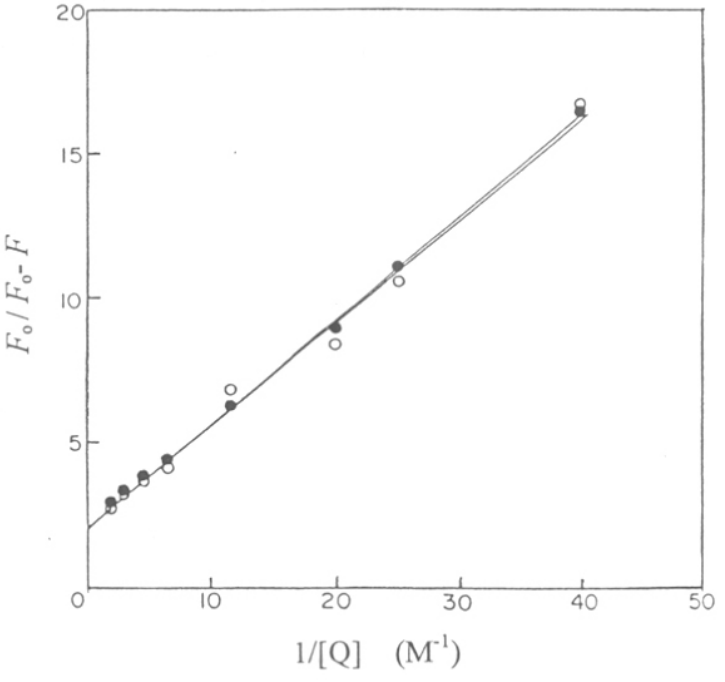

Fig. 3 **Acrylamide quenching of XR**
Modified Stern-Volmer plot for quenching of XR fluorescence (λ_{ex} 295 nm; λ_{em} 326 nm) by acrylamide in the absence (o) and presence of 0.2 M (•) Gdn/HCl.

Assessment of the polarity of XR-isoindole binding site

Earlier studies (*described in chapter 4*) have shown that OPTA reacts with the SH and NH_2 groups of XR resulting in the formation of fluorescent isoindole derivative at the active site. It has been reported that the variations in the thiol and amino substituents and solvent polarity have large effects on the position of the emission maximum of the isoindole derivative (Simons & Johnson, 1978b). This property was exploited to probe the polarity of the microenvironment at the active site of XR. The changes in the fluorescence emission maximum of an isoindole derivative compound EA adduct was determined in solvents of varying polarity. A linear relationship was observed between the emission maximum of EA adduct and molar transition energies of the various solvents. Solvents with higher polarity caused a red-shift in the fluorescence maximum of the EA adduct (Fig. 4). Based on the eq. $E_T = 2.985\ \lambda_{em} - 1087.28$, an E_T value of 137.2 kJ/mol was obtained for XR-isoindole derivative. As shown in Fig. 4, the emission maximum of the active site directed XR-isoindole at 410 nm corresponds to that of EA adduct in a mixture of *n*-hexane and toluene, indicating a nonpolar microenvironment at the active site of XR.

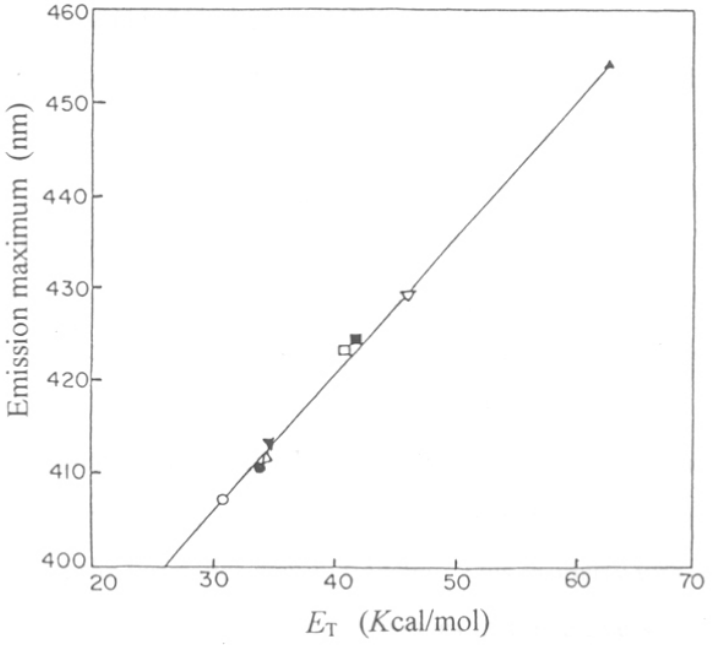

Fig. 4 **Correlation between fluorescence maximum of EA adduct and betaine iodide transition energies [E_T] in solvents of varying polarity**

Emission maximum of EA adduct (λ_{ex} 338 nm) in *n*-hexane (o); toluene (•); benzene (Δ); ethyl ether (▼); methylene chloride (□); acetone (■); acetonitrile (▽) and water (▲).

In the present investigation the active-site directed probe OPTA was used as a fluorescent affinity label to study the conformation and microenvironment at the active site of XR. The effect of Gdn/HCl on the activity of XR and isoindole fluorescence of OPTA-labeled XR were correlated to probe the conformation at the active site of the enzyme. Low concentrations of Gdn/HCl which was used as the active site perturbant, completely inactivated the enzyme without affecting the tryptophanyl (λ_{ex} 295 nm; λ_{em} 326 nm) and the XR-isoindole fluorescence (λ_{ex} 338 nm; λ_{em} 410 nm). Relatively higher concentrations of Gdn/HCl affected the microenvironment of the active site isoindole probe implicating a less fragile conformation at the active site of XR. This view was supported by various observations.

Fluorescence quenching studies were performed using acrylamide as the probing molecule, to detect any minor conformational change which accompanied inactivation of XR by Gdn/HCl. The quenching of XR by acrylamide resulted in a Stern-Volmer plot with a downward curvature suggesting that the fluorescence of certain tryptophans must be quenched much more easily than others. Based on the modified Stern-Volmer plot, 50 % of the total tryptophanyl fluorescence was available for quenching with a $K_{Q(eff)}$ value of 5.68 M^{-1}. The presence of Gdn/HCl had no effect on the exposure of tryptophan residues and a $K_{Q(eff)}$ value of 5.66 M^{-1} was obtained for the Gdn/HCl inactivated enzyme. The lack of effect of Gdn/HCl on the tryptophan emission and on quenching ability by acrylamide suggested that the inactivation is not due to secondary conformational change.

The quenching of the tryptophanyl fluorescence of a protein by its prosthetic group is due to resonance-energy transfer, provided this group is within a limited distance and the emission spectrum of tryptophan overlaps the absorbance spectrum of the prosthetic group (Guilbault, 1973). A disruption of the conformational integrity at the active site and therefore the spatial arrangement between the bound nicotinamide ring of the added coenzyme and the indole ring of tryptophan at or near the active site could lead to decrease in the efficiency of the resonance energy transfer. This property was exploited in the present investigation to probe the conformational changes at the active site of XR. The formation of XR-NADPH complex was accompanied by a decrease in the fluorescence of XR and enhancement of NADPH fluorescence with a concomitant shift in the emission maximum

from 465 to 445 nm. This observation is consistent with the binding of NADPH to the low affinity NADPH binding site of XR. It is interesting to note that the inactivation of XR by Gdn/HCl had no effect on the energy transfer process, further revealing the structural integrity at active site of the enzyme. Gdn/HCl induced inactivation of XR also failed to influence the binding of NADPH to the high affinity coenzyme binding site of XR (K_d 0.97 μM). Altogether the coenzyme binding studies suggested no change in conformation at the high- and low-affinity NADPH binding site of XR.

The variations in the thiol and amino substituents and solvent polarity have large effects on the position of the emission maximum of the fluorescent isoindole derivative (Simons & Johnson, 1978a). Changes in the fluorecence emission maximum of an isoindole derivative model compound 1-(β-hydroxyethylthio)-2-β-hydroxyethylisoindole (EA adduct) in solvents of varying polarity were studied. It was observed that solvents with higher polarity caused a red shift in the emission maximum of EA adduct. These properties were further utilized to interpret the fluorescence behaviour of XR-isoindole derivative, and thus enable to assess the polarity of the microenvironment at the active site of XR. Earlier studies have shown that the position of charge-transfer absorption band is remarkably sensitive to the polarity of the solvent and has been utilized for the creation of two most successful solvent polarity scales namely Z scale (Kosower, 1958) and E_T scale (Dimorth *et al*, 1963). In the present investigation E_T polarity scale was used which is based on the shifts in the charge transfer band in the visible spectrum of the pyridinium betaine in various solvents. The emission maximum values of the EA adduct obtained were correlated to the transition energies determined for various solvents and listed by Alder *et al* (1971). In comparison with other proteins (Weidekamm *et al*, 1973), the fluorescence emission maximum of the XR-isoindole derivative was observed at a shorter wavelength (λ_{em} 410 nm), and corresponds to the emission maximum of EA adduct in a mixture of *n*-hexane and toluene. Altogether these studies revealed that the microenvironment in XR which binds the fluorescent isoindole derivative is highly non-polar in nature.

The conformational integrity of an enzyme is essential for its activity. However, few attempts have been made to correlate the changes in the conformation of an enzyme to its catalytic properties. The unfolding of protein molecules during denaturation by urea or

guanidine hydrochloride is usually accompanied by loss in biological activity before significant conformational change can be detected. Studies have shown that in case of creatine kinase and glyceraldehyde-3-phosphate dehydrogenase the change in conformation at the active site parallels the inactivation of the enzyme by the denaturant suggesting that the active sites are located in relatively fragile parts of the enzyme (Xie & Tsou, 1987; Zhou *et al*, 1993). Hence a slight disturbance in the spatial arrangement of the active site destroys the enzyme activity before any gross conformational change can be detected. However, in case of XR, inactivation by Gdn/HCl preceded conformational changes in the active site and relatively higher concentrations of the denaturant were required to perturb the active site of the enzyme. The present studies revealed that the active site of XR is relatively less fragile and located in a highly nonpolar microenvironment. It has also been suggested that decrease in enzyme activity in Gdn/HCl could be due to reversible inhibition by the denaturant (Creighton, 1990). Gdn/HCl had no effect on the conformation and the NADPH binding sites of XR indicating that the inactivation may be due to specific interaction of the positively charged guanidino moiety of the denaturant with the negatively charged carboxyl group essential for catalysis, rather than unfolding of the molecule at the active site.

CHAPTER 6

Chaperone Assisted Folding of Xylose Reductase

Summary

Present investigations were undertaken to understand the folding of XR using the multimeric protein α-crystallin as a molecular chaperone. Denaturation studies using the structure-perturbing agent guanidinium chloride (GdmCl) indicated that XR folds through a partially folded state that resembles the molten-globule. Fluorescence and delay experiments revealed that α-crystallin interacts with the molten-globule state of XR (XR-m) and prevents its aggregation. Cold-lability of α-crystallin-XR-m interaction was revealed by temperature-shift experiments implicating the involvement of hydrophobic interactions in the formation of the complex. Reconstitution of active XR was observed on cooling the α-crystallin-XR-m complex to 4 °C or on addition of ATP at 37 °C. ATP hydrolysis is not a pre-requisite for XR release since the nonhydrolyzable analogue 5'-adenylyl imidodiphosphate (AMP-PNP) was capable of reconstitution of active XR. Experimental evidence has been provided for temperature and ATP mediated structural changes in the α-crystallin-XR-m complex that shed some light on the mechanism of reconstitution of active XR by this chaperone. The relevance of our finding to the role of α-crystallin *in vivo* is discussed.

Introduction

The folding and assembly of a protein into its biologically active conformation is a complex succession of reactions involving the formation of secondary and tertiary structures and domains, the pairing of domains and the oligomerization of folded monomers (Kim & Baldwin, 1982; Jaenicke, 1987). Elucidation of the various processes which govern protein folding has been the focus of intense research for the past decades. Numerous *in vitro* protein folding experiments have demonstrated that many proteins successfully achieve their correct native structures in the complete absence of other cellular factors and without input of energy. This led to the expectation that protein folding is determined by the information encoded by the amino acid sequence and proceeds *in vivo* by the same spontaneous mechanism (Kim & Baldwin, 1982; Jaenicke, 1987). However, *in vivo* folding and assembly of proteins occurs in a highly complex heterogeneous environment, in which high concentrations of proteins in various stages of folding, and with potentially interactive surfaces coexist that may change the folding potentials inherent in the sequence. Recently, a number of accessory proteins have been identified that affect the folding and subsequent assembly of proteins. These include the protein isomerases catalyzing *cis-trans* isomerization of peptide bonds or disulfide exchange (Freedman, 1984) and the polypeptide binding proteins termed as molecular chaperones (Hendrick & Hartl, 1993).

Protein disulfide isomerase– This enzyme facilitates the formation of the correct set of disulfide bonds during *de novo* folding of secreted proteins. It does not determine the folding pathway, but catalyses slow steps, presumably by reshuffling of incorrect disulfide bonds in the presence of a low molecular weight thiol compound which may be reduced or oxidized glutathione (Freedman, 1989). Generally, the secreted proteins contain disulfide bonds; hence, protein disulfide isomerase is localized in cell compartments such as the endoplasmic reticulum that form the secretory path (Freedman, 1984).

Peptidyl prolyl cis-trans isomerase– Some conformational steps in protein folding can be slow; therefore, enzymatic catalysis of folding is essential. An acceleration of crucial folding steps would decrease the risk of proteolytic degradation of partially folded chains, suppress competing unproductive pathways such as aggregation, and hence keep the protein on the correct productive folding pathway. Peptidyl prolyl cis-trans isomerase activities are widely

distributed in virtually all tissues and organisms ranging from mammals to bacteria. This enzyme accelerates efficiently the cis-trans isomerization of Xaa-Pro peptide bonds, one of the slow rate-determining steps in *in vitro* protein folding studies (Schmid & Baldwin, 1978; Lang *et al*, 1987).

Molecular chaperones– These proteins act sequentially in protein folding pathways by binding to folding intermediates that are in various stages of folding and then passing them on to next chaperone or chaperone complex in the cascade, eventually releasing a competent native protein. Binding usually involves interaction of the chaperones with hydrophobic residues on the surface of the unfolded proteins, and release often involves ATP hydrolysis. These proteins belong to the family of heat shock proteins (Pelham, 1988).

Elucidating the mechanistic details underlying the efficient refolding of proteins by chaperones now appears to be a important consideration for defining how proteins fold *in vivo*. The GroEL and GroES proteins from *E. coli* are among the most detailed characterized chaperones (Hendrick & Hartl, 1993). Horwitz (1992) and other workers have shown that α-crystallin acts as a molecular chaperone under various denaturing conditions including thermal inactivation, UV irradiation or reduction of disulfide bonds (Wang & Spector, 1994; Bakthisaran & Rao, 1994; Das & Surewicz, 1995). α-Crystallin is the major water soluble, multimeric structural protein of the eye lens made up of two types of highly homologous 20 kDa subunits, αA and αB. The A and B chains non-covalently self-associate to form a large macromolecular complex of approximately 40 subunits (Groenen, 1994). Until recently, α-crystallin was believed to be a lens specific protein; however, now has been reported to be present in many non-lenticular tissues (Iwaki *et al*, 1989). The expression of α-crystallin has been shown to be induced by thermal (Klemenz *et al*, 1991) or hypertonic stress (Dasgupta *et al*, 1992). Numerous studies have revealed that the ability of α-crystallin to suppress aggregation of damaged proteins plays a crucial role in maintaining the transparency of the ocular lens, and the failure of this function could contribute to the development of cataracts (Groenen *et al*, 1994; Kelly *et al*, 1993). Important recent development is the finding that α-crystallin shows extensive structural similarity with small heat shock proteins (sHsps) which are known to act *in vitro* as molecular chaperones (Merck *et al*, 1993; Jakob *et al*, 1993). α-Crystallin has been shown

to be functionally equivalent to the sHsps namely murine Hsp25 and human Hsp27 in refolding of α-glucosidase and citrate synthase *in vitro* (Jakob *et al*, 1993). It was however unable to refold rhodanase denatured in 6 M GdmCl (Das & Surewicz, 1995). Recently, α-crystallin has been reported to bind the temperature induced molten-globule state of proteins (Rajaraman *et al*, 1996; Das *et al*, 1996) and prevent photo- aggregation of γ-crystallin by providing hydrophobic surfaces (Bakthisaran & Rao, 1994).

Experimental evidence presented in the present work serves to implicate that the chaperone α-crystallin stabilizes the molten-globule state of XR and thus restrains the non-native conformer from exploring unproductive pathways. Lowering the temperature to 4 °C or presence of ATP at 37 °C induces a conformational change in α-crystallin-XR-m complex that is accompanied by a concomitant internalization of hydrophobic surfaces previously exposed. This acts to reduce the hydrophobic interactions that facilitates the dissociation of the complex further allowing reconstitution of the active XR. The present investigation reports for the first time the mechanism of α-crystallin-mediated reconstitution of active XR and the role of ATP in the function of α-crystallin as a molecular chaperone.

Materials and Methods

Materials

ATP (adenosine 5'-triphosphate), AMP-PNP(5'-adenylylimidodiphosphate) GdmCl (guanidinium chloride) and α-crystallin (c-4163) were purchased from Sigma and Centricon-100 micro-concentrators from Amicon. All chemicals used were of analytical grade.

Methods

Circular dichroism and Fluorescence studies

Circular dichroism (CD) spectra were recorded on a JASCO J600 model spectropolarimeter. XR was incubated with varying concentrations of GdmCl for 1.5 h at 28 °C in 0.05 M phosphate buffer, pH 7.2. Changes in the secondary structure of XR induced by the denaturant were monitored in the far-UV region (200-250 nm) using a 1 mm path length cell. The tertiary structure was monitored in the near-UV region (250-320 nm) using a 10 mm path length cell. The enzyme concentrations in these experiments was 0.5 mg/ml. Mean residue ellipticities [θ] (expressed as degree cm^2 $dmol^{-1}$) were determined according to Alder (1973). The ellipticity values obtained were normalized with respect to that in the absence of GdmCl.

Fluorescence spectra were recorded with a Perkin Elmer LS 50B spectrofluorimeter equipped with a Julabo F20 water bath or Aminco SPF-500 spectrofluorimeter. Corrections due to inner filter effect were made as described earlier (*refer chapter 4*).

ANS binding studies

XR was treated with varying concentrations of GdmCl as described above. Further, the GdmCl treated XR (final concentration 0.25 μM) was incubated with ANS (final concentration 10 μM) for 15 min and the spectra recorded on excitation at 375 nm.

Denaturation/Renaturation studies

All experiments described below were performed in the presence of 0.05 M sodium phosphate buffer, pH 7.2. XR-u and XR-m represents the completely unfolded and molten globule state of XR and were obtained on incubating the 25 μM enzyme with 6 M or 1.4 M

GdmCl respectively for 1.5 h at 28 °C. Renaturation was initiated by diluting 10 µl of the sample into a final volume of 1 ml of 0.05 M sodium phosphate buffer pH 7.2, under the specified conditions. 100 µl aliquots were withdrawn at various times of refolding and assayed for XR activity. The final concentration of XR-u/XR-m and α-crystallin in the refolding solution were 250 nM and 0.6 mg/ml respectively.

Renaturation of XR in the absence or presence of α-crystallin

The renaturation of XR-u/XR-m was initiated at 28 °C in phosphate buffer, with or without α-crystallin. After 30 min the samples were kept at a) 4 °C b) 28 °C or c) 37 °C. Small aliquots of the refolding solution were withdrawn at various times of refolding and assayed for XR activity. The refolding of XR-m was also investigated in the presence of varying concentrations of α-crystallin and the enzyme activity recovered after 6h at 4 °C was measured. The activity recovered was determined with reference to that of native XR.

Influence of α-crystallin on the stability of XR-m

Renaturation of varying concentrations of XR-m was initiated at 28 °C in phosphate buffer without α-crystallin. The chaperone was then added at various time intervals. After 30 min the samples were kept at 4 °C, aliquots were withdrawn after 6h and assayed for XR activity. The percentage activity recovered was determined with reference to equal concentration of native XR. The data obtained were normalized with respect to the time zero points for each XR-m concentration.

Tryptophanyl fluorescence of free and α-crystallin-bound XR

XR-m was renatured in phosphate buffer, containing α-crystallin at 37 °C. After 30 min the refolding solution was diluted to 2 ml and the tryptophanyl fluorescence was recorded. The fluorescence spectra of native and 6 M GdmCl denatured XR were also recorded. All samples were excited at 295 nm.

Influence of temperature on ANS fluorescence of α-crystallin-XR-m complex

Renaturation of XR-m was initiated at 37 °C in sodium phosphate buffer containing α-crystallin preincubated at the same temperature for 2h. After 30 min the samples were incubated at 37 °C or shifted to 4 °C; furthermore, ANS (final concentration 100 µM) was added after 12 h, and the fluorescence was recorded at the respective temperatures

(maintained ± 0.2 °C by Julabo F20 temperature water bath) at 1 h incubation, with the excitation wavelength fixed at 375 nm.

Reaction of α-crystallin renatured XR with *o*-phthalaldehyde

Renaturation of XR-m was initiated at 28 °C in phosphate buffer with or without α-crystallin. After 30 min the refolding solution was further incubated at 4 °C for 6h when maximum XR activity was recovered. The refolding solution was repetitively filtered through Centricon-100 microconcentrators (Amicon) to separate the released XR from α-crystallin. Furthermore, 10 µl of 3 mM OPTA was added to 2 ml of the filtrate, and the fluorescence spectra were recorded after 30 min with the excitation wavelength at 338 nm.

α-Crystallin mediated reactivation of XR in presence of ATP and XR substrates

Renaturation of XR-m was initiated at 37 °C by diluting the sample into phosphate buffer, with α-crystallin preincubated for 2 h at 37 °C. After 1 h following additions were made to the refolding solution a) ATP (1 mM), b) NADPH (0.5 mM), c) ATP (1 mM) + NADPH (0.5 mM) and d) xylose (250 mM). Further, small aliquots of the refolding solution were withdrawn at varying time intervals and the XR activity was determined. The activity recovered was determined with respect to the control containing native XR.

Renaturation of XR-m (*as described above*) was also studied in the presence of a) no nucleotide, b) ATP, c) AMP-PNP, d) ATP+NADPH, e) AMP-PNP + NADPH, f) ATP and g) AMP. The recoveries were determined after incubation for 3 h except for the samples d) and e) where the recoveries were determined after 12 h. The final concentration of the nucleotides in the various refolding solutions were 1.0 mM each of adenine nucleotides and 0.5 mM of NADPH. The percentage activity recovered is with respect to the control with native XR. In case of samples d) and e), the native XR was completely inactivated in 12h; therefore, the XR activity recovered is with respect to the activity of native enzyme incubated with 0.5 mM NADPH under identical conditions.

To investigate the dependence of renaturation on the order of addition of XR-m and ATP to α-crystallin, the renaturation of XR-m was initiated (*as described above*) in the presence of a) α-crystallin followed by addition of ATP after 1 h, b) α-crystallin preincubated with ATP for 1 h and c) in the presence of α-crystallin alone or its absence.

0.5 mM NADPH was added to all the samples. The final concentration of ATP in the refolding solution was 1.0 mM. The percentage of XR activity recovered was determined with respect to the control containing native enzyme.

Binding of ANS to ATP-free or bound α-crystallin-XR-m complex

ATP free α-crystallin-XR-m complex was obtained on renaturing XR-m in phosphate buffer with α-crystallin at 37 °C and incubating the sample for 30 min; whereas, the ATP-bound form was obtained on further incubation with the following concentrations of ATP a) 0.05 mM , b) 0.2 mM , c) 0.6 mM and d) 1.0 mM for 2 h at 37 °C. The complexes were incubated with ANS (final concentration 100 μM) and the fluorescence spectra were recorded at 37 °C with the excitation wavelength fixed at 375 nm.

Results and Discussion

Folding intermediates of XR

The CD spectrum of XR in the far-UV region (200-260 nm) exhibited a strong negative ellipticity in the region 215-222 nm and a weaker one at 208 nm, characteristic of a protein having an α-helix (*refer chapter 4*). XR was incubated with increasing concentrations of the denaturant GdmCl, and the changes in the negative CD band in the far-UV region were monitored. The mean residue ellipticities obtained at 220 nm $[\theta]_{220}$ were normalized with respect to that in the absence of GdmCl and plotted against the respective GdmCl concentration (Fig. 1). A decrease in the negative ellipticity was observed with the addition of GdmCl, and at 1.4 M GdmCl the $[\theta]_{220}$ decreased by almost 43% of that in the absence of GdmCl. Further increase in the denaturant resulted in a loss of negative ellipticity until there was a total loss of structure of the CD band in 6 M GdmCl indicating a considerable loss of secondary structure (Fig. 1). 6 M GdmCl converted XR into unfolded polypeptides and this state has been referred to as XR-u.

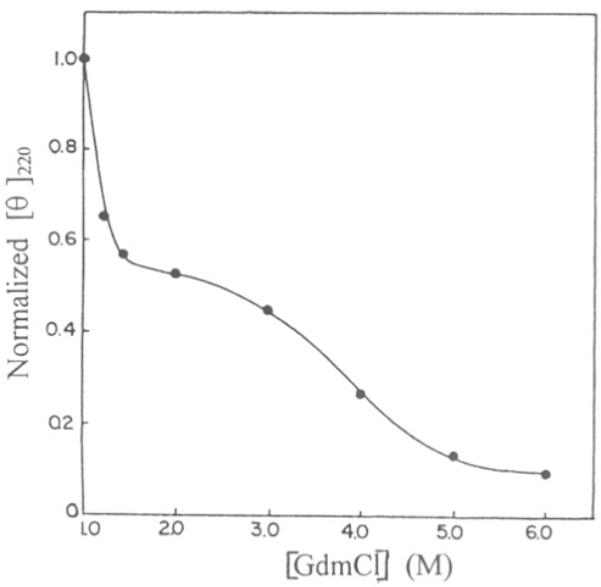

Fig. 1 Dependence of mean residue ellipticity of XR at 220 nm on GdmCl

The CD spectrum of XR was also monitored in the near-UV region (250-320 nm) to study GdmCl induced changes in the environment of tryptophan and tyrosine side chains. In the absence of the denaturant, the spectrum exhibited a broad negative band with a double minimum at 278 and 285 nm. However, the presence of 1.4 M GdmCl resulted in a decrease in the negative ellipticity in this region similar to that of the unfolded XR in 6 M GdmCl indicating that the aromatic residues in this state were no longer in an asymmetric environment.

In the present investigation the fluorophore ANS was used to determine the relative amount of exposed hydrophobic surfaces in the folding intermediates of XR. ANS is not fluorescent in aqueous solutions (λ_{em} 525 nm); however, on addition of proteins containing hydrophobic pockets its emission maximum shifts to shorter wavelengths, and the emission intensity is enhanced. As shown in Fig. 2, the binding of ANS to XR was measured as a function of GdmCl. A maximum increase in the ANS fluorescence (λ_{em} 475 nm) was observed at 1.4 M GdmCl indicating maximum exposure of hydrophobic surfaces in this state of XR. At high concentrations of the denaturant, a decrease in the intensity of the dye fluorescence was observed which was accompanied by a shift in the λ_{em} toward red indicating unfolding of XR. ANS has been widely used to detect the formation of molten-globule like intermediates in the folding pathways of several proteins (Ptitsyn *et al*, 1990). This state is characterized to be as compact as the native protein with solvent accessible hydrophobic regions and appreciable amount of secondary structure but no rigid tertiary structure (Fink, 1995; Ptitsyn, 1995). It was evident from the CD studies that at 1.4 M GdmCl, XR retains substantial amount of secondary structure (Fig. 1) but very little tertiary structure. Altogether the CD and ANS binding studies revealed that at 1.4 M concentration of GdmCl XR partially unfolded to its molten-globule state which has been referred to as XR-m. The existence of molten-globule like intermediates has been demonstrated with several proteins and are known to be involved in various cellular functions (Bychkova *et al*, 1988; Hendrick & Hartl, 1993; Tanford, 1968; Pace, 1986). Interest in such intermediates is strong since they have been proposed to be an obligatory intermediate formed early in the folding pathway.

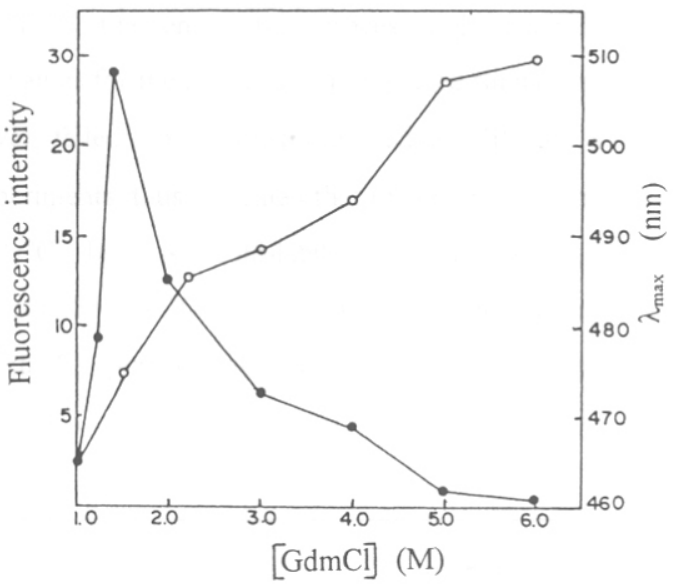

Fig. 2 ANS fluorescence of GdmCl treated XR

ANS fluorescence intensity at 475 nm (•) and λ_{max} (o) on incubation with XR treated with varying concentrations of GdmCl.

Chaperone-assisted renaturation of XR

Attempts to refold XR from the XR-u state in the absence and presence of α-crystallin were unsuccessful (Fig. 3). Similar results were obtained for progressively less denatured states of XR (XR denatured with 2-4 M GdmCl). Further investigations were carried out to study the influence of α-crystallin on the renaturation of XR-m. The refolding of XR-m was initiated at 28 °C in the absence/presence of α-crystallin; after 30 min the samples were shifted to varying temperatures (Fig. 3), and the XR activity recovered at different time intervals was measured. As shown in Fig. 3, XR-m lacked the ability to spontaneously reconstitute active XR. However, in the presence of α-crystallin the renaturation process at 4 °C followed a sigmoidal time course. As can be observed from *inset* of Fig. 3, there was no measurable XR activity for the first 15 min (lag phase). Thus similar to renaturation of oligomeric proteins (Jaenicke, 1987), inactive XR monomers may be produced in an early folding step which then undergo additional folding and/or association prior to the assembly of XR into active oligomers. The rate of reactivation

beyond the lag phase was slow and a maximum 55% of the XR activity was recovered in 6 h. A value of 112 min was observed for $t_{1/2}$,where the activity recovered was half of the maximal extent. At 28 °C, the renaturation process yielded a maximum 14% of the XR activity, whereas the values for the lag phase and $t_{1/2}$ were similar to that observed at 4 °C. α-Crystallin, however, failed to reconstitute active XR at 37 °C (Fig. 3). These temperature-shift experiments thus revealed that the complex of α-crystallin and the bound X R is stable at 37 °C but is cold-labile since lowering the temperature of the renaturation process from 28 to 4 °C resulted in the reconstitution of active XR. Unlike the observations at 28 °C, α-crystallin failed to reconstitute active XR when the refolding process was initiated at 4 °C.

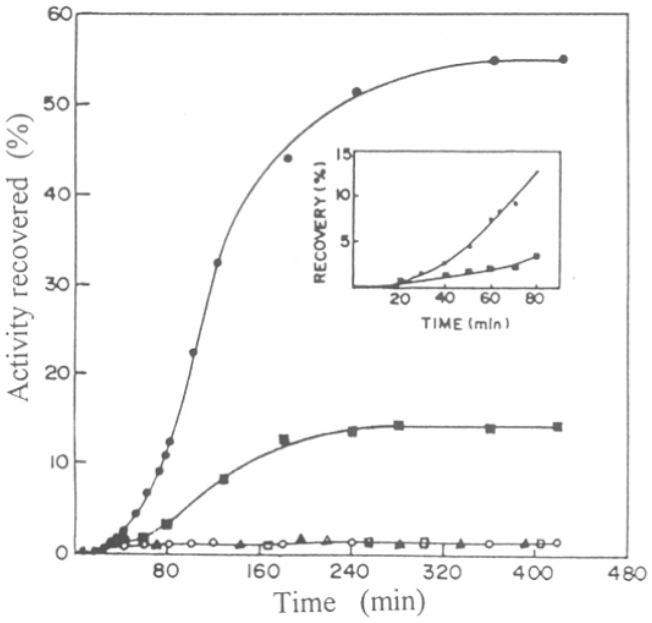

Fig. 3 **Renaturation of XR in the absence or presence of the α-crystallin**
Renaturation of XR-m in the absence of α-crystallin (o) and in its presence at 4 °C (•); 28 °C (■); and 37 °C (□). (Δ) and (▲) represents the refolding of XR-u and progressively less denatured states of XR (XR denatured with 2-4 M GdmCl) in the absence and presence of α-crystallin.
Inset: Early time course of α-crystallin assisted renaturation of XR.

Dependence of renaturation of XR on the concentration of α-crystallin

The α-crystallin mediated renaturation of XR was examined as a function of the chaperone concentration. As shown in Fig. 4, 5% of the original XR activity was recovered at the lowest concentration of α-crystallin (0.05 mg/ml). The extent of renaturation increased in a concentration dependent manner and a maximum 55-57% of the original activity was recovered at α-crystallin concentration of 0.6-0.8 mg/ml. The concomitant increase in the extent of renaturation with an increase in α-crystallin can be attributed to simple mass action effects, wherein an increase in the α-crystallin concentration would increase the collisional frequency so as to favour the formation of α-crystallin-XR-m complex as opposed to forming non-native XR. To test the specificity of α-crystallin, the renaturation of XR-m was also investigated in the presence of bovine serum albumin alone under the conditions described for renaturation with α-crystallin. It was observed that unlike α-crystallin bovine serum albumin failed to mediate the reconstitution of active XR.

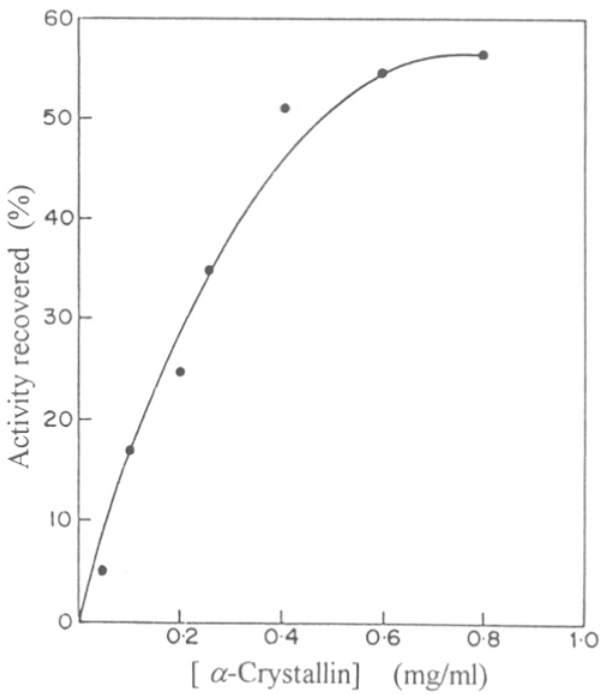

Fig. 4 Reactivation of XR-m at varying concentrations of α-crystallin

Delay experiments

α-Crystallin mediated reconstitution of active XR only from its XR-m state (Fig. 3), indicating that probably the chaperone traps the oxido-reductase in a conformation resembling the molten-globule. Evidence for this observation was provided by delay experiments wherein refolding of XR-m was initiated in a solution lacking α-crystallin which was then added at the indicated times. As shown in Fig. 5, a decrease in the ability of α-crystallin to reconstitute active XR from the XR-m state was observed with an increase in the time between the dilution of XR-m and the addition of α-crystallin. The increase in XR-m concentration also resulted in a decrease in the yield of reconstituted XR indicating that the loss of recoverable XR was due to aggregation and not due to some irreversible isomerization. The delay experiments revealed that when XR-m is diluted into a solution containing α-crystallin two competitive processes occur, namely aggregation or formation of α-crystallin-XR-m binary complex. Since aggregation is a second-order process it can be much faster than first-order folding (Zettmeissl *et al*, 1979) and hence predominant with increasing concentrations of XR-m.

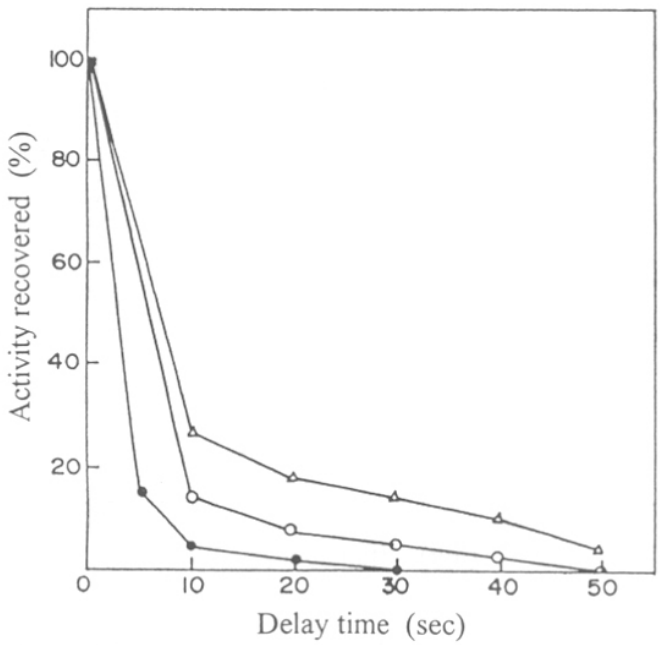

Fig. 5 **The lability of XR-m in the absence of α-crystallin.** Refolding of 200 (Δ), 300 (o) and 400 nM (•) XR-m when α-crystallin was added at the indicated times.

α-Crystallin forms a complex with folding intermediate of XR

Fluorescence studies were performed to confirm that the XR bound to α-crystallin exists in the molten-globule state. The tryptophanyl fluorescence of native, denatured and α-crystallin bound XR is shown in Fig. 6. Native XR exhibited an emission maximum at 326 nm while in 6 M GdmCl the emission maximum was shifted to 350 nm which corresponds to the fluorescence maximum of tryptophan in aqueous solution. The XR bound to α-crystallin exhibited an emission maximum at 334 nm indicating that the tryptophans in the bound form of XR are more exposed to the solvent than the native enzyme. The increase in fluorescence intensity of the α-crystallin bound XR may be attributed to the denaturant induced changes in the microenvironment of the tryptophans of XR or may be due to interactions of the partially unfolded protein with α-crystallin. Altogether these results revealed that the conformation of XR bound to α-crystallin is neither native like nor completely unfolded but a partially folded intermediate resembling the molten-globule. Thus by sequestering the molten-globule state of XR in the form of a stable binary complex, α-crystallin is able to suppress their interaction that would otherwise lead to aggregation.

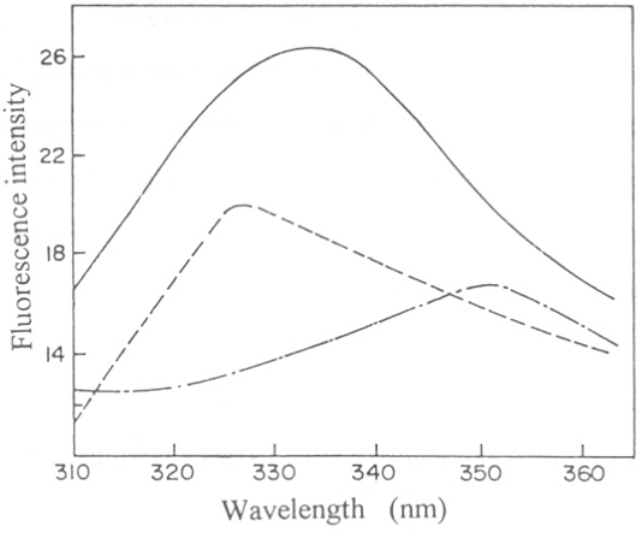

Fig. 6 **Typtophanyl fluorescence of native (----), denatured (—·—) and α-crystallin- bound (—) XR**

Temperature dependence of the exposure of hydrophobic surfaces of α-crystallin-XR-m complex

The temperature dependence of the hydrophobic interactions in protein folding has been studied earlier by Baldwin (1986). Maximum stabilization of these interactions is observed at high temperature where the enthalpy is the dominating factor in determining the stability, and as the temperature is decreased the interactions are weakened. Our temperature-shift experiments (Fig. 3) revealed an increase in the α-crystallin-mediated reconstitution of XR with the decrease in the temperature of the refolding solution implying that the hydrophobic interactions play a crucial role in the formation of α-cystallin-XR-m complex. Attempts were made to correlate temperature-mediated alterations in the hydrophobic surfaces of the α-crystallin-XR-m complex to reconstitution of active XR, using ANS a probe for apolar binding sites whose fluorescence is dependent on the hydrophobicity of the environment. As shown in Fig. 7, presence of α-crystallin-XR-m complex incubated at 37 °C resulted in a blue-shift in the ANS fluorescence from 525 to 475 nm accompanied by an increase in fluorescence intensity; however, in presence of the complex incubated at 4 °C a 35% decrease in the dye fluorescence was observed compared to that at 37 °C (Fig. 7). These results indicate that, at 37 °C the complex exists in a state with hydrophobic binding sites that are accessible to ANS; however, a decrease in the incubation temperature to 4 °C probably mediates a conformational change in the complex that is accompanied by internalization of the hydrophobic surfaces previously exposed. This further acts to weaken the hydrophobic interactions holding the α-crystallin-XR-m complex and thus reduces the affinity of α-crystallin for the substrate protein further allowing reconstitution of active XR (Fig. 3). This observation also explains for the cold-lability of α-crystallin-XR-m complex and the inability of α-crystallin to reconstitute active XR when refolding was initiated at 4 °C.

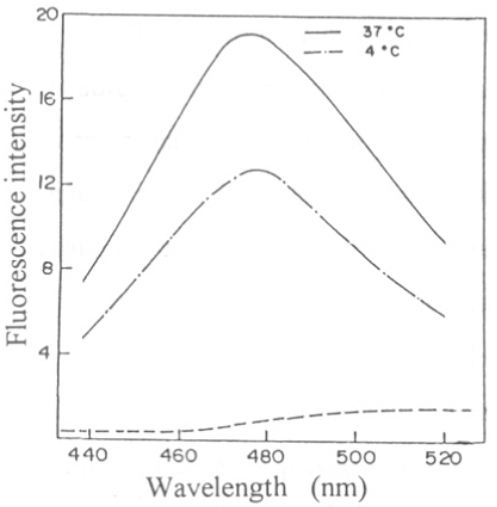

Fig. 7

ANS fluorescence (λ_{em} 475 nm) in the presence of α-crystallin-XR-m complex at 37 and 4 °C

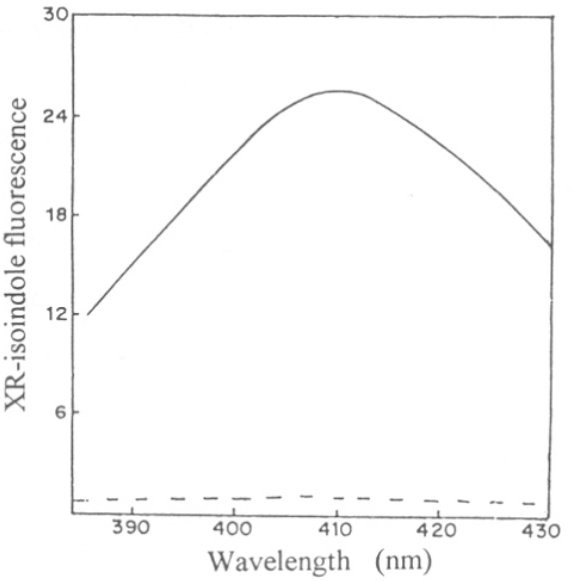

Fig. 8

Isoindole fluorescence (λ_{em} 410 nm) of α-crystallin renatured XR on reaction with OPTA

Fluorescent chemoaffinity labeling of XR renatured in the presence of α-crystallin

Fluorescent chemoaffinity labeling studies were performed using OPTA as the chemical initiator to shed some light on the conformation of XR renatured in the presence of α-crystallin. Chemoaffinity labeling is a powerful technique and combines some of the advantages associated with the photoactivated and electrophilic affinity labeling. *o*-Phthal-aldehyde is a bifunctional agent that cross-links SH and NH_2 groups situated in close proximity to form an isoindole derivative that exhibits strong fluorescence (Simons, 1979). XR reacts with *o*-phthalaldehyde resulting in the formation of fluorescent XR-isoindole derivative at the active site (λ_{ex} 338 nm; λ_{em} 410 nm) (*refer chapter 4*). As shown in Fig. 8, incubation of the α-crystallin renatured XR with OPTA resulted in the formation of XR-isoindole derivative as observed with the native enzyme. However, XR when renatured in the absence of α-crystallin failed to form the derivative. These results suggested that α-crystallin mediated the refolding of XR to a conformation similar to that of the native enzyme.

Influence of ATP and XR substrates on α-crystallin mediated renaturation of XR

The inability of α-crystallin to reconstitute active XR at 37 °C (Fig. 3) cannot be attributed to lack of binding of the chaperone to XR as shown in Fig. 6 but may be due to either an inability to release the bound XR at high temperature or due to the polypeptide being released in a temperature-sensitive conformation. Earlier the role of ATP in the renaturation of the proteins rhodanese, rubisco and β-protein (Mendonza *et al*, 1991; Schmidt & Buchner, 1992) by the chaperone GroEL has been reported. Recently evidence for the binding of ATP to α-crystallin was provided by ^{31}P-NMR spectroscopy (Caines *et al*, 1990) and fluorescence studies (Palmisano *et al*, 1995). Hence, studies were undertaken to find out if ATP played any role in the chaperone function of α-crystallin. For this functional *in vitro* analysis refolding of XR-m was initiated in a buffer containing α-crystallin at 37 °C and further incubated in the absence/presence of ATP. As shown in Fig. 9, α-crystallin mediated reconstitution of active XR was not observed in the absence of ATP. However, with ATP the renaturation process followed a sigmoidal time course and values of 10 and 53 min were observed for the lag time (Fig. 9 *inset*) and $t_{1/2}$ respectively. A maximum 22% of the XR activity was recovered in 1.5 h and further decrease in the yield may be attributed to temperature mediated inactivation of the released XR. The effect of XR substrates NADPH and xylose on the α-crystallin mediated renaturation of XR-m was investigated. It was observed that the percentage of XR activity recovered in the presence of ATP and NADPH in 1.5 h was approximately 2.5 fold higher than that observed in the presence of ATP alone (Fig. 9). However, the lag time (10 min) (Fig. 9 *inset*) and $t_{1/2}$ (53 min) values observed in both cases were identical indicating that the presence of NADPH did not alter the rate of the initial slow reaction (refolding of monomer and/or correct formation of dimer) nor the overall rate. The phosphorylated coenzyme, however, failed to mediate the reconstitution of active XR in the absence of ATP (Fig. 9). This ruled out the possibility of interaction of NADPH with XR bound to α-crystallin and alter the equilibrium between the bound and free enzyme. However, this may also be unlikely because the bound XR is in a non-native state (Fig. 6) and lacks enzymatic activity. In light of these data we propose that the release of α-crystallin bound XR is mediated by ATP, and the phosphorylated coenzyme NADPH traps the free XR in a conformation stable

at the physiological temperature. The XR substrate xylose failed to exert its effect on α-crystallin mediated reconstitution of active XR in the presence of ATP (Fig. 9). This may be due to the fact that the enzyme follows an *iso-ordered bi bi* mechanism wherein xylose binds to XR-NADPH binary complex.

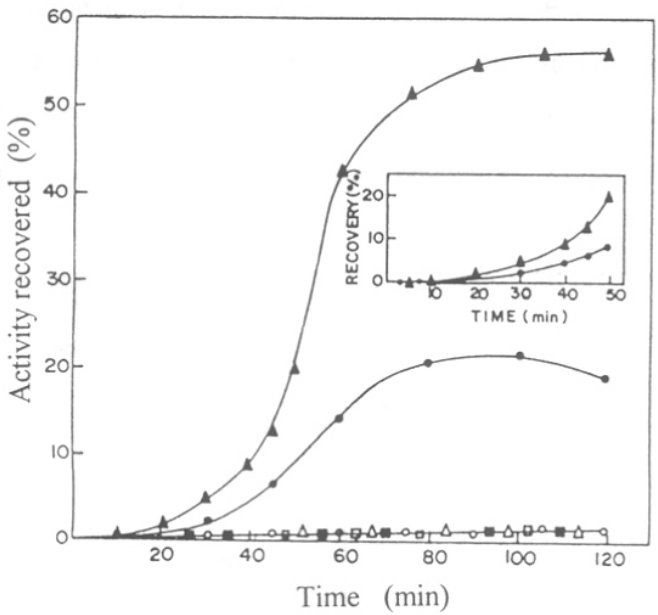

Fig. 9 **Influence of ATP and XR substrates on the α-crystallin mediated reactivation of XR-m**

α-Crystallin mediated renaturation of XR-m in presence of no nucleotide (o), ATP (•), NADPH (Δ) , ATP + NADPH (▲) and xylose (■). (□) represents α-crystallin-mediated renaturation of XR-u in the presence of the nucleotides/ XR substrates.

Inset: Early time course of the α-crystallin assisted renaturation of XR-m in the presence of ATP (•) or ATP + NADPH (▲).

Influence of adenine nucleotides on the α-crystallin mediated renaturation of XR

The effects of adenine nucleotides upon the α-crystallin mediated reconstitution of active XR were investigated. As shown in Fig. 10, addition of 5'-adenylyl imidodiphosphate (AMP-PNP) an ATP analog with a nonhydrolyzable β-γ bond resulted in a maximum 18% of XR activity in 1.5 h from its partially folded state compared to the maximum activity recovered in the presence of ATP. Further increase in the incubation period resulted in a decline in the yield of reconstituted XR which can be attributed to the thermal inactivation

of the free XR. Hence, the experiments were repeated wherein the coenzyme NADPH was added 30 min after the addition of the adenine nucleotides ATP/AMP-PNP so as to stabilize the released XR. Under these conditions a maximum 53% of XR activity was recovered in the presence of AMP-PNP in 12 h compared to the maximum observed in the presence of ATP in 5 h and which did not increase with further incubation. These results indicated differential ability of the adenine nucleotides ATP and AMP-PNP to reconstitute active XR which may be attributed to their different binding constants. α-Crystallin mediated reconstitution of active XR was not observed in the presence of AMP or ADP (Fig. 10), implying the involvement of the P_γ of ATP upon binding to α-crystallin-XR-m complex.

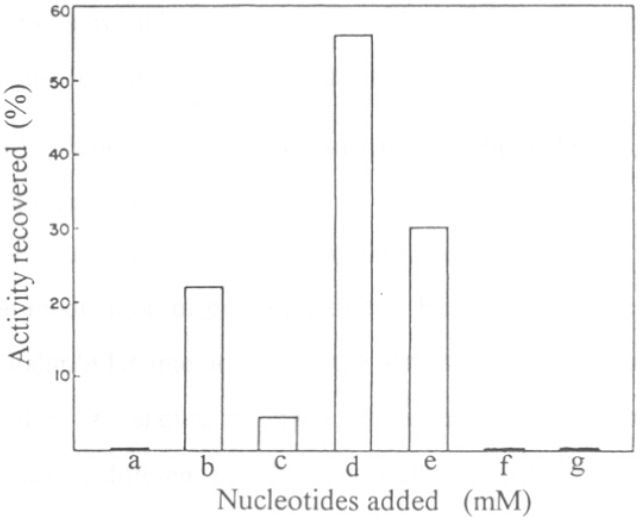

Fig. 10 **Effect of adenine nucleotides on the α-crystallin mediated reactivation of XR**
Reactivation of XR-m in the presence of a) no nucleotide, b) ATP, c) AMP-PMP, d) ATP + NADPH, e) AMP-PNP + NADPH, f) ADP and g) AMP.

Studies on the α-crystallin mediated renaturation of XR-m in the presence of various adenine nucleotides supported the notion that ATP hydrolysis is not a pre-requisite for release of XR bound to α-crystallin since the nonhydrolyzable analogue AMP-PNP was capable of reconstitution of the active XR. Instead, the release of XR may be mediated in part through the binding of ATP or AMP-PNP producing a similar conformational change in

the chaperone which weakens its interactions with XR further allowing reconstitution of the active enzyme. In contrast to 37 °C (Fig. 9) the α-crystallin mediated renaturation of XR-m was observed in the absence of ATP at 4 °C (Fig. 3). Also, when the renaturation was initiated at 37 °C and later the temperature shifted to 4 °C a maximum 55% of the original XR activity was recovered in 24 h. These differences in the ATP requirement supported the notion that the role of adenine nucleotide would seem to be linked with the need to provide a rapid dissociation pathway for the α-crystallin-XR-m complex at 37 °C, and is not essential for correct folding of XR. In light of these data it is tempting to speculate that a weak interaction exists between α-crystallin and the non-native XR. Tightly bound substrate proteins would probably reduce the flexibility of α-crystallin; hence, the binding of ATP alone or its hydrolysis would not be sufficient to induce conformational change necessary for the dissociation of the α-crystallin-protein complex.

Dependence of α-crystallin assisted renaturation on the order of addition of partially folded XR and ATP to α-crystallin

The highly selective nature of protein-ligand interaction provides a sensitive mechanism for the modulation of protein activity. Experiments were carried out to define the role of α-crystallin/ATP interaction on the structure and mechanism of action of the chaperone α-crystallin. As shown in Fig. 1, the order of addition of ATP and XR-m to α-crystallin resulted in a difference in the α-crystallin mediated renaturation profiles. The renaturation process of XR-m carried out in the presence of preformed α-crystallin-ATP complex followed a sigmoidal time course and values of 15 and 40 min were obtained for the lag phase (Fig. 11 *inset*) and $t_{1/2}$ respectively. However, when α-crystallin-XR-m complex was allowed to form prior to addition of ATP the renaturation process had a $t_{1/2}$ of 53 min and an initial lag time of 10 min. Though the value of $t_{1/2}$ was increased by 13 min in the later case, the final extent of XR activity recovered was 5.5 fold higher than that observed with the preformed α-crystallin-ATP complex. This indicated that the ATP-free form of α-crystallin mediates reconstitution of active XR more effectively than the ATP-bound form.

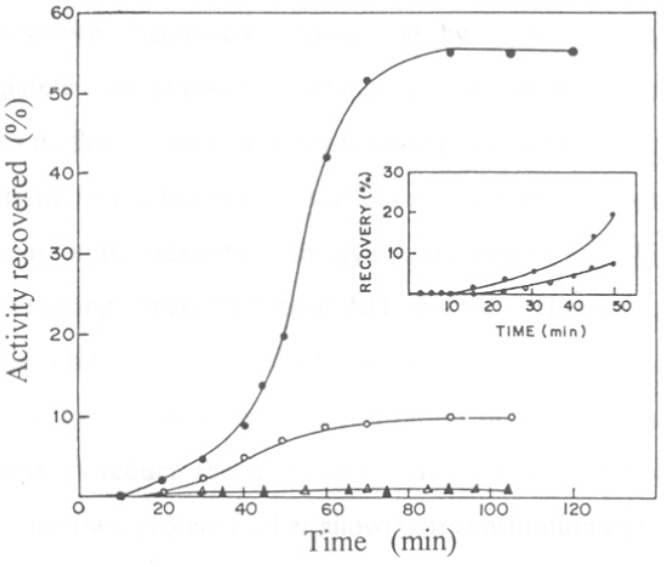

Fig. 11 **Influence of changes in the order of addition of XR-m and ATP to α-crystallin on the α-crystallin mediated renaturation of XR**

Refolding of XR-m in the presence of a) α-crystallin followed by addition of ATP (•); b)α-crystallin preincubated with ATP (o); c) α-crystallin alone (Δ) or in its absence (▲). **Inset:** Early time course of renaturation demonstrating the lag phase values of 10 and 15 min for sample a) and b) respectively.

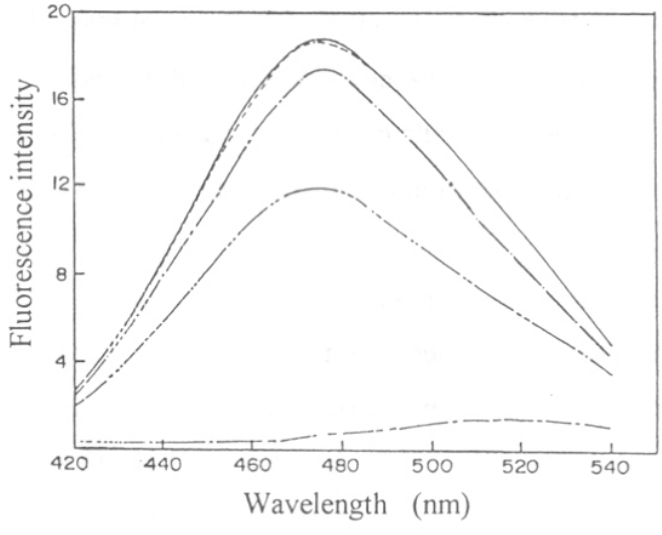

Fig.12 **Exposure of hydrophobic surfaces in the presence of ATP-free or bound crystallin-XR-m complex measured by ANS binding**

Spectra for ANS in the presence of α-crystallin-XR-m complex (ATP-free) (—) or α-crystallin-XR-m complex in presence of ATP (ATP-bound) at the following concentrations: 0.05 mM (—), 0.2 mM (---) , 0.6 mM (- - -) and 1.0 mM (- - - -). Bottom spectrum represents that of ANS alone.

The structural differences in ATP-free and bound form of α-crystallin-XR-m were probed by fluorescence spectroscopy using the hydrophobic probe ANS. As shown in Fig. 12, ANS exhibited an emission maximum at 525 nm; however, in the presence of α-crystallin-XR-m its fluorescence intensity increased and the emission maximum shifted to 475 nm characteristic of the transfer of ANS into a hydrophobic environment. Further, a concomitant decrease in the intensity of the dye fluorescence (λ_{em} 475 nm) was observed in the presence of increasing concentrations of ATP (Fig. 12). These results imply that binding of the adenine nucleotide to α-crystallin-XR-m complex induces a conformational change that is accompanied by a concomitant internalization of hydrophobic surfaces previously exposed. This acts to reduce the hydrophobic interactions and thus the affinity of the chaperone for the substrate protein further allowing reconstitution of the active XR.

Evidence for the ATP/α-crystallin binding has earlier been provided by ^{31} P-NMR spectroscopy (Caines *et al*, 1990) and fluorescence studies (Palmisano *et al*, 1995). ATP failed to influence the tryptophanyl fluorescence of XR in 1.4 M GdmCl (XR-m) indicating inability of the adenine nucleotide to bind XR-m. Altogether these results imply that in presence of α-crystallin-XR-m complex, ATP binds α-crystallin and not the bound XR which is quite likely because as shown in Fig. 6 the α-crystallin bound XR exists in a non-native state. In light of these data we propose that α-crystallin operates by providing hydrophobic surfaces that interact with the molten-globule state of XR and the hydrophobic interactions play an important role in the formation of α-crystallin-XR-m complex.

Conformational changes have been proposed to play a major role in the binding of folding intermediates and in the discharge of polypeptides from molecular chaperones. One of the signals for inducing such structural changes is the hydrolysis of ATP as reported in case of the chaperone DnaK (Liberek *et al*, 1991) and GroEL (Mendonza *et al*, 1991; Goboubinoff *et al*, 1989). However, reports are also available wherein the chaperones GroEL (Schmidt & Buchner, 1992) and BiP (Kassenbrock & Kelly, 1989) do not require ATP hydrolysis. Instead, the mere binding of the adenine nucleotide to the chaperone induces a typological change in the chaperone which weakens its interaction with the bound protein. This acts to release the protein, further allowing it to assume its native state. Our

investigations reveal that the mechanism of chaperoning of α-crystallin also requires the binding of ATP to the chaperone and not its hydrolysis.

Earlier studies have indicated that chaperones functioned post-translationally before the formation of the folded functional enzyme. The present investigation was carried out to gain some insight into the conformation of XR interacting with the chaperone α-crystallin and the mechanistic details underlying the reconstitution of active enzyme. The conditions for the unfolding of native XR were sought in the belief that the unfolded enzyme or its folding intermediates would serve as a substrate for the α-crystallin mediated reconstitution of active XR. Our denaturation studies using the structure-perturbing agent GdmCl revealed that the folding of XR involves an intermediate that resembles the molten-globule. The existence of molten-globule like intermediates has been demonstrated with several proteins and are known to be involved in various cellular functions such as membrane translocation of proteins (Bychkova *et al*, 1988; van der Goot *et al*, 1991), chaperone-assisted protein folding (Hendrick & Hartl, 1993) and also in various genetic diseases (Tanford, 1968; Pace, 1986). Interest in such intermediates is strong since they have been proposed to be an obligatory intermediate formed early in the folding pathway (Kim & Baldwin, 1990). A common feature of the molten-globule state is the exposure of hydrophobic surfaces that lead to aggregation of proteins during folding. Our *in vitro* studies using XR revealed that the chaperone α-crystallin operates by interacting with the hydrophobic regions that appear on the surface of molten-globule state of XR. This reduces the concentration of the free partially folded XR (XR-m) during renaturation and thus prevents loss of enzyme activity due to their hydrophobic aggregation. Lowering the temperature to 4 °C or presence of ATP at 37 °C induces a conformational change in the α-crystallin-XR-m complex that is accompanied by a concomitant internalization of previously exposed hydrophobic surfaces. This acts to reduce the hydrophobic interactions involved in the formation of the complex and thus the affinity of the chaperone for the substrate protein further allowing reconstitution of the active XR. The results presented here are consistent with the notion that the complete folding of XR resulting in the formation of catalytically active dimer does not occur while it is bound to the surface of α-crystallin. Our investigation reveals for the first time the mechanism of α-crystallin-mediated reconstitution

of an active enzyme and the role of temperature and ATP in its mechanism of chaperoning. Earlier it has been reported that α-crystallin does not prevent the photoaggregation of γ-crystallin at low temperatures. However, it can do so at temperatures above 30 °C (Bakthisaran & Rao, 1994). Our present investigation also supports this view, since α-crystallin mediated reconstitution of XR was observed when the refolding process was initiated at 28 and 37 °C and not when initiated at 4 °C which is attributed to the inability of the chaperone to prevent aggregation of XR-m at low temperature.

Delay experiments revealed the inability of α-crystallin to dissolve XR aggregates formed in its absence implying that the chaperone α-crystallin should be present during stress condition. The dependence of protein aggregation reactions on temperature and concentration is known. Our results support the notion that one of the functions of α-crystallin *in vivo* may be to protect non-native protein from intracellular aggregation during high rate of protein synthesis and/or thermal stress. The inability of XR-u and XR-m to spontaneously reconstitute active XR under the conditions used in the present investigation is due to the fact that aggregation competes with the correct folding pathway. The kinetic competition between refolding and aggregation has been reported to be a major determinant for lower yields or irreversibility in refolding of proteins *in vitro* (Jaenicke & Rudolph, 1986). However, refolding of XR may be possible under different experimental conditions, but regardless of this observation we are left with the fact that presence of α-crystallin resulted in a substantial amount of reconstitution of active XR from the XR-m state.

It has been reported that in *E.coli* a cascade of molecular chaperones mediate folding of proteins. The chaperone DnaK interacts with polypeptides in their extended conformation and prevents premature misfolding and aggregation after which GroEL stabilizes folding intermediates resembling the molten-globule and mediates proper folding. The transfer of DnaK/DnaJ-bound protein to GroEL requires GrpE as the coupling factor (Langer *et al,* 1992). Such a mechanism is likely to exist in eukaryotes also (Langer *et al,* 1992; Ellis, 1990). Our investigation reveals that α-crystallin is able to reconstitute XR *via* interaction with its non-native conformer characterized by an increased surface hydrophobicity but a remarkably low degree of unfolding. The inability of α-crystallin to

reconstitute XR from its extended conformation implies that *in vivo* other chaperones may be involved in binding to the unfolded polypeptides and prevent premature misfolding and aggregation, whereas the proper folding and assembly may depend on the subsequent transfer of the partially folded polypeptide to α-crystallin. Further evidence is provided by the observation that α-crystallin prevents aggregation of lens proteins induced by oxidative stress and UV radiation. These conditions are not likely to unfold protein molecules completely but induce formation of partially folded state with hydrophobic surfaces that result in its aggregation (Das *et al*, 1996). For many years α-crystallin was thought to be a lens specific structural protein where it played a role to facilitate proper transmission of light. However, recently α-crystallin has been demonstrated to be present in various non-lenticular tissues such as brain, spleen and heart and also found in NIH 3T3 cells expressing Ha-*ras* and v-*mos* (Iwaki *et al*, 1989; Klemenz *et al*, 1991). α-Crystallin has been reported to be induced by thermal or hypertonic stress (Klemenz *et al*, 1991; Dasgupta *et al*, 1992) and its expression is markedly increased in a number of neurological diseases such as Creutzfeld-Jacob disease, Alexander disease and Lewy body disease (Iwaki *et al*, 1992; Dugid *et al*, 1988; Lowe *et al*, 1990). Our present investigation on α-crystallin adds to the information available on its chaperone function which may assist to shed some light on its diverse roles *in vivo*.

BIBLIOGRAPHY

Bibliography

Alder, A., Greenfield, N. J. & Fasman, G. D. (1973) *Methods Enzymol.* **27,** 675-735.

Alder, R. W., Baker, R. & Brown, J. (1971) *Mechanisms of organic chemistry* pp. 40-51 Wiley Interscience, New York.

Ambrose, M. C. & Perham, R. N. (1976) *Biochem. J.* **155,** 429-432.

Amore, R., Wilhelm, M. & Hollenberg, C. (1989) *Appl. Microbiol. Biotechnol.* **30,** 351.

Andrews, P. (1965) *Biochem. J.* **96,** 595-60.

Bai, Y. & Hayashi, R. (1979) *J. Biol. Chem.* **254,** 713-718.

Bakthisaran, R. & Rao, M. C. (1994) *J. Biol. Chem.* **269,** 27264-27268.

Baldwin, R. L. (1986) *Proc. Natl. Acad. Sci.* USA **83,** 8069-8072.

Banerjee, M. (1985) Ph.D. Thesis, Indian Institute of Technology, Delhi.

Bannerjee, S., Archana, A. & Satyanarayana, T. (1994) *Curr. Microbiol.* **29,** 349-352.

Barbosa, M. F. S., de Medeiros, M. B., de Mancilha, I. M., Schneider, H. & Lee, H. (1988) *J. Ind. Microbiol.* **3,** 241-251.

Barnett, J., Payne, R. W. & Yarrow, D. (1983) *Yeasts: Characteristics and identification,* Cambridge University Press, New York.

Basran, J., Casarotto, I.L., Barsukov, I.L. & Roberts, G.L.K (1995) *Biochemistry* **34,** 2872.

Batt, C. A., Carvallo, S., Easson, D. D., Akedo, M. & Sinskey, A. J. (1986) *Biotechnol. Bioeng.* **28,** 549-553.

Bicho, P. A, Runnals, P. L., Cunningham, J. D. & Lee, H. (1988) *Appl. Environ. Microbiol* **54,** 50-54.

Birken, S. & Pisano, M. A. (1976) *J. Bacteriol.* **125,** 225-232.

Bolen, P. L. & Detroy, R. W. (1985) Biotechnol. Bioeng. **27,** 302-307

Bradford, M. N. (1976) *Anal. Biochem.* **72,** 248-254.

Bruinenberg, P. M, van Dijkes, J. & Scheffers, W. (1983) *J. Gen. Microbiol.* **129,** 965-971.

Bruinenberg, P M., de Bot, P. H. M., van Dijken, J. P. & Scheffers, W. A. (1984) *Appl. Microbiol. Biotechnol.* **19,** 256-260.

Burstein, Y., Walsh, K. A. & Neurath, H. (1974) *Biochemistry* **13,** 205-210.

Bychkova, V. E., Pain, R. H. & Pititsyn, O. B. (1988) *FEBS Lett.* **238,** 231-234.

Caines, G. H., Schleich, T., Morgan, C. F. & Farnsworth, P. N. (1990) *Biochemistry* **29,** 7547-7557.

Callens, M., Kersters-Hilderson, H., van Opstal, O. & Debruyne, C. K. (1986) *Enzyme Microb. Technol.* **8,** 696-700.

Callens, M., Kersters-Hilderson, H., Vangrysperre, W. & Debruyne, C. K. (1988) *Enzyme Microb. Technol.* **10,** 695-700.

Carraway, K. L. & Koshland, D. E. Jr. (1969) *Biochem. Biophys. Acta* **160,** 272-274.

Chakravorty, M., Veiga, L., Bacila, M. & Horecker, B. (1962) *J. Biol. Chem.* **237,** 1014.

Chan, E. C., Ueng, P. P. & Chen, L. F. (1989) *Appl. Microbiol. Biotechnol.* **31,** 524-528.

Chen, S. & Engel, P. C. (1975) *Biochem. J.* **149,** 619-626.

Chen, W. P. (1980) *Process Biochem.* **15,** 30-35.

Chiang, L. C. & Knight, S. G. (1960) *Nature (London)* **188,** 79-81.

Christakopoulos, P., Macris, B. & Kekos, D. (1990) *Appl. Microbiol. Biotechnol.* **33,** 18.

Christakopoulos, P., Macris, B. J. & Kekos, D. (1989) *Enzyme Microb. Technol.* **11,** 236.

Clark, T. & Cronan, J. E. (1980) *J. Bacteriol.* **141,** 177-183.

Creighton, T. E. (1990) *Biochem. J.* **270,** 1-161.

Culbert, S. J. & Wang, Y. M. (1986) *Nutr. Res.* **6,** 913-922.

Curtis, S. J. (1974) *J. Bacteriol.* **120,** 295-300.

D'Amore, T. & Stewart, G. G. (1987) *Enzyme Microb. Technol.* **9,** 322-330.

Dahlquist, F. W. & Raftery, M. A. (1968) *Biochemistry* **7,** 3277-3280.

Dahn, K. M., Davis, B. P., Pittman, P. E., Kenealy, W. R. & Jeffries, T. W. (1996) *Appl. Biochem. Biotechnol.* **57-58,** 267-276.

Dann, L. G. & Britton, H. G. (1974) *Biochem. J.* **137,** 405-411.

Das, K. P. & Surewicz, W. K. (1995) *Biochem. J.* **311,** 367-370.

Das, K. P., Petrash, J. M. & Surewicz, W. K. (1996) *J. Biol. Chem.* **271,** 10449-10452.

Dasgupta, S., Hohman, T. C. & Carper, D. (1992) *Exp. Eye Res.* **54,** 461-470.

David, J., Wiesmeyer, H. (1970) *Biochim. Biophys. Acta* **208,** 45-55.

Dekker, R. F. (1986) *Biotechnol. Bioeng.* **28,** 605-609.

Dellweg, H., Klein, C., Prahl, S., Rizzi, M. & Weigert, B. (1990) *Food Biotechnol.* **4,** 137.

Dellweg, H., Rizzi, M., Methner, H. & Debus, D. (1984) *Biotechnol. Lett.* **6,** 395-400.

Deshpande, V., Kesksar, S., Mishra, C. & Rao, M. (1986) *Enzyme Microb.Technol.* **8,** 149.

Dickens, F. (1938) *Biochem. J.* **32,** 1626-1645.

Dimorth, K., Reichardt, C., Siepmann, T. & Bohlmann, F. (1963) *Ann. Chim.* **661,** 1-37.

Dische, Z. & Borenfreund, E. (1951) *J. Biol. Chem.* **912,** 583-587.

Ditzelmuller, G., Kubicek, C. P., Wohrer, W. & Rohr, M. (1984) *Can. J. Microbiol.* **30,** 1330-1336.

Ditzelmuller, G., Kubicek-Pranz, E. M., Rohr, M. & Kubicek, C. P. (1985) *Appl. Microbiol. Biotechnol.* **22,** 297-299.

du Preez, J. C., Bosch, M. & Prior, B. A. (1986) *Enzyme Microb. Technol.* **8,** 360-364.

du Preez, J. C., Prior, B. A. Manteiro, M. (1984) *Appl. Microbiol. Biotechol.* **19,** 261-266.

du Preez, J. C., van Driesell, B. & Prior, B. A. (1989) *Appl. Microbiol. Biotechnol.* **25,** 143.

Dugid, J. R., Rohwer, R. G. & Seed, B. (1988) *Proc. Natl. Acad. Sci.* USA **57,** 5738-5742.

Eftink, M. R. & Ghiron, C. A. (1976) *Biochemistry* **15,** 672-680.

Ellis, R. S. (1990) *Science* **250,** 954-959.

Ellman, G. L. (1959) *Arch. Biochem. Biophys.* **82,** 70-77.

Emodi, A. (1978) *Food Technol.* **32,** 28-32.

Eyzaguirre, J. (1986) *Chemical modification of Enzymes, Active site studies* (ed. Eyzaguire) John Wiley and Sons.

Fink, A. L. (1995) *Annu. Rev. Biophys. Biomol. Struct.* **24,** 495-522.

Freedman, R. B. (1984) *Trends Biochem.* **9,** 438-441.

Freedman, R. B. (1989) *Cell* **57,** 1069-1072.

Freisheim, J. H., Ericsson, L. H., Bitar, K. G., Dunlap, R. B. & Reddy, A. V. (1977) *Arch. Biochem. Biophys.* **180,** 310-317.

Girio, F. M., Peito, M. A. & Amaral-Collaco, M. T. (1989) *Appl. Microbiol. Biotechnol.* **32,** 199-204.

Goboubinoff, P., Christeller, J. T., Gatenby, A. A. & Lorimer, G. H. (1989) *Nature* **342,** 884-888.

Gong, C. S. (1983) *Annu. Rep. Ferment. Proc.* **6,** 253-297.

Gong, C. S., Chen, L., Flickinger, M. & Tsao, G. (1981a) *Adv. Biochem. Eng/Biotechnol.* **20,** 93-118.

Gong, C. S., Claypool, T. A., McCracker, L. D., Mann, C. M., Ueng, P. P. & Tsao, G. T. (1983) *Biotechnol. Bioeng.* **25,** 85-102.

Gong, C. S., Mann, C. M. & Tsao, G. T. (1981b) *Biotechnol. Lett.* **3,** 77-82.

Groenen, P. J., Merck, K. B., de Jong, W. E. & Bloemendal, H. (1994) *Eur. J. Biochem.* **225,** 1-19.

Guilbault, G. G. (1973) in *Practical fluorescence: theory methods and techniques*, Marcel Dekker, New York.

Gupthar, A. S. (1992) *Can. J. Microbiol.* **38,** 1233-1237.

Hahn-Hagerdal, B., Jonsson, B. & Lohmeier-Vogel, E. (1985) *Appl. Microbiol. Biotechnol.* **21,** 173-175.

Hallborn, J. M., Walfridsson, M., Airaksinen, U., Ojamo, H., Hahn-Hagerdeal, B., Penttila, M. & Keraren, D. (1991) *Biotechnology* **9,** 1090-1095.

Helmut, B., Hildburg, B. & Hans, J. G. (1987) *Electrophoresis* **8,** 93-99.

Hendrick, J. P. & Hartl, F. U. (1993) *Annu. Rev. Biochem.* **62,** 349-384.

Herrero, A. A., Gomez, R. F., Snedecor, B., Tolman, C. J. & Roberts, M. F. (1985) *Appl. Microbiol. Biotechnol.* **22,** 53-62.

Ho, N. Y. & Chang, S. F. (1989) *Enzyme Microb. Technol.* **11,** 417-421.

Hoare, D. G. & Koshland, D. E. Jr. (1967) *J. Biol. Chem.* **242,** 2447-2453.

Hofer, M. & Nassar, F. R. (1987) *J. Gen. Microbiol.* **133,** 2163-2172.

Horecker, B. L. (1962) in *Pentose metabolism in bacteria*, Wiley Interscience, New York.

Horitzu, E. J. & Ordal, Z. J. (1970) *J. Bacteriol.* **102,** 369-375.

Horton, H. R. & Koshland, D. F. Jr. (1965) *J. Am. Chem. Soc.* **87,** 1126-1132.

Horwitz, J. (1992) *Proc. Natl. Acad. Sci.* USA **89,** 10449-10453.

Hyvönen, L. & Koivistoinen, P. (1983) *Adv. Food Res.* **28,** 273-403.

Ingram, L. O. & Buttke, T. M. (1984) *Adv. Microb. Physiol.* **25,** 253-300.

Ingram, L. O. (1986) *Trends Biotechnol.* **4,** 40-44.

Iwaki, T., Kume Iwaki, A., Liem, R. & Goldman, J. E. (1989) *Cell* **57,** 71-78.

Iwaki, T., Wisniewski, T. & Iwaki, A. (1992) *Am. J. Pathol.* **140,** 345-356.

Jaenicke, R. & Rudolph, R. (1986) *Methods Enzymol.* **131,** 218-250.

Jaenicke, R. (1987) *Prog. Biophys. Mol. Biol.* **49,** 117-237.

Johnson, S., Bailey, T. & Cardenas, J. (1979) *Biochem. Biophys. Res. Commun.* **90,** 525.

Jeffries, T. W., Fady, J. H. & Lightfoot, E. (1985) *Biotechnol. Bioengg.* **27,** 171-176.

Jakob, U., Gaestel, M., Engel, K. & Buchner, J. (1993) *J. Biol. Chem.* **268,** 1517-1520.

Jeffries, T. W. & Sreenath, H. K. (1988) *Biotechnol. Bioeng.* **31,** 502-506.

Jeffries, T. W. (1981) *Biotechnol. Lett.* **3,** 213-218.

Jeffries, T. W. (1983) *Adv. Biochem. Eng/Biotechnol.* **27,** 1-32.

Jeffries, T. W. (1984) *Enzyme Microb. Technol.* **6,** 254-258.

Jones, R. P. (1989) *Enzyme Microb. Technol.* **11,** 130-153.

Kassenbrock, C. K. & Kelly, R. B. (1989) *EMBO J.* **8,** 1461-1467.

Kasumi, T., Hayashi, K. & Tsumura, N. (1982) *Agric. Biol. Chem.* **46,** 21-30.

Kelly, M. J., David, L., Iwasaki, N., Wright, J. & Shearen, T. R. (1993) *J. Biol. Chem.* **268,** 18844-18849.

Kim, P. S. & Baldwin, R. L. (1982) *Annu. Rev. Biochem.* **51,** 459-489.

Kim, P. S. & Baldwin, R. L. (1990) *Annu. Rev. Biochem.* **59,** 631-660.

Kise, S., Koizumi, N. & Maeda, H. (1988) *J. Ferment. Technol.* **66,** 615-623.

Kitada, M., Dobashi, Y. & Horikoshi, K. (1989) *Agric. Biol. Chem.* **53,** 1461-1468.

Klemenz, R., Frohli, E., Steiger, R. H., Schafer, R. & Aoyama, A. (1991) *Proc. Natl. Acad. Sci.* USA **88,** 3652-3656.

Kosower, E. M. (1958) *J. Am. Chem. Soc.* **80,** 3253-3260.

Kotter, P. & Ciriacy, M. (1993) *Appl. Microbiol. Biotechnol.* **38,** 776-783.

Kotter, P., Amore, R., Hollenberg, C. P. & Ciriacy, M. (1990) *Curr. Genet.* **18,** 493-500.

Kulbe, K. D., Schmidt, H., Schmidt, K. & Scholze, H. A. (1972) *Progress in Biotechnol.* 7, 565-572.

Kumar, P., Singh, A. & Schugerl, K. (1991a) *Appl. Microbiol. Biotechnol.* **34,** 570-572.

Kumar, P., Singh, A. & Schugerl, K. (1991b) *Process Biochem.* **26,** 209-216.

Kurose, N., Murata, K. & Kimura, A. (1987) *Agric. Biol. Chem.* **59,** 2575-2578.

Kurtzman, C. P. (1984) in *The Yeast: A Taxonomic Study* (K. V. Rij, ed.) pp. 289-295, Elsevier, Amsterdam.

Kwon, H. J., Kitada, M. & Horikoshi, K. (1987) *Agric. Biol. Chem.* **51,** 1983-1989.

Laemmli, U. K. (1970) *Nature* **227,** 680-685.

Lakowicz, J. R. (1983) *Principles of Fluorescence Spectroscopy* pp. 45 Plenum Press.

Lang, K., Schmid, F. X. & Fischer, G. (1987) *Nature* **329,** 268-270.

Langer, T. Lu, C., Echols, H., Flanagan, J., Hayer, M. K. & Hartl, U. F. (1992) *Nature* **356,** 683-689.

Lee, H. (1992) *FEMS Microbiol. Lett.* **92,** 1-4.

Lee, H., James, A. P., Zahab, D., Mahmourides, G., Maleszka, R. & Schneider, H. (1986) *Appl. Environ. Microbiol.* **51,** 1252-1257.

Lefevre, J. F., Ehrlich, R. & Remy, P. (1980) *Eur. J. Biochem.* **103,** 155-160.

Lehrer, S. S. (1971) *Biochemistry* **10,** 3254-3263.

Levy, H. M., Leber, P. D. & Ryan, E. M. (1963) *J. Biol. Chem.* **238,** 3654-3659.

Liberek, K., Skowyra, D., Zylicz, M., Johnson, C. & Georgopoulos, C. (1991) *J. Biol. Chem.* **266,** 14491-14496.

Lieberthal, S., Oldfield, M. & Shanley, B.C. (1979) *Adv. Exp. Med. Biol.* **132,** 797-805.

Liu, J. K. & Dunlap, R. B. (1974) *Biochemistry* **13,** 1807-1814.

Lokman, B. C., van Santen, P., Verdoes, J. C., Kruse, J., Leer, R. J., Posno, M. & Pouwels, P. H. (1991) *Mol. Gen. Genet.* **230,** 161-169.

Lowe, J., Landon, M., Pike, I., Spendlove, I., Mc Dermott, H. & Mayer, R. J. (1990) *Lancet.* **336,** 515-516.

Lowry, O. H., Rosebrough, N. J., Farr, A. L. & Randall, R. J. (1951) *J. Biol. Chem.* **193,** 265-275.

Lucas, C. & van Uden, N. (1986) *Appl. Microbiol. Biotechnol.* **23,** 491-495.

Maleszka, R. & Schneider, H. (1982) *Can. J. Microbiol.* **28,** 360-363.

Manderson, G. J. & Newland, M. (1987) *J. Biotechnol.* **6,** 167-171.

March, J. (1977) in *Advanced Organic Chemistry: Reactions Mechanisms & Structure*, pp. 22 McGraw-Hill, New York.

McCracken, L. D. & Gong, C. S. (1983) *Adv. Biochem. Eng./Biotechnol.* **27,** 33-55.

Melchior, W. B. & Fahrney, D. (1970) *Biochemistry* **9,** 251-258.

Mendonza, J. A., Rogers, E., Lorimer, G. H. & Horowitz, P. M. (1991) *J. Biol. Chem.* **266,** 13044-13049.

Merck, K. B., Groenen, P. J., Voorter, C. E. M., de Haard-Hoekam, W. A., Horwitz, J., Bloemendal, H. & de Jong, W. (1993) *J. Biol. Chem.* **268,** 1046-1052.

Miles, E. W., (1977) In *Methods in Enzymology* Vol. **43,** Acad. Press, N.York pp 431

Meyrial, V., Delgenes, J., Moletta, R. & Navarro, J. M. (1991) *Biotechnol. Lett.* **13,** 281.Miles, E. W. (1977) *Methods Enzymol.* **47,** 431-442.

Mishra, C., Keskar, R. & Rao, M. (1984) *Appl. Environ. Microbiol.* **48,** 224-228.

Morimoto, S., Matsuo, M., Azuma, K. & Sinskey, A. (1986) *J. Ferment. Technol.* **64,** 219

Mortlock, R. P. & Wood, W. A. (1964) *J. Bacteriol.* **88,** 838-844.

Mühlrad, A., Hegyi, G. & Toth, G. (1967) *Acta Biochim. Biophys. Acad. Sci. Hung.* **2,** 19.

Neirinck, L. G., Maleszka, R., & Schneider, H. (1984) Arch. Biochem. Biophys. **228,** 13-21

Neuhauser, W., Haltrich, D., Kulbe, K. D. & Nidetzky, B. (1997) *Biochem. J.* **326,** 683.

Ovadi, J., Libor, S. & Elodi, P. (1967) *Acta Biochem. Biophys. Acad. Sci. Hurg* **2,** 455-458.

Pace, N. C. (1986) *Methods Enzymol.* **131,** 266-279.

Palczewski, K., Hargrave, P. & Kochman, M. (1983) *Eur. J. Biochem.* **137,** 429-435.

Palmisano, D. V., Groth-Vasselli, B., Fransworht, P. N. & Reddy, M. C. (1995) *Lancet* **336,** 515-516.

Pampulha, M. E. & Loureiro-Dias, M. C. (1989) *Appl. Microbiol. Biotechnol.* **31,** 547-550.

Parekh, S. R., Parekh, R. S. & Wayman, M. (1988) *Enzyme Microb. Technol.* **10,** 660-668.

Pawar, H. S., Bodhe, A. M., Rele, M. V. & Vartak, H.G. (1988) *J. Biosci* **13,** 43-46.

Pelham, H. R. B. (1988) *Nature* **332,** 776-777.

Perlman, D. (1949) *Am. J. Bot.* **36,** 180-188.

Perlman, D. (1950) *Am. J. Bot.* **37,** 237-242.

Peterson, D. L., Gleisner, J. M. & Blakley, R. L. (1975) *Biochemistry* **14,** 5261-5267.

Pradel, L. A. & Kassab, R. (1968) *Biochem. Biophys. Acta* **167,** 317-325.

Ptitsyn, O. B. (1995) *Adv. Protein Chem.* **17,** 83-229.

Ptitsyn, O. B., Pain, R. H., Semisotnov, G. V., Zerovnik, E. & Razgulyaev, O. I. (1990) *FEBS Lett.* **262,** 20-24.

Racker, E. (1948) *Fed. Proc. Fed. Am. Soc. Exp. Biol.* **7,** 180-184.

Rajaraman, K., Raman, B. & Rao, C. M. (1996) *J. Biol. Chem.* **271,** 27595-27600.

Rao, M., Deshpande, V., Keskar, S. & Srinivasan, M. C. (1983) *Enzyme Microb. Technol.* **5,** 133-136.

Ratledge, C. & Botham, P. A. (1977) *J. Gen. Microbiol.* **102,** 391-395.

Rhodes, C., Germershausen, J. & Suskind, S. R. (1971) *Methods Enzymol.* **22,** 80-86.

Ringold , H. J. (1966) *Nature* **210,** 535-536.

Riordan, J. F. & Vallee, B. L. (1972) *Methods Enzymol.* **25,** 449-456.

Riordan, J. F., Wacker, W. E. C. & Vallee, B. L. (1965) *Biochemistry* **4,** 1758-1765.

Rizzi, M., Erlemann, P., Bui-Thanh, N. & Dellweg, H. (1988) *Appl. Microbiol. Biotechnol.* **29,** 148-154.

Rizzi, M., Harwart, K., Bui-Thanh, N. & Dellweg, H. (1989b) *J. Ferment. Bioeng.* **67,** 25.

Rizzi, M., Harwart, K., Erlemann, P., Bui-Thanh, N. & Dellweg, H. (1989a) *J. Ferment. Bioeng.* **67,** 20-24.

Rosenberg, S. L. (1980) *Enzyme Microb. Technol.* **2,** 185-193.

Schellenberg, G. D., Sarthy, A., Larson, A. E., Backer, M. P., Crabb, J. W., Lidstrom, M., Hall, B. D. & Furlong, C. E. (1984) *J. Biol. Chem.* **259,** 6826-6832.

Schmid, F. X. & Baldwin, R. L. (1978) *Proc. Natl. Acad. Sci.* USA **75,** 4764-4768.

Schmidt, M. A. & Buchner, J. (1992) *J. Biol. Chem.* **267,** 16829-16833.

Schneider, H. (1989) *Crit. Rev. Biotechnol.* **9,** 1-40.

Segel, I. (1976) *Enzyme Kinetics,* Wiley, New York.

Sgorbati, B., Lenaz, G. & Casalicchio, F. (1976) *Antonie van Leeuwenhoeck* **42,** 49-53.

Simons, S. S. Jr. & Johnson, D. F. (1978a) *Anal. Biochem.* **90,** 705-725.

Simons, S. S. Jr. & Johnson, D. F. (1978b) *J. Org. Chem.* **43,** 2886-2891.

Simons, S. S. Jr., Thompson, E. B. & Johnson, D. F. (1979) *Biochemisty* **18,** 4915-4922.

Singh, A. & Kumar, P. K. R. (1991) *CRC Crit. Rev. Biotechnol.* **11,** 129-147.

Singh, A. & Schugerl, K. (1992) *Biochem. Int.* **28,** 481-488.

Singh, A., Kumar, P. K. R. & Schugerl, K. (1991) *Biotechnol. Lett.* **13,** 527-532.

Skoog, K., Hahn-Hagerdal, B. (1988) *Enzyme Microb. Technol.* **10,** 66-80.

Slinger, P. J., Bothast, E. J., van Canwenberge, J. E. & Kurtzman, C. P. (1982) *Biotechnol. Bioeng.* **24,** 371-384.

Smile, K. L., and Bolen, P. L. (1982) *Biotechnol. Lett.* **4,** 607-610.

Soumalainen, I., Londesborough, J. & Korhola, M. (1989) *J. Gen. Microbiol.* **135,** 1537.

Spande, T. F. & Witkop, B. (1967) *Methods Enzymol.* **11,** 498-506.

Stern, O. & Volmer, M. (1919) *Phys. Z.* **20,** 183-193.

Stevis, P. E., Huang, J. J. & Ho, N. W. Y. (1987) *Appl. Environ. Microbiol.* **53,** 2975.

Stinson, R. A. & Holbrook, J. J. (1973) *Biochem. J.* **131,** 719-728.

Suihko, M. -L., Suomalainen, I., and Enari, T. M. (1983) *Biotechnol. Lett.* **5**, 525-530.

Takahashi, K. (1968) *J. Biol. Chem.* **243,** 6171-6179.

Tanford, C. (1968) *Adv. Protein Chem.* **23,** 121-282.

Tomoyeda, M. & Horitsu, H. (1964) *Agric. Biol. Chem.* **28,** 139-143.

Topham, C. M. & Dalziel, K. (1986) *Eur. J. Biochem.* **155,** 87-94.

van der Goot, F. G., Gonzales-Manas, J. M., Lakey, J. H. & Pattus, F. (1991) *Nature* **354,** 408-410.

van Uden, N. (1989) in *Alcohol Toxicity in yeast and bacteria* CRC Press, Boca Raton, F.L.

Veiga, L. A., Bacila, M., and Horecker, B. L. (1960) *Biochem. Biophys. Res. Commun.* **2**, 440-448.

Verduyn, C., van Kleef, R., Frank, J., Schreuder, H., van Dijken, J. P. & Scheffers, W. A. (1985) *Biochem. J.* **226,** 669-677.

Walfridsson, M., Anderlund, M., Bao, X. & Hahn-Hagerdal, B. (1997) *Appl. Microbiol. Biotechnol.* **48,** 218-224.

Walsh. C. Enzymatic reaction mechanisms, W. H. Freeman & Co. San Francisco, CA.

Wang, G. S. & Wang, L. H. (1989) *Rept. Taiwan Sugar Res. Inst.* **124,** 39-37.

Wang, K. & Spector, A. (1994) *J. Biol. Chem.* **269,** 13601-13608.

Watson, N. E., Prior, B. A., du Preez, J. C. & Lategan, P. M. (1984) *Enzyme Microb. Technol.* **6,** 447-450.

Webb, S. R. & Lee, H. (1992) *J. Gen. Microbiol.* **138,** 1857-1863.

Wedlock, D. N. & Thornton, R. J. (1989) *J. Gen. Microbiol.* **135,** 2013-2018.

Wedlock, D. N., James, A. P. & Thornton, R. J. (1989) *J. Gen. Microbiol.* **135,** 2019-2026.

Weidekamm, E., Wallach, D. F. & Fluckiger, R. (1973) *Anal. Biochem.* **54,** 112-114.

Whitaker, J. R. & Perez, V. J. (1968) *Arch. Biochem. Biophys.* **124,** 70-75.

Wiegel, J. (1980) *Experientia* **36,** 1434-1446.

Wu, J. F., Lastik, S. M. & Updegraff, D. M. (1986) *Nature (London)* **321,** 887-889.

Xie, G. F. & Tsou, C. L. (1987) *Biochim. Biophys. Acta.* **911,** 19-24.

Yang, V. W. & Jeffreis, T. (1990) *Appl. Biochem. Biotechnol.* **26,** 197-206.

Yu, S., Wayman, M. & Parekh, S. K. (1987) *Biotechnol. Bioeng.* **29,** 1144-1150.

Zettmeissl, G., Rudolph, R. & Jaenicke, R. (1979) *Biochemistry* **18,** 5567-5571.

Zhang, Y. & Lee, H. (1997) *FEMS Microbiol. Lett.* **147,** 227-232.

Zhou, H. M., Zhang, X. H., Yin, H. & Tsou, C. L. (1993) *Biochem. J.* **291,** 103-107.